universität wien

MASTERARBEIT

Titel der Masterarbeit

„Radiosynthesis of the DAT-PET-Tracer [^{18}F]FE@IPCIT“

verfasst von

Cornel Fink, BSc

angestrebter akademischer Grad

Master of Science (MSc)

Wien, 2013

Studienkennzahl lt. Studienblatt:	A 066 862
Studienrichtung lt. Studienblatt:	Masterstudium Chemie
Betreut von:	assoc. Professor Dr. Wolfgang Wadsak

meinen Eltern

Table of Content

1 **INTRODUCTION 1**

1.1 RADIOACTIVITY 1

1.1.1 Radioactive Decay 1

1.1.2 Activity 2

1.1.3 Half-life 2

1.1.4 Decay Modes 2

1.1.4.1 Alpha (α) Radiation 2

1.1.4.2 Beta (β) Radiation 3

1.1.4.2.1 β^- Decay (Electron Emission) 3

1.1.4.2.2 β^+ Decay (Positron Emission) 3

1.1.4.3 Electron Capture 4

1.1.4.4 Gamma (γ) Radiation 4

1.1.5 Nuclides 5

1.1.5.1 Non-metallic Radioisotopes 5

1.1.5.1.1 Carbon-11 5

1.1.5.1.2 Fluorine-18 5

1.1.5.1.3 Nitrogen-13 6

1.1.5.1.4 Oxygen-15 7

1.1.5.2 Metallic Radioisotopes 7

1.1.5.2.1 Gallium-68 7

1.1.5.2.2 Technetium-99m and Technetium-94m 8

1.2 INSTRUMENTATION IN NUCLEAR CHEMISTRY AND NUCLEAR MEDICINE 8

1.2.1 Production of Radioactive Isotopes 8

1.2.1.1 Cyclotron 8

1.2.1.2 Nuclear Reactor 9

1.2.1.3 Generator 9

1.2.2 Imaging Techniques 10

1.2.2.1 X-ray 10

1.2.2.2 Computed Tomography 10

1.2.2.3 Magnetic Resonance Imaging 11

1.2.2.4 PET Positron Emissions Tomography and Single-photon Emission Computed Tomography 11

1.2.2.4.1 Positron Emissions Tomography 12

1.2.2.4.2 Single-photon Emission Computed Tomography 12

1.2.3 Synthesis Modules 12

1.2.3.1 Automated Synthesis Modules 13
1.2.3.2 Manually Operated Synthesis Modules 13
1.2.4 High performance liquid chromatography 13
1.2.4.1 Basic Principles 13
1.2.4.2 Instrumentation 14
1.2.4.3 Analytical HPLC vs. Semi-preparative HPLC 15
1.3 SYNAPTIC TRANSDUCTION 15
1.3.1 Neurotransmitter 16
1.3.1.1 Definition of a Neurotransmitter 16
1.3.1.2 Characteristics 16
1.3.1.3 Classification System 16
1.3.2 Neurotransmitter Substances (Selection) 17
1.3.2.1 Catecholamines 17
1.3.2.1.1 Dopamine 17
1.3.2.1.2 Epinephrine and Norepinephrine 18
1.3.2.1.3 Serotonin 18
1.3.3 Neurotransmitter Receptors 18
1.3.3.1 Dopamine Receptors 19
1.3.3.2 Epinephrine and Norepinephrine Receptors 19
1.3.3.3 Serotonin Receptors 19
1.3.4 Mechanisms of Reuptake and Decomposition of Neurotransmitters 19
1.3.4.1 Neurotransmitter Transporter Sites 19
1.3.4.1.1 Dopamine Transporters 20
1.3.4.1.2 Serotonin Transporters 20
1.3.4.1.3 Norepinephrine Transporter 20
1.3.5 Illicit Drugs: Mechanism of Action 21
1.4 RADIOPHARMACY 22
1.4.1 Radiopharmaceuticals 22
1.4.2 Characteristics and General Consideration for Radiopharmaceuticals 23
1.4.3 Effective Half-life 24
1.4.4 Specific Activity 24
1.5 TRACER 24
1.6 FROM COCAINE TO FE@IPCIT 25
1.6.1 Cocaine 25
1.6.1.1 General 25
1.6.1.2 Metabolism 26
1.6.1.3 Neurobiology 26

1.6.1.4 Addiction 27
1.6.1.5 Summarized Effects of Cocaine 27
1.6.2 Development of a New Drug 28
1.6.2.1 Cocaine as a precursor 28
1.6.2.2 Methylecgonidine 28
1.6.2.3 Troparil 29
1.6.2.4 Halogenated Analogues of Troparil 30
1.6.2.4.1 WIN 35,428 30
1.6.2.4.2 RTI-31 31
1.6.2.4.3 RTI-51 31
1.6.2.4.4 RTI-55 32
1.6.2.4.5 FE@CIT 33
1.6.2.4.6 PE2I and FE-PE2I 33
1.6.3 FE@IPCIT 34
1.6.3.1 Synthesis of IPCITacid and FE@IPCIT 35
1.6.3.2 Preclinical tests 35
1.6.3.2.1 Selectivity and Affinity 35
1.6.3.2.2 BBB Penetration Experiments 36
***2* AIM 38**
***3* MATERIALS AND INSTRUMENTATION 39**
3.1 MATERIALS 39
3.1.1 Solvents 39
3.1.2 Catalytic Substances 39
3.1.3 Chemicals 39
3.1.4 Formulation of the Pharmaceutical 39
3.1.5 Miscellaneous 39
3.2 INSTRUMENTATION 40
***4* METHOD 42**
4.1 MANUALLY OPERATED SYNTHESIS OF [^{18}F]BFE AND [^{18}F]FE@IPCIT 42
4.1.1 Synthesis of [^{18}F]BFE 42
4.1.1.1 Set-up for Fluoride-18 Extraction 42
4.1.1.2 Example Experiment for Manually Operated Synthesis: First Part – Extraction of $^{18}F^-$ 42
4.1.1.3 Set-up for [^{18}F]BFE Synthesis 43
4.1.1.4 Example Experiment for Manually Operated Synthesis: Second Part - Azeotropic Drying of [^{18}F]F^- and Synthesis of [^{18}F]BFE 43
4.1.2 Synthesis of [^{18}F]FE@IPCIT 44

4.1.2.1 Set-up for [^{18}F]FE@IPCIT Synthesis 44
4.1.2.2 Example Experiment for Manually Operated Synthesis: Third Part - Synthesis of [^{18}F]FE@IPCIT 44
4.1.2.3 Digitalized Laboratory Protocol 45
4.2 MODULE ASSISTED SYNTHESIS OF [^{18}F]BFE AND [^{18}F]FE@IPCIT 46
4.2.1 Set-up for [^{18}F]BFE and [^{18}F]FE@IPCIT Synthesis 46
4.2.2 Example Experiment for an Automated Module Synthesis 47
4.2.2.1 Protocol 47
4.2.2.2 Digitalized Laboratory Protocol 48
***5* EXPERIMENTS 49**
5.1 SYNTHESIS OF 2-BROMOETHYL TRIFLUOROMETHANESULFONATE 49
5.2 MANUALLY OPERATED SYNTHESIS OF [^{18}F]BFE AND [^{18}F]FE@IPCIT 49
5.2.1 Legend 49
5.2.2 Protocols 51
5.2.2.1 Experiment M.1 51
5.2.2.2 Experiment M.2 52
5.2.2.3 Experiment M.3 53
5.2.2.4 Experiment M.4 54
5.2.2.5 Experiment M.5 55
5.2.2.6 Experiment M.6 56
5.2.2.7 Experiment M.7 57
5.2.2.8 Experiment M.8 58
5.2.2.9 Experiment M.9 59
5.2.2.10 Experiment M.10 60
5.2.2.11 Experiment M.11 62
5.2.2.12 Experiment M.12 63
5.2.2.13 Experiment M.13 64
5.2.2.14 Experiment M.14 65
5.2.2.15 Experiment M.15 66
5.2.2.16 Experiment M.16 67
5.2.2.17 Experiment M.17 68
5.2.2.18 Experiment M.18 69
5.2.2.19 Experiment M.19 70
5.3 MODULE ASSISTED SYNTHESIS OF [^{18}F]BFE AND [^{18}F]FE@IPCIT 71
5.3.1 Experiment A.1 71
5.3.2 Experiment A.2 72
5.3.3 Experiment A.3 73

5.3.4 Experiment A.4 ..... *74*
5.3.5 Experiment A.5 ..... *75*
5.3.6 Experiment A.6 ..... *76*
5.3.7 Experiment A.7 ..... *77*
5.3.8 Experiment A.8 ..... *78*
5.3.9 Experiment A.9 ..... *79*
5.3.10 Experiment A.10 ..... *80*
5.4 HPLC 81
5.4.1 Analytical HPLC *81*
5.4.1.1 Assay for Separation of Fluoride-18 and [^{18}F]BFE 81
5.4.1.2 Assay for Separation of IPCITacid and [^{18}F]FE@IPCIT 81
5.4.2 Semi-preparative HPLC *83*
5.4.2.1 Assay 83
***6* RESULTS 84**
6.1 MANUALLY OPERATED SYNTHESES OF [^{18}F]FE@IPCIT 84
6.1.1 Synthesis Results of [^{18}F]BFE and [^{18}F]FE@IPCIT *84*
6.1.2 Catalysts *85*
6.2 MODULE ASSISTED SYNTHESIS OF [^{18}F]FE@IPCIT 86
***7* DISCUSSION 87**
***8* CONCLUSION 94**
***9* REFERENCES 95**
***10* APPENDIX 103**
10.1 ABSTRACT ENGLISH 103
10.2 ABSTRACT GERMAN 103
10.3 CURRICULUM VITAE 105
10.4 ACKNOWLEDGMENT 106

Table of Figures

Figure 1: Most important ^{11}C-precursors and direct derivatives 5
Figure 2: Basic components of a neuron [1] 15
Figure 3: general structure of catecholamines 17
Figure 4: Cocaine 25
Figure 5: Degradation of cocaine by esterases 26
Figure 6: Schematic representation of cocaine as a SNDRI 26
Figure 7: Schematic representation of the interaction of cocaine and its receptor [78] 27
Figure 8: Methylecgonidine 28
Figure 9: Synthesis route of methylecgonidine 29
Figure 10: Cocaine derivate troparil 29
Figure 11: WIN vinyl analogue 30
Figure 12: Fluorinated troparil analogue WIN 35,428 30
Figure 13: Chlorinated troparil analogue RTI-31 31
Figure 14: Brominated troparil analogue RTI-51 31
Figure 15: β-CIT: iodinated troparil analogue 32
Figure 16: nor-β-CIT 32
Figure 17: Structural formula of FE@CIT 33
Figure 18: PE2I - a more advanced troparil analogue 33
Figure 19: FE-PE2I (structural formula) 33
Figure 21: Candidate substance: FE@IPCIT 34
Figure 20: From cocaine to FE@IPCIT 34
Figure 22: Schematic synthesis route for IPCITacid and FE@IPCIT 35
Figure 23: Schematic representation of affinity tests 36
Figure 24: Schematic drawing: extraction of $^{18}F^-$ from $H_2{}^{18}O$ via an anion-exchange cartridge 42
Figure 25: Schematic drawing of the experimental set-up for [^{18}F]BFE synthesis 43
Figure 26: Reactants for [^{18}F]BFE synthesis: 2-Bromoethyl trifluoromethanesulfonate (BET) and $^{18}F^-$ 43
Figure 27: Schematic drawing of the set-up for [^{18}F]FE@IPCIT synthesis 44
Figure 28: [^{18}F]FE@IPCIT forms in a single step by reacting the precursor IPCITacid with [^{18}F]BFE 44
Figure 29: Laboratory protocol of a manual [^{18}F]FE@IPCIT synthesis 45
Figure 30: Schematic drawing of the synthesis module 46
Figure 31: Protocol of a module assisted [^{18}F]FE@IPCIT synthesis 48
Figure 32: Schematic synthesis route for BET 49

Figure 33: Chromatogram from fluoride-18 and [^{18}F]BFE (experiment M.16)..... 81
Figure 34: Chromatogram of IPCITacid (UV-detection); first peak is caused by the solvent of IPCITacid (DMSO) 82
Figure 35: Chromatogram of FE@IPCIT (UV-detection); first peak is caused by the solvent of FE@IPCIT (DMSO) 82
Figure 36: Chromatogram of FE@IPCIT by semi-preparative HPLC (colored area), IPCITacid elutes in the second peak 83

1 Introduction

Medicine has always strived for innovation, modernization and improvement. The treatment of neurodegenerative diseases such as Alzheimer´s or Parkinson's disease is still ineffective. Nuclear medicine can make a valuable contribution to improve the current situation by using radioactive substances for diagnosis and treatment. Nuclear chemistry can provide suitable compounds. By definition, nuclear chemistry is the branch of chemistry concerned with radioactive substances. Especially the subfield of medical nuclear chemistry focusses on the development and the production of radiopharmaceuticals, with radiopharmaceutical being defined as any drug containing a radioactive isotope. General nuclear chemistry covers many areas such as inorganic, organic, physical, and analytical chemistry.

The objective of the present work was the synthesis of a new compound FE@IPCIT (or [^{18}F]FE@IPCIT when labeled with radioactive fluorine-18). The reason for the molecule design is the combination of structural advantages from two clinically applied substances, β-CIT and PE2I. FE@IPCIT showed promising results in preliminary preclinical examinations.

1.1 Radioactivity

The word "radioactivity" evokes mostly negative associations in general public. In nuclear medicine however, radioactivity is an important tool. Hazardous effects caused by radioactive irradiation must be weighed carefully against its benefits in terms of detectability in minuscule amounts. In any case, radioactive substances must be handled with great care to avoid the contamination of persons and equipment.

1.1.1 Radioactive Decay

Radioactive decay is a process of unstable elements reaching stability by emitting one or more corpuscules particles. The process occurs randomly and unprompted and cannot be slowed down or speeded up. Decaying atomic nuclei are called parent radionuclides while newly-formed products are known as daughter nuclides. In some cases, daughter nuclides are different chemical elements (nuclear transmutation), while in other cases they are isotopes of the same element. Already in 1913, two scientists, Soddy and Fajans, developed a rule governing the transmutation of elements during radioactive decay [2]. Radioactive decay is always related to a change in the number of neutrons and protons. For a huge number of atoms, the laws of statistic prevail.

$$N_t = N_0 \cdot e^{-\lambda t}$$

N_0 represents size of a population of radioactive atoms in the original sample (t = 0), N_t the number of radioactive atoms after the time t, and λ is known as decay constant, a proportionality factor between the number of radioactive atoms and the decay rate. The radioactive decay follows an exponential law, as outlined in Soddy and Fajans rule [2-6].

1.1.2 Activity

Activity is measured in Becquerels (Bq) and defined as the rate of decay:

$$A = -\frac{dN}{dt}$$

One Bq corresponds to one decay per second. Becquerel is most often a too small unit to specify the activities handled in laboratories and industry. Therefore, MBq (10^6) or GBq (10^9) are frequently used. High activities indicate a fast decrease of radioactivity and high irradiation at the beginning (t = 0).

1.1.3 Half-life

The half-life of a radioactive isotope is the time required for one-half of the original quantity to decay. How long the individual half-life of the different atoms is depends on the type of nucleus. Half-life may range from a tiny fragment of a second ($3.03 \cdot 10^{-7}$ s for ^{212}Po [7]) up to trillions of years ($7 \cdot 10^{24}$ years for ^{128}Te [8]). No information about the life time of a single atomic nucleus can be obtained, because half-life is a statistical measure only applicable on huge numbers. The symbol for half-life is $T_{½}$.

$$T_{\frac{1}{2}} = \frac{\ln(2)}{\lambda} = \frac{0.693}{\lambda}$$

A long half-life stands for an almost stable isotope, while short half-life indicates a fast decay and a large λ-value.

1.1.4 Decay Modes

1.1.4.1 Alpha (α) Radiation

Alpha (α) radiation is a corpuscular radiation. Alpha-particles consist of two protons and two neutrons and they are doubly positively charged. It is known that helium-4 has an identical atomic nucleus. No other particles that are emitted by radioactive decay are nearly as massive as α-particles. This mode of decay is most common for heavy isotopes such as ^{224}Ra or ^{232}Th.

Since α-particles possess a limited range, a purely α-particles emitting source is not dangerous as long as enough distance is kept. All emitted α-particles from one type of isotope exhibit the same

amount of kinetic energy. Furthermore, they only have low penetration power and can be shielded easily e.g. by human skin. However, when incorporated into the body, they have the most destructive power of all particles emitted by radioactive decay because of their high ionization potential. Therefore, alpha particles are classified as high linear energy transfer (LET, energy transferred per unit length track [9]) radiation [10].

The hazardous effect of alpha radiation on organic tissue excludes its use in diagnostic nuclear medicine [11, 12]. Nonetheless, more recent developments in nuclear chemistry have led to an increased interest in alpha-particle emitting radionuclides for therapeutic purposes [13, 14].

1.1.4.2 Beta (β) Radiation

Beta (β) radiation appears when unstable nuclei emit electrons (e^-) or positrons (e^+). Charged particles have an ionizing effect and they are also known as beta rays. Their designation is done with the Greek letter β (beta) and a superscripted sign (+ or -) indicating the corresponding charge of the particle. Both kinds of β-radiation exhibit the mass of an electron ($9.1 \cdot 10^{-31}$ kg) and share a related mechanism of formation.

Beta-particles have a higher penetration power then α-particles. The ionization power of β-particles is intermediate and they are always single charged. Kinetic energies of emitted β-particles are not constant even though the total released energy is identical for each radioactive decay. This fact is caused by co-emitted particles. They were identified as neutrinos and contain the missing kinetic energy.

1.1.4.2.1 β^- Decay (Electron Emission)

In an atomic nucleus, a neutron is converted into a proton. Therefore, this mode of decay is typical for neutron-rich isotopes (^{40}K, ^{248}Bk).

In nuclear medicine β^--radiation is used for therapeutic purposes.

1.1.4.2.2 β^+ Decay (Positron Emission)

Positron emission (PE) is a typical decay mode for nuclei with an excess of protons. An unstable core emits a positively charged particle to reach stability by changing its proton-neutron-ratio. After PE the atomic number decreases by one.

β^+-particles consist of antimatter. Antimatter and normal matter cannot coexist. If a subatomic particle collides with its corresponding antiparticle, both are extinguished. This phenomenon is known as annihilation. The mass of both particles is turned into energy. The energy right before the blast is conserved in the combined matter-antimatter particle (gluon) and amounts to 1.022 MeV. Right after its formation, the gluon undergoes annihilation and two gamma blasts with the discrete

energy signature of 511 keV are released. The photons are accelerated in exact opposite directions (180°) [15].

PET (1.2.2.4.1 Positron Emissions Tomography) is based on this process. Hence, PE radionuclides are of great importance for nuclear medicine.

1.1.4.3 Electron Capture

Electron capture (EC) is a phenomenon that exists only for unstable proton-rich nuclei. An inner-shell electron (K-shell) is incorporated by a proton and a cavity is left behind. The proton is transformed into a neutron and a neutrino is released. Alongside electromagnetic radiation from two sources is emitted. The first source is the newly-formed excited daughter nucleus. The second source is the cavity in the inner shell. When it is filled up with an outer orbit electron, energy is released as gamma radiation. Also, auger electrons may arise in this process. These monoenergetic electrons are produced when energy is directly transferred to an outer sphere electron. As a result, the electron is ejected by the atom. In round terms the process could be described as an internal photoelectric effect.

EC and PE are competing decay modes. EC is the primary mode of decay for nuclei with a relative superabundance of protons but lacking of the energy to decay via PE [16].

1.1.4.4 Gamma (γ) Radiation

Gamma (γ) radiation is fundamentally different from α- and β-radiation. Gamma radiation has the same nature as light but the photon energy is much higher. Gamma radiation is co-emitted with other radioactive decay event. The mechanism behind this is that daughter nuclei are usually in an excited state after formation. Gamma rays emerge during the relaxation process, normally happening immediately after transmutation (10^{-12} s). Gamma radiation may also occur in combination with other nuclear reactions such as nuclear fission, positron emission or electron capture.

On the one hand, gamma rays have a high penetration power and thick slabs of concrete or lead shieldings are required to block them. On the other hand, they have only low ionization power since they pass through tissue almost without interaction.

Gamma rays are frequently used in nuclear medicine. Methods like PET or SPECT (1.2.2.4.2 Single-photon Emission Computed Tomography) are based on gamma rays. Also, roentgen radiation is closely related to gamma irradiation only with less energetic photons.

1.1.5 Nuclides

A nuclide is an atom with a specific atomic- and mass number. The designation *nuclide* is used to describe atoms of different elements, whereas the designation *isotope* is used to describe different types of atoms of the same element [17]. Nowadays, more than 3000 nuclides are known whereof approximately 270 are stable, the remaining are radioactive [18].

1.1.5.1 Non-metallic Radioisotopes

In this section the focus is on the most import non-metallic nuclides for PET. Together, they account for the majority of PET radiopharmaceuticals in diagnosis, treatment, and research [19].

1.1.5.1.1 Carbon-11

The chart of nuclei lists 15 nuclides for carbon [20]. All but two (^{12}C, ^{13}C) are unstable. The only radioactive nuclide that exists as such in nature is carbon-14 with a half-life of 5730 years [21]. It decays by β^--emission to ^{14}N. If a closer look is taken on artificial nuclides of carbon, only ^{11}C ($T_{½}$=20.4 min) has a suitable half-life and the right decay mode for PET [22].

Carbon is part of almost every natural or synthetic drug. This characteristic makes ^{11}C an important positron emitting isotope for labeling biomedically relevant molecules without altering their physiological or chemical behavior. The short half-life limits the number of steps in syntheses. The most common way to produce ^{11}C in a cyclotron is by proton bombardment of a ^{14}N filled target. A nitrogen-14 nucleus, which absorbs a proton ($^{14}N(p,\alpha)^{11}C$), decays by emitting an alpha particle to ^{11}C. Cyclotrons usually deliver ^{11}C in two chemicals forms: $[^{11}C]CO_2$ and $[^{11}C]CH_4$ [23]. Production can be controlled by adding traces of oxygen (yields CO_2) or hydrogen (yields CH_4) to the target gas.

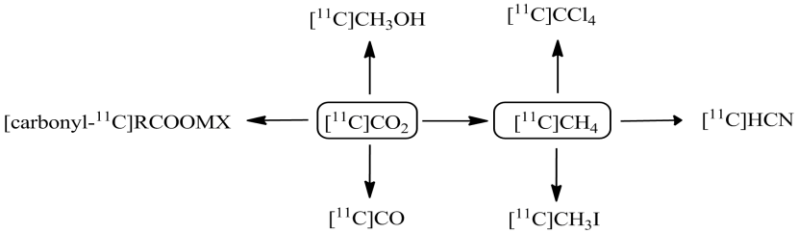

Figure 1: Most important ^{11}C-precursors and direct derivatives

1.1.5.1.2 Fluorine-18

Fluorine has nine protons. It is the most electronegative element in the periodic table. Today there are 16 known isotopes but only one is stable (^{19}F). Only two isotopes have a half-life of more than one minute [20]. ^{18}F has a half-life of 110 minutes and is the radionuclide, which is most widely used for PET imaging [24]. The following reasons for the dominance of this nuclide can be found: 1) the half-life (sufficient time to perform multistep syntheses but short enough not to harm the patient), 2) the decay of ^{18}F is almost exclusively via positron emission (97 %), and 3) the short positron linear

range in tissue (2.39 mm in water) because of the relatively low energy of the emitted positron (maximum 0,635 MeV) [25]. The short range allows the production of the highest resolved PET images of all the available positron emitters [23]. But there are also two negative aspects when dealing with ^{18}F: 1) the low natural abundance of fluorine in biological structures and 2) the unknown physiological effects when labeling a compound with "unnatural" fluorine [26]. Compared to other PET nuclides, the radioisotope is easily available from both cyclotron and nuclear reactors. The focus here is on the preparation using particle accelerators, and therefore the following nuclear reactions can be formulated:

	Reaction	Target
1	^{19}F (γ,n) ^{18}F	Teflon
2	^{23}Na (γ,αn) ^{18}F	NaOH or $NaSO_4$
3	^{18}O (p,n) ^{18}F	$H_2{}^{18}O$
4	^{18}O (p,n) ^{18}F-^{19}F	$^{18}O_2$
5	^{20}Ne (d,α) ^{18}F	0.1 % F_2 in Ne
6	^{16}O (^{3}He,n) ^{18}F	H_2O
7	^{16}O (α,d) ^{18}F	H_2O
8	^{16}O (t,n) ^{18}F	Li_2CO_3
9	^{23}Na (p,αx) ^{18}F	Na

Table 1: Production of fluorine-18 and fluoride-18 via particle accelerators [25]

The most common and effective way to produce ^{18}F uses the reaction #3 (Table 1), ^{18}O (p,n) ^{18}F. The yield is 216 mCi/µA for 14 MeV protons. Compared to the reaction #5, the yield is twice as high, whereas the deuteron energy is similar [25]. However, there are also drawbacks when $^{18}F^-$ is produced using this method: The enrichment of [^{18}O]water is a costly process, and an additional drying step is required when water-free radionuclides are mandatory.

Fluorine itself (line 4), consisting of one radioactive ^{18}F and one stable isotope ^{19}F, is not so common in nuclear chemistry because ^{18}F-^{19}F is corrosive and on account of that, the handling is more complicated and the equipment is more expensive. Instead many techniques were developed to use $^{18}F^-$ nuclide as radioactive source for labeling molecules instead of dealing with the highly reactive ^{18}F-^{19}F.

1.1.5.1.3 Nitrogen-13

Nitrogen is the 7th element in the periodic table. Nowadays, there are 15 known isotopes. Amongst these only two, ^{14}N and ^{15}N, are stable. All the remaining isotopes are radioactive and except one too short-lived to be of medical relevance. ^{13}N has a half-life of 9.97 minutes [27]. The nuclear reaction for the formation of the nuclide in cyclotrons is $^{16}O(p,\alpha)^{13}N$ [28]. Such a short half-life does not allow complex syntheses. [^{13}N]ammonia is the most commonly used modification for PET studies [22]. The

radiopharmaceutical is applied as an intravenous injection and it is mainly used for diagnostic cardiac imaging in association with coronary artery diseases or after myocardial infraction to measure the remaining perfusion of the heart [28, 29].

1.1.5.1.4 Oxygen-15

Oxygen has 15 isotopes whereof only three are stable (^{16}O, ^{17}O, ^{18}O). Two of the radioactive isotopes have a half-life in the range of 1-2 minutes. ^{15}O decays by β^+-emission after a half-life of exactly 122.24 seconds and it is used in nuclear medicine. The $^{14}N(d,n)^{15}O$ reaction is the most widely used process of formation [30] whereas the $^{16}O(p,pn)^{15}O$ reaction can be used only when specific activity (1.4.4 Specific Activity) is not important [31]. Its half-life is too short to use the nuclide for complex chemical synthesis. Possible forms of application are the inhalation of $C^{15}O$, $C^{15}O_2$, or $^{15}O_2$. These three gases are used to perform the so called oxygen-15 steady-state model [32]. [^{15}O]Water and [^{15}O]butanol are also possible modifications for application in perfusions studies [30].

1.1.5.2 Metallic Radioisotopes

Some metallic nuclides for PET can be provided by generators. This characteristic is of advantage for facilities without particle accelerators or nuclear reactors. Chemical reactions to introduce metallic PET nuclides into molecules are different from those for non-metallic nuclides, and the products are often metal complexes using radionuclides as central ions.

1.1.5.2.1 Gallium-68

There are 34 known isotopes of gallium [20]. However, only three of them are of medical interest. Two of these isotopes, ^{66}Ga ($t_{½}$ = 9,45 h) and ^{68}Ga ($t_{½}$ = 67.6 min), decay by β^+-emission (89 %) while ^{67}Ga ($t_{½}$ = 78 h) decays by γ-emission [19]. Gallium is a rare element with no known biological function. So, every application of a gallium containing radiopharmaceutical introduces a compound into an organisms that would not be there naturally [33].

The isotope ^{68}Ga has become one of the most used metallic PET nuclides for diagnosis. One of the reasons for this is the considerably long half-life of the parent nuclide ^{68}Ge ($t_{½}$ = 279.8 d). It allows the construction of generators (1.2.1.3 Generator) that last for a long period (up to one year). The half-life (68 min) of ^{68}Ga matches the pharmacokinetics of many peptides and other small molecules [34] and the generators can be eluted every six hours (high availability of ^{68}Ga).

These characteristics make it an ideally suited on-demand available radionuclide for biomedical experiments and clinical applications. A generator can deliver gallium in different chemical forms depending on the applied technique for elution. Most common forms are [^{68}Ga]EDTA and [^{68}]$GaCl_3$ in HCl. ^{68}Ga is applied in the assessment of blood-brain barrier (BBB) integrity as well as in tumor localization [35].

1.1.5.2.2 Technetium-99m and Technetium-94m

In the periodic table technetium is located in the second row in group-VII of transition metals. It can take many different oxidation states and adopts to scores of different coordination geometries. Technetium does not exist in nature because the half-life for the most stabile isotope ^{97}Tc lasts only $2.6 \cdot 10^6$ years. It was the first artificially produced element (in 1937) [36]. ^{99m}Tc is the most used metallic isotope for nuclear medicine today because of two reasons: 1) ^{99m}Tc is available from generators and 2) it has a suitable half-life of 6.01 hours (^{99m}Tc -- 6 h --> ^{99}Tc, Eγ = 140.5 keV, Iγ = 87.2 %). Because of its pure gamma radiation, ^{99m}Tc is perfect for SPECT diagnosis.

More recently, ^{94m}Tc (t½ = 52.5 min, $E_{\beta+max}$ of 2.44 MeV) has been examined in greater detail. It can be produced in biomedical particle accelerators (^{94}Mo(p,n)^{94m}Tc) and decays by β^+-emission (72 % positron branching ratio) [19, 37]. The chemistry of technetium is well understood and methods developed for ^{99m}Tc can be adopted for ^{94m}Tc as well. The use of ^{94m}Tc would be an improvement in diagnostic imaging because the resolution of PET is superior compared to SPECT [38].

1.2 Instrumentation in Nuclear Chemistry and Nuclear Medicine

1.2.1 Production of Radioactive Isotopes

1.2.1.1 Cyclotron

A cyclotron is a cyclical particle accelerator for the production of radioactive isotopes. In contrast to linear accelerators, the negatively charged particles are kept on a spiral trajectory during acceleration by strong magnetic fields. The acceleration is caused by an oscillating radio field (RF). Beside nuclear reactors, cyclotrons are a main tool for production of radionuclides. Especially the production of positron emitting nuclides for PET is an advantage of cyclotrons [18].

Every cyclotron consists of three major components: an electromagnet to generate a magnetic field (1.5 - 2.0 tesla), two hollow copper electrodes, right in between the pole pieces of the electromagnet known as “Dees” (D_1 and D_2) because of their semicircular shape, and an ion source in the center. The whole system is kept under a high vacuum (approx. 10^{-7} torr). Between the two Dees, there is a narrow gap where the particles are accelerated. The orientation of the magnetic field is perpendicular to the plane of the Dees. The injected ions have a low kinetic energy. By the time the negatively charged ions are released into the central chamber, one of the Dees is charged positively and the particles are accelerated towards it. The applied magnetic field forces the particles along a semicircular path. Just when the particles arrive at the gap between the Dees, the potential of the Dee is reversed and the particles are accelerated once more. They are faster when they enter the

second Dee. The particles describe a circular trajectory of greater radius since the magnetic field still has the same strength. After several iterations, the particles acquire their maximum kinetic energy. During the extraction process, the particles are passed through a stripping foil (ultrathin graphite), which removes (strips) electrons from the particles. Finally, a particle beam consisting of positively charged ions is directed on the target molecules to enchain nuclear reactions [15, 39, 40].

1.2.1.2 Nuclear Reactor

A nuclear reactor sustains a controlled nuclear fission. If heavy nuclei (such as uranium-235) absorb neutrons, they reach an unstable state that frequently results in nuclear fission. The spallation process releases two lighter fission fragments, gamma radiation, kinetic energy (heat) and two or three free neutrons [41]. The free neutrons move with high kinetic energy. For further nuclear fission, they have to be slowed down by a moderator (e.g. heavy water or graphite) to become so called "thermal neutrons". If they now strike a fissionable nucleus it may undergoes fission and the process of fissions continues. A nuclear chain reaction is established. One method to keep the chain reaction under control is to ensure that each fissioning nucleus can only initiate one new nucleus to fission. This is realized by using neutron poisons and control rods to eliminate excess neutrons [42].

Neutrons, which are not needed to sustain the nuclear chain reaction, can serve as neutron source for other purposes. When stable isotopes (target) are placed in a reactor and are exposed to thermal neutrons, nuclear reactions may happen (n, γ). The result is the creation of unstable neutron-rich nuclei. Since these nuclei are still of the same element, separation is chemically impossible. For that reason, the products are of low specific activity. The dominating decay mode for the new cores is the emission of β^--particles.

The nuclear reaction with fast neutrons (n,p) results in different products. It leads to the creation of other elements, which are hence chemically separable from the target nuclei. If the element is used in its natural isotopic composition, the results are different unstable isotopes, which lead to different decay products (^{131}I production from $^{126\text{-}131}$Te isotopes). It is chemically impossible to separate different iodine isotopes from each other. The final product is the desired ^{131}I, which is however diluted with other iodine isotopes (no-carrier-added, n.c.a.). A way to drastically improve the specific activity is the use of monoisotopical or isotope-enriched target material. The gained radionuclide would be carrier-free (c.f.) and of high specific activity, but its production is very expensive.

1.2.1.3 Generator

A basic requirement for nuclide generators is that the maternal nuclide has a longer half-life than the daughter nuclide. The decay of the maternal nuclide continuously produces new daughter nuclides. The daughter nuclides are yielded by elution. Therefore it is essential that mother and the daughter

are different elements. Generators are known to provide radioactive nuclides of great purity and high specific activity [18, 40]. The isotopic purity of the eluted radionuclides (c.f. or at least n.c.a.) depends on the composition of the maternal matrix. The medically important isotope ^{99m}Tc is a generator nuclide. For the production of its maternal isotope ^{99}Mo nuclear reactors are required. The spallation of ^{235}U shows a higher abundance of fragments in the range of 85 - 105 units, among which ^{99}Mo (6 %) is found. The extraction of the nuclide is difficult but it can be obtained in high purity. The nuclear reaction is described with the following formula [43]:

$$^{235}\text{U} + \text{n} \text{ ---fission---> } ^{99}\text{Mo-} + \text{other fragments.}$$

1.2.2 Imaging Techniques

Molecular imaging is a more and more upcoming technology. Its aim is to provide detailed images of molecular events in living organisms. Clinical medicine uses different technologies such as ultrasound (US), computed tomography (CT), magnetic resonance imaging/tomography (MRI or MRT), and scintigraphy. Each method has its merits and drawbacks. However, only scintigraphic methods are able to provide the high specificity and sensitivity that is needed to visualize molecular events at tracer (*vide infra* 1.5 Tracer) levels. Tools for clinical scintigraphy are single-photon emission computed tomography (SPECT) and positron-emissions-tomography (PET). Both technologies depend on radiopharmaceuticals [44].

All the presented techniques can be used for non-invasive investigative imaging of living organisms.

1.2.2.1 X-ray

X-ray focuses high-energetic ionizing electromagnetic rays (X-rays) on the object to be viewed. The process of producing an image is based on the different absorption abilities of materials of various density and composition. Material of higher density (bones) absorbs X-rays more effectively than material of lower density (water-rich tissues). The images show parts of higher density in white shades, whereas the more transparent parts are pictured in blackish colors. The method is used to produce two-dimensional (planar) pictures of anatomic structures. The limitations are reached if the aim is to observe dynamic processes or if spatial resolution is required.

1.2.2.2 Computed Tomography

CT is a more advanced version of the X-ray method. The word “tomography” can be interpreted as “imaging of the body in multiple slices” [45]. The innovative idea was to rotate the X-ray source around the patient taking a large number of images. Computer software is used to calculate volumetric representations. A disadvantage of this method is to exposure the patient to high amounts of ionizing radiation [46, 47].

1.2.2.3 Magnetic Resonance Imaging

MRT uses a different physical effect than X-ray-based techniques to generate three-dimensional images of objects. The underlying phenomenon is known as nuclear magnetic resonance.

The method is based on the fact that nuclei with an odd number of protons or neutrons absorb and re-emit electromagnetic radiation when they are exposed to a strong and constant magnetic field B_0. The effect is based on the Larmor precession of the nuclear spin around the axis of the magnetic field. Under the influence of the magnetic field, the atomic nuclei can orientate themselves with or against the external force field (longitudinal relaxation). Orientation with the field is energetically favored. Therefore it is defined as ground state, whereas the opposite orientation (against the external field) is called excited state. The difference between the two states is very small at body temperature, but slightly more nuclei are in the ground state (Boltzmann factor). The really important difference for the measurement is only 0.00049 %. The irradiation of a high-frequency magnetic field (RF) allows excitation of atomic nuclei. A requirement for this is that the RF matches the Larmor frequency (resonance condition) [48].

MRT shows good results with soft (water-rich) tissues. Hence this method is well-suited for imaging of muscle, heart, tumor, or brain. The produced three-dimensional images are of good quality without exposing the patient to harmful X-ray irradiation as it would be the case with CT. The time for a full scan is an important differentiating factor between the two techniques: Computed tomography takes approximately five minutes, while a MRT scan runs approximately for 30 minutes. So, an indication for a CT scan could be an acute trauma or, more generally for any emergency situations when time is limited [49].

1.2.2.4 PET Positron Emissions Tomography and Single-photon Emission Computed Tomography

The principle used by PET and SPECT to gain information is different from the one applied for CT and MRI. The source of the signals for PET and SPECT is a radioactive nuclide inside the object. The examined object is surrounded by detection units, that record emitted radiation. A computer collects the amplified signal from the detector units and calculates a three-dimensional model corresponding to these signals. The information is normally presented as cross-sectional slices through the body. It is possible to freely manipulate or reformat the data set since it is a computer model.

The differences between PET and SPECT results from the use of different radionuclides and slightly altered recording technique.

1.2.2.4.1 Positron Emissions Tomography

PET scanners can provide quantitative and qualitative information about processes such as perfusion, distribution, or metabolism *in-vivo*. It is based on the decay of radionuclides by positron emission. The characteristics of this decay mode are involved in the detection process. The requirements for a valid signal are 1) two events must be detected simultaneously at two or more detectors, 2) both recorded photons must lie on one line (line of response, LOR) and 3) their energy signature must match exactly 511 keV. If an incident does not fulfill all three conditions, no signal is recorded [50]. This protocol leads to an decreased number of wrong positive signals and results in improved images [15].

PET scanners are not designed to resolve anatomic structures. There are other methods that are way better suited for this task. For this reason, modern PET scanners are hard-wired back to back to MRT scanners (earlier, CT scanners were combined for the same reason). The MRT scanner is used to generate a model of the morphology, while the PET scanner generates a molecular image by recording the tracer (*vide infra* 1.5 Tracer) signals. A computer program can link the tracer signals to anatomic structures and calculate a single image from both data sets [51, 52].

1.2.2.4.2 Single-photon Emission Computed Tomography

SPECT also requires a radioactive source incorporated by the patient. Accordingly, the first action is the application of a radiopharmaceutical. The tracers are distributed in the body by blood flow and diffusion. Finally, they bind to receptors or certain structures. The radionuclides linked to the ligands release gamma radiation during their radioactive decay. This radiation is recorded by a rotating gamma camera. The signal is sent to a computer unit as an electrical pulse together with the exact position of the event. SPECT can provide spatial resolution by combining a lot of individual 2-D pictures in a row [45]. The efficiency is 10-20 times lower than for PET scanner [15].

1.2.3 Synthesis Modules

Manual methods of synthesizing radiopharmaceutical reach their limits if high activities are involved, more complex reactions are performed, and high throughput is necessary. However, there are several reasons for automation. In particular short-lived PET nuclides such as carbon-11, nitrogen-13, oxygen-15, and fluorine-18 are problematic because they emit high radiation in a short time. The gamma radiation originating from annihilation requires solid lead as protective barrier.

The principle how synthesis modules work is to reduce complex operations to many single steps and execute them one after another. Typical basic processes are hydrolysis, evaporation, chromatographic procedures, purification, and sterile filtration. All these operations are controlled by a computer program. It allows the supervisor to observe the on-going processes and set actions if required. A detailed report including date, time and estimated yield is shown when the synthesis is

finished. The protocols are important sources for identifying errors since pharmaceuticals have zero error tolerance.

The dominating systems are fully-automated –and half-automated modules [18, 40, 53].

1.2.3.1 Automated Synthesis Modules

The application area for automated synthesis modules (ASM) is routine work and commercial production. Automation has played an important role in reducing radiation exposure of staff and also in granting a constant high quality of the produced pharmaceuticals. Especially for [^{18}F]FDG, ready-for-use cassettes (cartridges) are commercially available, allowing production under good manufacturing practice (GMP) conditions. It is a future goal to offer such cassettes for other frequently used tracers (*vide infra* 1.5 Tracer) as well. The cassettes consist of tubes, templates and prefilled vials with all required chemicals. After the installation of the cartridge in the ASM, only the radioactivity, provided by a cyclotron, has to be added and the automatized production of a radiopharmaceutical can be started. The final product is delivered ready for use. For each synthesis is a new cassette required, which raises the production costs [19, 54].

1.2.3.2 Manually Operated Synthesis Modules

The application area for user operated synthesis modules (USM) is mostly in research facilities. USMs are structured as flexible toolkits. One advantage is the variable and individual combination of different modules, allowing easy adaptation of the system to the requirements of new syntheses.

1.2.4 High performance liquid chromatography

1.2.4.1 Basic Principles

Separation in liquid chromatography (LC) is based on the different retention times of various analyte molecules in between a stationary phase (adsorbent, small particles) and a mobile phase (eluent). The stationary phase is packed into columns manufactured of steel, plastic or glass. Frequently used packing materials are silica gel, alumina celite or glass beats coated with a porous material (pellicular particles). The use of plastic material is critical because of the high applied pressures.

Some frequently used characteristics for the separation of a sample are size (SEC, size exclusion chromatography), shape (GF, gel filtration), hydrophobic properties (HIC, hydrophobic interaction chromatography; RPC, reversed phase chromatography), net charge and charged groups (pH depending, IEC, ion exchange chromatography), isoelectric point (CF, chromatofocusing), and metal binding (IMAC, immobilized metal ion affinity chromatography e.g. His-tagging).

Affinity chromatography (AC) is a powerful separation method based on highly specific interactions between suitable ligands and the interested analyte. High costs are a drawback of this method.

A second factor, that has an enormous effect on the separation efficiency, is the mobile phase. Depending on the analyte, a premixed mobile phase with an exact ratio of the deployed solvents may be the best choice (isocratic), or it could be obliged to drive a gradient elution. Certain properties such as charge and solvation shell can be influenced by the solvent composition (pH value, ionic strength, organic or aqueous solvents). Further parameters are possible by adding various additives (detergents, metals, reducing agents) to the solvent.

Other adjustable parameters are temperature and flow rate. Furthermore, in some cases it may be advantageous to combine two columns in a row to achieve an optimal separation (pre- or post-columns). Normally separations are carried out at room temperature (RT), but in some cases it may be beneficial to heat or cool down the AC. During a separation process external conditions should be constant, because small changes in the overall setup can significantly alter the outcome [55, 56].

1.2.4.2 Instrumentation

High performance liquid chromatography (HPLC) systems consist of some basic components. The mobile phase is stored in reservoirs. They are placed in front of a degassing system. It is important to remove dissolved gases from the solvents to avoid gas bubbles in the column. The techniques used for this task are vacuum pumps or in more modern systems ultrasonic devices. The simplest setup is to use a single reservoir (isocratic). Depending on the composition of the analyte it may be necessary to use more than one solvent to carry out the separation. For this purpose, some HPLCs have a mixing chamber installed, which allows altering the composition of the solvent during the separation (gradient elution).

HPLC pumps have output pressures from 2 – 20 MPa and maximal flow rates up to 20 mL/min. If a reciprocating pump is used then a damper unit is required for laminar flow. The solvent is conducted through a pre-filter to the injection valve. The construction of the valve allows injecting the sample without a reducing pressure in the column (laminar flow). A pre-column (PC) can be installed to protect the analytical column (AC) from contaminations originating from impurities in the solvent. The length of AC can vary from 8 cm up to 1.5 meters with an inner diameter of 2 - 4 mm.

A very important part of an HPLC system is the detector unit. Most detection techniques are based on ultraviolet light (UV), infrared light absorption (IR), fluorescence, conductance, polarography, and radioactive measurement. IR, UV and fluorometric detectors are temperature sensible. Detection of radioactivity is the most sensitive method but it requires radioactive nuclides in the sample [57, 58].

1.2.4.3 Analytical HPLC vs. Semi-preparative HPLC

A definition to explain the field of operation for preparative HPLC (pHPLC) and analytical HPLC (aHPLC) could be phrased like this: The purpose of pHPLC is the purification of samples while aHPLC is used for the identification of compounds. pHPLC is an expensive separation technique compared to traditional methods such as distillation, extraction or crystallization. Normally, it is only used for the purification and isolation of valuable products. In general this modification uses bigger columns and higher flow rates than aHPLC. The separation efficiency is worse than for aHPLC but it allows much bigger sample volumes. The working area ranges from µg up to kilograms of compound (industrial scale), while aHPLC samples lie in the range of µg or less and the sample volumes are much smaller than the column volume (< 1:100) [59, 60].

1.3 Synaptic Transduction

Communication is a fundamental process in living organisms. Nerves are the wires that transmit information. A nerve cell consists of three fundamental parts: axon, cell body and dendrites (figure 2). Along the axon, the propagation of a signal is done by an electric current. The transmission of the signal from one axon terminal to another cell is a chemical process. The complex process of transmitting a signal can be reduced to three components: 1) a neurotransmitter that bridges the synaptic cleft (20 nm) between the neurons by diffusion, 2) a receiver (receptor), which re-converts the chemical signal into an electrical signal and, 3) a tool (reuptake transporter) to stop the signal by cleaning the synaptic cleft from NTs [61].

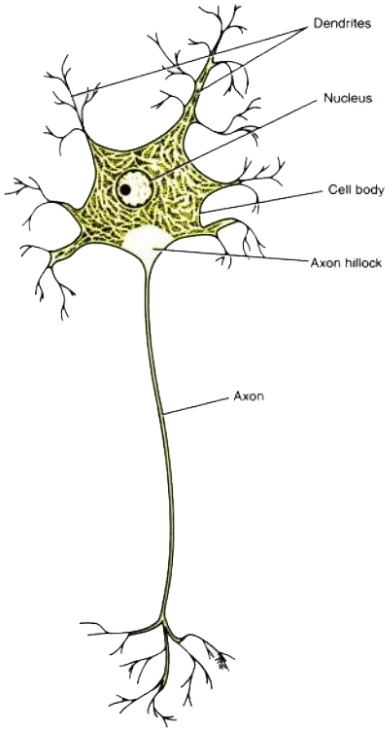

Figure 2: Basic components of a neuron [1]

When an action potential arrives at the synaptic cleft (from the presynaptic neuron), voltage-gates calcium channels are opened by membrane depolarization. The influx of Ca^{2+} ions initiates exocytosis within the cell, a process of transferring substances from the intracellular space (cytoplasm) into the extracellular matrix. Therefore, the NTs are encapsulated inside the cell with plasma membrane (vesicle) [62]. The content of the vesicles is released into the synaptic cleft and the NTs diffuse to the postsynaptic neuron and trigger a new action potential by binding to receptors. The NTs must be removed from the synaptic cleft immediately after the successful transmission of the signal [63] by different mechanisms (1.3.4 Mechanisms of Reuptake and Decomposition of Neurotransmitters). The whole

transduction process lasts approximately 0.5 milliseconds [64]. Many drugs compromise this well-balanced system and cause psychedelic effects.

1.3.1 Neurotransmitter

1.3.1.1 Definition of a Neurotransmitter

The *Oxford English Dictionary* (2nd edition) defines a neurotransmitter (NT) as…

"…a substance which is released at the end of a nerve fibre by the arrival of a nerve impulse and, by diffusing across the synapse or junction, effects the transfer of the impulse to another nerve fibre, a muscle fibre, or some other receptor. [65]"

1.3.1.2 Characteristics

Based on the definition a substance must possess particular features to be a NT: the substance must be released at the presynaptic end of a nerve fibre, and the enzymes for the production of the substance are located in the nerve cell. The release of the substance is triggered by depolarization, and the postsynaptic cell has specialized receptors for this substance. An action potential can also be initiated by artificial application of a suitable substance (NT, drug). However, inhibiting the release of further neurotransmitters or blocking of receptors leads to the opposite effect: No nerve pulses are forwarded [66].

There are hundreds of potential substances in the nerve system, which meet at least some of these conditions. The term "*putative neurotransmitters*" includes all potential NTs [67]. Nowadays, there are 200 substances known to function as neurotransmitters [68].

1.3.1.3 Classification System

There are several classification systems. A simple one divides the NT into the two groups "fast NTs" and "slow NTs" according to their mechanism of activation. The fast NTs (glutamate or GABA) bind to receptors, which directly open ion channels, while the slow NTs (catecholamines e.g. dopamine or epinephrine) bind to G protein-coupled receptors and trigger the release of second messengers inside the cell, which activate ion channels [66]. Another classification distinguishes between "small-molecule NTs" and neuropeptides. Table 2 shows the major classes of NTs according to the latter classification system [69].

Major Classes of Neurotransmitters	
Small-molecules NTs	**Neuropeptides**
Acetylcholine	Opioid peptides
Excitatory amino acids	Endomorphins
Aspartate	beta-Endorphin
Glutamate	Nociceptin
Inhibitory amino acids	Leucine-enkephalin
GABA	Substance P
Glycine	
Biogenic amines (monoamines)	
Catecholamines	
Dopamine	
Norepinephrine	
Epinephrine	
Indoleamine	
Serotonin (5-HT)	
Imidazole amine	
Histamine	
Purines	
Adenosine	
ATP	

Table 2: Major classes of neurotransmitters

1.3.2 Neurotransmitter Substances (Selection)

1.3.2.1 Catecholamines

Some of the most important NTs are catecholamines. Members of this group are simple biogenic amines such as epinephrine, norepinephrine, and dopamine. They all share a common basic structure and are derived from the amino acid tyrosine [70].

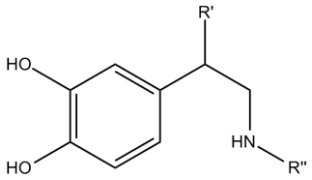

Figure 3: general structure of catecholamines

	R’	R’’
dopamine	H	H
norepinephrine	OH	H
epinephrine	OH	$-CH_3$

Table 3: Different functional groups of catecholamines

1.3.2.1.1 Dopamine

Dopamine (DA) plays a central role in many physiological processes. One field of action for DA is the area of emotional states. An increased level of DA is stimulating, while a decrease in dopamine has the opposite effect. Diminished dopamine levels are linked to major depression, Alzheimer’s and Parkinson’s disease [71, 72]. DA also plays an import role in the coordination of movements.

Characteristic symptoms, shown by people suffering from Parkinson's disease, are motoric abnormalities such as resting tremor, bradykinesia, or even akinesia [73]. The dopamine-generating cells of the midbrain (substantia nigra) are diminished in the beginning and completely destroyed when the disease progresses [74]. A possible treatment is the application of L-DOPA. This precursor of dopamine can penetrate the BBB [75], while the direct application/injection of dopamine into the blood stream would not show any effects on the dopamine levels in the brain, since DA itself cannot cross the BBB [76].

1.3.2.1.2 Epinephrine and Norepinephrine

Epinephrine (EPN) and Norepinephrine (NE) are also known as adrenaline and noradrenaline. The molecules have various functions in the body. They can act as hormones or as neurotransmitters. The fight-or-flight response is a commonly known effect triggered by the release of these two substances [77]. They are secreted under all kinds of stress [78]. Not all effects of these substances are excitatory; also inhibitory processes are associated with them. Two different types of adrenergic receptors are responsible for the contrary effects [79].

1.3.2.1.3 Serotonin

Serotonin (5-Hydroxytryptamin, 5-HT) is an inhibitory biogenic amine and most abundant in the upper brain stem. The precursor for the biosynthesis of serotonin is tryptophan. Serotonin plays a role in the regulation of hunger, sensory perception, pain (directly via nociceptors), body temperature and sleep. The treatment of depression often involves selective serotonin re-uptake inhibitors (SSRIs) [80].

1.3.3 Neurotransmitter Receptors

The receptors are also known as neuroceptors. They are membrane proteins and the majority is located in postsynaptic membranes. Neuroceptors are activated directly by NTs, which are released from the presynaptic neurons. It has been discovered that a NT can activate many different receptors whereupon one type of receptor never binds various NTs [66]. Receptor subtypes bind to the same NTs, but showing different effects and having slightly altered amino acid sequences. Furthermore, some postsynaptic neurons express more than one receptor subtype.

The binding of a NT can result in the direct opening of an ion channel (ligand gated ion channel), or initiate a G protein-coupled receptor (GPCRs) cascade. GPCRs are transmembrane proteins with a poly peptide chain crossing the lipid bilayer seven times. A structural change is initiated when a ligand binds on the outside of the receptor, which leads to the release of a G protein in the cell [81]. Ionotropic receptors have a significantly shorter time of response than metabotropic receptors [67]. The different response times are used to trigger time shifted events: A first rapid response (ion channel gated) and a second slower onset of action (G protein-coupled).

There are also receptors in the presynaptic nerve terminal that act as autoreceptors, controlling the concentration of NT in the synaptic cleft: If a preset level of NT is reached, the receptors stop any further release of NT from the presynaptic neuron (negative feedback loop) [82].

1.3.3.1 Dopamine Receptors

Dopamine receptors are divided in the subtypes D_1 - D_5 [83]. They can be found in discrete brain regions (forebrain circuit [67]) as well as in peripheral regions. Dopamine receptors are involved in many neuronal processes including learning, pleasure, motivation, cognition, fine motor skills, and the endocrine system [84].

1.3.3.2 Epinephrine and Norepinephrine Receptors

The receptors are GPCRs with the subtypes α_1-, α_2-, and β-adrenergic receptors. The subtypes trigger contrary effects [85]. α-adrenergic receptors are associated with various excitatory (peripheral vasoconstriction) and one inhibitory effect (relaxation of intestinal), whereas β-adrenergic receptors are mainly associated with inhibitory effects (vasodilation and bronchialdilation), except for one excitatory function (stimulation of myocardium) [79].

1.3.3.3 Serotonin Receptors

Receptors for serotonin are also known as 5-hydroxytryptamine receptors (5-HT receptors). This group includes GPCRs and ligand-gated ion channels (LGICs) [86]. At present, there are seven confirmed receptors (5-HT_1 - 5-HT_7) and many subtypes [87]. The highest density is found in raphe nuclei and the hippocampus. The serotonin agonist lysergic acid diethylamide (LSD) directly stimulates this receptor [88].

1.3.4 Mechanisms of Reuptake and Decomposition of Neurotransmitters

So far, several mechanisms for the removal of the NTs from the synaptic cleft have been discovered. An effective and most frequently used technique is a recycling process: The NTs are taken back up into the presynaptic neuron by specialized transporter sites. Moreover, decomposition with enzymes (e.g. mono-amine oxidase, MAO) is another way to eliminate NTs [83]. These enzymes are frequently point of action for drugs and pharmaceuticals [89]. Simple diffusion of the NTs is also involved in the removal process.

1.3.4.1 Neurotransmitter Transporter Sites

The purpose of transporter sites is to terminate the signal transduction after a successful transmission by executing a re-uptake of the NTs from the synaptic cleft back into the presynaptic neuron. Due to their high substrate specificity, transporters are an interesting target for drug

development. The aim is to develop substances, which selectively attack one transporter type in order to avoid side effects [83].

NTs are transported through the membrane together with Na^+ -and Cl^--ions (cotransport). The main energy source is the Na^+ gradient generated by Na^+/K^+ ATPase (secondary transport). The stoichiometry of the transport can be written as a ratio of the involved species: 1 Cl^- : 2 Na^+ : 1 NT. The combined use of two ionic gradients allows concentrating NTs 10.000-fold higher inside the neuron than outside in the extracellular space [90].

Since the transporters are substrate specific, each NT requires its own reuptake transporter. The most common transporters are DAT (dopamine), NET (norepinephrine), and SERT (serotonin). There are also isoforms of the transporters [91]. Based on the recent development in the field of neuro-imaging it was possible to localize the transporter binding sites in specific regions of the brain. Also, the quantification of dopamine transporters *in-vivo* is now feasible [92].

1.3.4.1.1 Dopamine Transporters

Dopamine transporters consist of 619 amino acids [93] and they are located in the presynaptic membrane of neurons. The highest observed transporter densities can be observed in the putamen (forebrain, telencephalon), the caudate nucleus (basal ganglia), and the nucleus accumbens (ventral striatum), whereas decreased densities are found in the nucleus amygdalæ (medial temporal lobes), the substantia nigra (striatum), the hypothalamus (ventral diencephalon), and at the low-end cerebellum [94, 95] . Several diseases, such as PD, Tourette Syndrome, and progressive supranuclear palsy (PSP), are associated with DATs [96, 97]. Several drugs and pharmaceuticals block the DAT to delay the resorption of the NTs [98, 99].

1.3.4.1.2 Serotonin Transporters

The human serotonin transporter consists of 630 amino acids and it is assumed that it transverses the membrane 12 times [100]. The highest densities were found in the amygdala and raphé nuclei and in the midline thalamic nuclei. Other tissues exhibiting high concentrations of SERT are nucleus interpeduncularis, substantia nigra, locus coeruleus, nucleus nervi hypoglossi, nucleus nervi facialis, and partly the hypothalamus [101-103]. Abnormalities in the serotonin system have been shown to correlate with a number of diseases including PD [104], major depression, obsessive-compulsive and panic disorders [105], and suicide (post mortem examinations) [106].

1.3.4.1.3 Norepinephrine Transporter

The human norepinephrine transporter is built of 617 amino acids [107]. It is a transmembrane protein and closely related with SERT since it has been shown that they are members of the same Na^+/Cl^- transporter gene family [108]. Psychiatric conditions associated with the reduction or

aberration of NET are PD [109], seizure [110], depression [111], attention-deficit/hyperactivity disorder (ADHD) [112], and suicide (postmortem in depressed beings) [113].

1.3.5 Illicit Drugs: Mechanism of Action

As explained before, NTs are crucial for the communication between neurons. Any interference caused by foreign substances in this fragile and highly complex system of chemically mediated transmission results in malfunctions. Illicit drugs are substances that exploit this critical step in the signal propagation, but also legal drugs use similar mechanisms. There are several ways how a chemical may influence the cell-to-cell-communication in human brains. The reuptake sites for NTs - preferential SERT, DAT, and NET - are often the point of attack for drugs and more selectively for pharmaceuticals [114].

The psychotropic effects of potent stimulants, such as cocaine, 3,4-Methylendioxy-N-methylamphetamin (MDMA), amphetamines and methylphenidates (*vide infra*), are caused by their ability to inhibit transporter sites (DAT, NET and SERT) in the presynaptic membrane of neurons [115]. As a direct consequence, the removal of the NTs is delayed and the NTs remain therefore longer in the synaptic cleft. In this process, the absolute amount of released NT into the synaptic cleft is only insignificantly increased. Antidepressants also use this mechanism, but it is intended that pharmaceuticals target transporters more selectively [83].

It is known that amphetamines and phentermines use an additional mechanism: They stimulate a massive efflux of monoamines (dopamine, less norepinephrine) into the synaptic cleft. After a rapid uptake into the neuron terminals via transporter sites, they act as substrate for intracellular vesicular monoamine transporters (VMAT). These VMATs transport amphetamine from the cytoplasm into storage vesicles. These actions lead to an increased efflux of stored NTs into the cytoplasm. Recently, it was discovered that transporter sites function in a bidirectional manner (DAT). This explains why high dopamine levels in the cytoplasm lead to an increased efflux of dopamine into the synaptic cleft [116].

A short overview how drugs can affect the nerve system's communication is outlined in table 4 [117].

Neurochemical mechanisms of drug influence		
1	NT synthesis	a drug may decrease or increase the synthesis of NT
2	NT transport	a drug may disturb the transport of the NT to the axon terminals
3	NT reuptake	drugs may hinder the transporters to reuptake the NTs from the synaptic cleft
4	Receptor blocking	a drug may inactivate a receptor by blocking it
5	NT storage	a drug may derange the storage of NT molecules in vesicles of the axon terminal
6	NT release	a drug may interfere with the axon terminals to release the NT prematurely or make more NT in the synaptic cleft available
7	NT degradation	a drug may inhibit the breakdown of NT molecules
8	Receptor activation	drugs may imitate NTs and thus activate receptors (prop. permanently)

Table 4: Neurochemical mechanisms of drug influence

1.4 RADIOPHARMACY

Radiopharmacy is the division of pharmaceutics dealing with radioactive isotopes for drug compounding. Experts from many disciplines such as pharmacists, technicians, chemists, biologists and physicists work in this field. Being a nuclear pharmacist requires a rational understanding of drug design, production, and quality control. Further tasks are distribution, storage, and disposal of radiopharmaceuticals [118, 119].

1.4.1 Radiopharmaceuticals

Radiopharmaceuticals are all pharmaceutical products, which contain radioactive isotopes, when they are ready to use. So far, this generic definition includes radiopharmaceuticals for diagnosis as well as for therapeutic purposes. The definition does not specify the composition of the drugs. Hence, a radiopharmaceutical can be a radioactive element (^{18}O-^{16}O), a salt ([^{131}I]NaI), a small molecule, a peptide, or a whole protein linked to a radionuclide. Commonly, they consist of two parts, a radionuclide and a ligand (pharmaceutical). All radiopharmaceuticals are prescription drugs [22].

The main fields of application for radiopharmaceuticals in clinical nuclear medicine are diagnostic issues (95 %), whereas therapeutic questions only account for 5 %. It must be kept in mind that radioactive substances entail a detrimental effect on the patient. Thus, radiopharmaceuticals are never administered without cause. In order to minimize the aversive effects of radiation, radiopharmaceuticals are normally applied only once to a patient in a life. The goal of diagnostic procedures is to obtain images that show the distribution of the radiopharmaceutical in the body.

Any effects on cells, caused by radioactive irradiation, are negative side effects of this method. In contrast, therapeutic radiopharmaceuticals are meant to destroy the target cells by exposing them to radioactive radiation. The fact that cells in the neighborhood of target cells are also affected by radiation without being hit directly is known as “cross-fire effect”.

A remarkable difference between conventional drugs and radiopharmaceuticals is that no verifiable dose-response-relationship can be observed for the latter. The reason can be found in the fact that the amount of administered drug in a single dose is in the range of pico- to nanograms. Another exception for radiopharmaceuticals is that they cannot be prepared, tested, controlled, stored and distributed in the same manner as conventional drugs. It is common praxis to prepare a radiopharmaceutical and administer it immediately after testing relevant parameters such as pH-value, concentration of organic solvents, (radio-)chemical purity and osmolality [119]. Sterility- and endotoxin tests are performed after complete decay of the radionuclide.

1.4.2 Characteristics and General Consideration for Radiopharmaceuticals

The development of a radiopharmaceutical is based on various considerations. In a first step, the radionuclide must be selected. This choice is fundamental, because the half-life of the radionuclide should be adequate to the therapeutic or diagnostic purpose. In addition, the radionuclide must be compatible with the ligand. Not every radioactive element can be attached to every chosen molecule. A factor directly depending on the radionuclide is the decay mode. Diagnostic methods use γ-radiation, electron capture (EC), and positron emission, while β^--decay is used for therapeutic procedures. Elements exhibiting α-decay are rarely used in conventional nuclear medicine [120]. In some cases it is possible to replace atoms in the molecular structure by a radioactive isotope. Hereby, the native structure of the ligand is not altered and the physiological behavior of the labeled compound corresponds with the behavior of the original compound.

Another important factor is time. The preparation of the radiopharmaceutical should not be too time consuming, especially when short-lived PET nuclides are involved. The whole labeling process should not take more than three half-lives of the radionuclide [121].

Moreover, other properties such as charge of the molecule, lipophilicity, affinity, specific activity and stability should be taken into account. An effective separation assay for reactants, side products, solvents, and product also has to be carried out. The final product must be an administrable drug for human patients: sterile, safe, pyrogen-free, and without toxins. Therefore, reliable and efficient purification protocols have to be developed. Additionally, there have to be analytical procedures to guarantee a feasible pharmaceutical quality control before tracer application [44].

1.4.3 Effective Half-life

The effective half-life of a radiopharmaceutical is influenced by two different parameters: a) the biological half-life, which depends on metabolic and excretion processes, and b) the physical half-life, which is determined by the radioactive decay of the nuclide. Effective half-life and intended use should correspond to each other. For diagnostic purposes a short period (hours) is sufficient, while a longer effective half-life (days) is mandatory for therapeutic radiopharmaceuticals [119].

1.4.4 Specific Activity

Utmost importance should be paid to the specific activity (SA) in connection with tracers (*vide infra* 1.5 Tracer) for neurotransmitter systems, because the cold and hot molecules are competing for the same structures and their number is limited. For metabolic tracers, the SA plays a less important role because there is no limited number of binding sites.

SA is defined as the radioactivity per unit mass (or mol) of a radionuclide or a labeled compound. For example, if a 50 mg sample contains 370 MBq, then the SA is given as 370/50 = 7.4 MBq/mg. It is also possible to calculate the molar amount of a product and divide the activity by it. The result would be given as MBq/mol [122, 123].

1.5 TRACER

A tracer is a substance that follows ("traces") a physiological or biochemical process [124]. The term tracer includes free radionuclides, peptides, large biomolecules, and complex compounds. In most cases, a tracer is built up of two main parts: a non-radioactive ligand and a radioactive nuclide. Ligands may be substances occurring in nature, chemically modified natural derivatives or completely new designed molecules. Often, a structural element from a naturally occurring substance is used as basic structure and certain properties are added or enhanced [125]. In clinical terms these molecules are often called radiotracers or radiopharmaceuticals. There are some requirements for a suitable tracer: 1) it should act like the native compound, 2) specific activity should be high (more important for neurotransmitter tracers e.g. [^{18}F]fallypride because *in-vivo* receptor quantities are limited and easily saturated [126], less important for metabolic tracers), and 3) isotopic effects on the tracer caused by the radionuclide should be negligible or at least predictable [124].

It is more complicated to predict the behavior of substances with artificially added atoms. This concerns especially elements with a low natural abundance in biological systems. In some cases, addition of radionuclides may change the biological and metabolic properties of the native compound. For example, examinations with [^{18}F]FDG are based on such an effect [127]. The introduced fluorine does not only prevent enzymatic decomposition, it also traps the molecules within the cells. The result is a fast accumulation in metabolic active cells [128].

Metallic radionuclides, such as ^{68}Ga, ^{99m}Tc, ^{111}In, and ^{188}Re, are very challenging because they are usually not present in biological substances [129]. For this reason, it is not possible to directly compare the behavior of labeled compounds with naturally occurring molecules. As a logic consequence, a careful examination and evaluation of the new substances is required. The advantage of replacing native atoms (e.g. carbon) in structures by their one radioactive isotope is, that the labeled compound does not differ from natural compounds in biological meanings [124]. A quick penetration of the BBB is advantageous because the available time for accumulation in the tissue is limited by the effective half-life (1.4.3 Effective Half-life). Besides studying the complex interaction of neurotransmitters, tracers can be used for evaluation of much simpler physiological processes such as excretion, perfusion, transport, and distribution.

Analog tracers are a group of modified natural compounds. There are manifold reasons for modifying a molecule, such as the improvement of imaging quality, a more specifically targeting of a desired structure, the change of metabolism, or improved clearance properties [130]. Very often, native substances lack a binding site for desired radionuclides. Construction and linkage of artificial binding sites to native compounds can cause severe changes in the biological behavior.

1.6 From Cocaine to FE@IPCIT

1.6.1 Cocaine

1.6.1.1 General

Cocaine was discovered in 1859 by A. Niedermann. In 1884, S. Freud recommended the use of the drug in psychotherapy to treat depression.

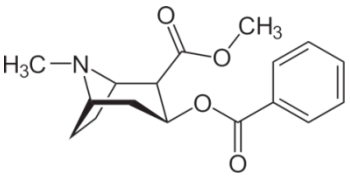

Figure 4: Cocaine

The generic name (INN) for the substance is benzoylmethylecgonine, a crystalline tropane alkaloid. The major source is the plant *Erythroxylum coca*. After an extraction process, the substance is available as a salt, cocaine hydrochloride. It can be used directly for consumption or it can be chemically modified to obtain the free base ("freebase"), the pure basic form of an amino function. It is relatively insoluble in water, whereas the salt is highly water soluble [131].

Cocaine primarily stimulates the cortex cerebri, the hypothalamus and the cerebellum in the brain. This leads to euphoria and improved psychical and physical performance whereas hunger and thirst(anorectic effect) are suppressed [132, 133].

1.6.1.2 Metabolism

In humans, 95 % of cocaine (**1**) is decomposed by cleavage of the ester functions after a half-life of 40 to 60 minutes [134]. The most important enzymes for the biological deactivation are carboxylesterases. The wavy red line in figure 5 marks the bond that is cleaved. According to this, the

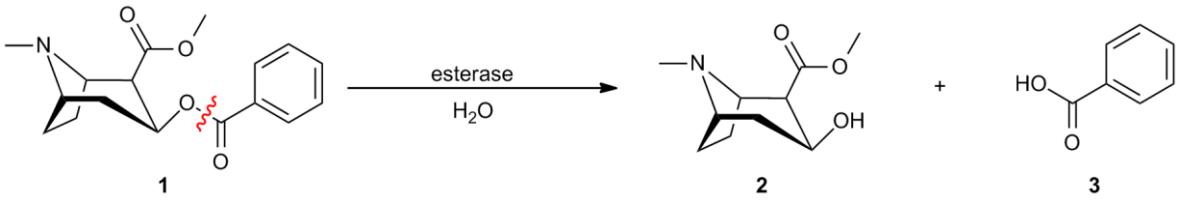

Figure 5: Degradation of cocaine by esterases

primary metabolites are ecgonine methyl ester (**2**) and benzoic acid (**3**) [135]. The metabolites are largely excreted in the urine [136].

1.6.1.3 Neurobiology

Cocaine enhances monoamine (serotonin, norepinephrine and dopamine) activity in the CNS and PNS by blocking reuptake pumps (transporters) [137]. The reinforcing effect seems to result from interaction with the brain's own reward system [138]. The effects of cocaine appear to be caused by its action at the DAT and D2 receptor [115, 139]. The native molecule can be seen as a serotonin–norepinephrine–dopamine reuptake inhibitor (SNDRI) or triple reuptake inhibitor (TRI). This action indirectly leads to a higher concentration of transmitters in the synaptic gap because the removal of the transmitter is inhibited and it remains active in the synapsis for a longer time. The total amount of released transmitters from the presynaptic neuron is only slightly increased by cocaine [137].

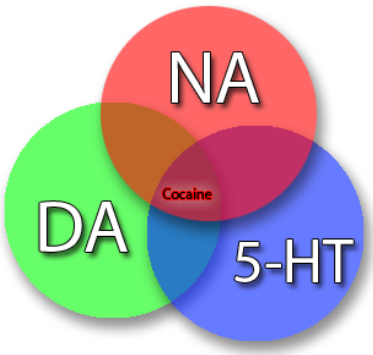

Figure 6: Schematic representation of cocaine as a SNDRI

Cocaine penetrates easily the BBB, causing a rapid onset of the psychedelic effect. Especially when smoked (usually the free base of cocaine), a "high" is produced in less than ten seconds [140], plasma values peaking at about 5 to 10 minutes after inhalation [141]. It seems that not only the abuse liability is higher for drugs with a short onset time, also the reinforcing effect appears to be stronger [142]. Another finding was that the transporter occupancy correlates with the degree of lipophilicity [143].

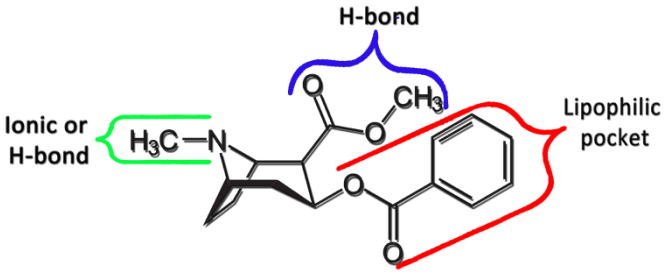

Figure 7: Schematic representation of the interaction of cocaine and its receptor [78]

1.6.1.4 Addiction

A person can be described as "addicted" when the further use of the substance is compulsive. The individuals have lost every control over the consumption. Neural areas of the brain that are involved in the addiction process are impulse control (prefrontal cortex, cingulate gyrus), motivation (orbito frontal cortex), memory (amygdala, hippocampus), and reward (ventral pallidum, striatum [144]). These are also the areas, which can be observed easily with nuclear neuroimaging by applying radiolabeled cocaine or cocaine congeners. Thus it was discovered that the D_2 receptor availability was decreased (15 – 20 %) in humans and non-human primates when they consume cocaine [116].

1.6.1.5 Summarized Effects of Cocaine

Cocaine can induce many effects such as increase of vigilance (reduced need of sleep), nasal drip, mydriasis, coronary vessel constriction, release of thyroid hormone (followed by glucose release), vasodilation (better muscle perfusion), vasoconstriction (skin), release of NTs (primary epinephrine and norepinephrine), blocking of reuptake of NT (DAT), glycogen mobilization (muscle and liver), higher muscle tone of the large intestine and supraventricular tachycardia, deleterious effects on cardiac rhythm, and myocardial contractility resulting in the increase of blood pressure [145].

The cardiotoxicity of cocaine is a serious problem. Drug-related deaths are most often connected to the cardiovascular manifestation of the drug. The drug can irreversibly harm the heart structure, speed up existing cardiovascular disease or cause sudden death by cardiac failure (myocardial infraction and ventricular fibrillation). The anesthetic and adrenergic effects combined in cocaine are a possible reason for cardiac problems [146]. The molecular mechanism of action can be found in the behavior of cocaine regarding the blockage of K^+ channels, increased Ca^{2+} channel current, and inhibition of Na^+ influx during depolarization. Besides the acute effects, there are also pathologic changes of the heart related to chronicle abuse of cocaine, such as dilated cardiomyopathy, left ventricular hypertrophy, and myocarditis [147, 148].

1.6.2 Development of a New Drug

A promising way to develop a pharmaceutical is to start with modification of suitable natural compounds. Cocaine can effectively block transporter sites, but the psychedelic effects are unwanted in research and the selectivity is insufficient. The aim is to synthesize derivatives without the negative effects and emphasize the desired aspects.

1.6.2.1 Cocaine as a precursor

First efforts to target transporters were carried out with ^{11}C-labeled cocaine. The primary target was the DAT [40]. As mentioned, cocaine is not specific for one transporter site [114]. Therefore, it is not a suitable tracer for accurate measurements. The chemical industry produced many derivatives from cocaine, trying to find a treatment for addicted persons. The pharmaceutical company Sterling-Winthrop, Inc. synthesized many derivatives. The manufacturing code for their substances consists of a three letter code WIN (from **Win**throp) followed by a number. Bayer AG acquired the company in 1994 [149, 150]. Another company, which synthesized important compounds based on cocaine is the Research Triangle Institute (RTI). They also used an abbreviation to label their compounds: RTI followed by a number [151], e.g. the iometopane RTI-55 (beta-CIT). Nowadays, many of these substances are used in scientific research.

The precursor for the syntheses is normally natural cocaine because the full synthetic production of a similar precursor would be very work-intensive (4 chiral centres – 16 possible stereoisomers) and therefore expensive while the natural compound is cheap and easily available.

1.6.2.2 Methylecgonidine

The anhydroecgonine methyl ester (AEME) emerge from a pyrolytic process when the freebase of cocaine ("crack cocaine") is smoked [152]. It has been shown that the substance manifests a severe cytotoxicity [153]. The compound is used in scientific research as a precursor for phenyltropane analogues.

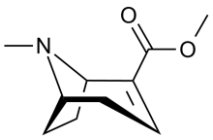

Figure 8: Methylecgonidine

A synthesis of AEME for scientific purposes was proposed by S. Singh [154]. Methylecgonidine was prepared from (R)-cocaine as precursor in three steps: 1) hydrolysis (HCl), 2) dehydration, and 3) esterification as shown in figure 9.

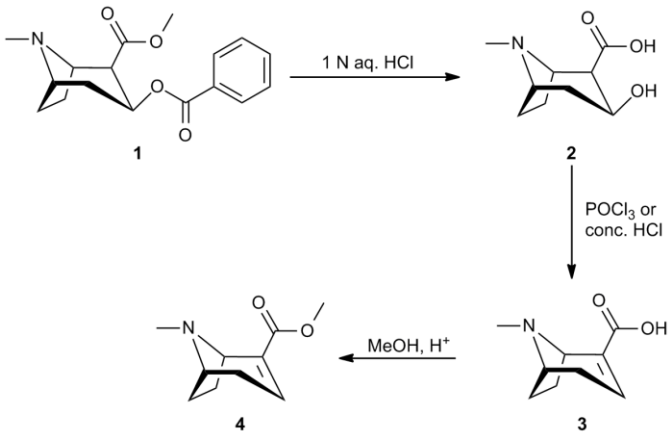

Figure 9: Synthesis route of methylecgonidine

During the reaction ecgonine (2) and ecgonidine (3) are formed as intermediates. Both are useful precursors for further syntheses.

1.6.2.3 Troparil

Troparil is a stimulant drug and is used in scientific research. Other names for the compound are WIN 35,065-2 and β-CPT. The molecular structure is identical for troparil and cocaine except an ester function of the cocaine molecule, which links an aryl ring to the tropane [155]. It is an important precursor for many phenyltropanes derivatives. Some analogues will be explained in more detail (*vide infra*). They all have a *para*-halogen atom linked to their 3β-phenyl ring.

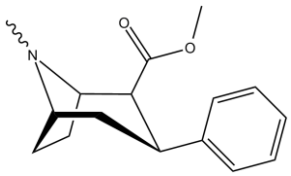

Figure 10: Cocaine derivate

WIN 35,065-2 has a 4.4-fold higher binding potency for the DAT than cocaine [154]. *In-vivo*, this results in a higher ratio between specific and unspecific binding. An attempt to explain the increased affinity was done by measuring the interatomic distances. The distance between the bridging nitrogen and the center of the aromatic ring was seen as significant for binding potency. The interatomic distance in cocaine and WIN 35,065-2 are 7.7 and 5.6 Å, respectively. Probably, the 3β-phenyl ring is in a more favorable position in WIN 35,065-2 [154]. WIN 35,065-2 saturates the DAT in a biphasic manner by characteristic bonding to high- and low-affinity sites like cocaine [156].

There is also evidence that the binding potency and selectivity depends highly on the substituents at the aromatic ring. The comparison of 3β-phenyl ring derivatives demonstrated, that a high electron density around the aromatic ring increased the affinity to DAT [154]. Further structural features, which are crucial for high ligand potency, have been identified: the tropane nitrogen, a 2β-substituent, and a 3β-aryl group [157]. The removal of the intermediate ester linkage suppressed the local anesthetic properties of the molecule [158].

Moreover, the metabolism of 3-phenyltropanes is slower as compared to the one of cocaine and therefore these substances have longer durations of action [159]. The reason for this is the absence of an ester function. The phenyl ring in troparil is directly attached to the tropane structure with a non-hydrolyzable carbon-carbon bond. The removal of the ester linkage did not alter the affinity to SERT [160]. In PET, this leads to a signal in DAT and SERT rich regions, respectively. Hence, there are signals in the striatal area (caudate nucleus and putamen), caused by radioligand binding to DAT and also from the hypothalamus (mesencephalon) is caused by binding to SERT [161].

Three substances were chosen and compared in more detail to explain the different binding behavior of similar compounds. These substances were cocaine, WIN 35,065-2 and a WIN vinyl analogue (Figure 11). Solvation effects were the first evaluated property. It was calculated that cocaine is favored solvated than the WIN compounds because of the two ester groups (position 2β and 3β). The pK_a values for the tropane nitrogen in cocaine, WIN 35,065-2, and the WIN vinyl analogue are 8.65, 9.55, and 11.95, respectively. The WIN and the WIN vinyl analogue are more conformationally restricted than cocaine. The restriction is associated with the steric interaction between the 2β and 3β moieties. Accordingly, the higher binding potency of the WIN compounds was correlated with their decreased conformation flexibility, the reduced aqueous solvation, and the higher pK_a values [154, 162].

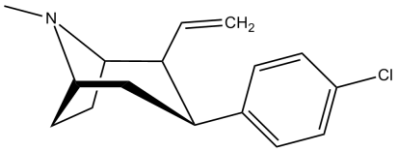

Figure 11: WIN vinyl analogue

1.6.2.4 Halogenated Analogues of Troparil

It has been shown that a slow onset of a drug weakens the reinforcing effect [29]. This was the incentive to create numerous cocaine analogues to find a suitable substance, fitting for the treatment of addicts. Some developed compounds showed increased affinities to DAT with similar affinities to SERT and NET as cocaine [142]. In nuclear medicine theses derivatives are used for studying the distribution of DAT [163].

1.6.2.4.1 WIN 35,428

WIN 35,428 is also known as β-CFT. The structure is identical to troparil, except the fluorine atom which is attached to the 3β-aromatic ring. The fluorine within the substance is advantageous for PET experiments, because it can be labeled with the radioactive nuclide ^{18}F without altering the structure of the molecule. The molecule possesses additional functions for labeling with ^{11}C, but the use of ^{18}F is advantageous because of the longer half-life. The short half-life of ^{11}C is a problem because of the slow uptake process into the brain (striatum peak: 91 min after injection, approx. 4.5 $T_{½}$) [164].

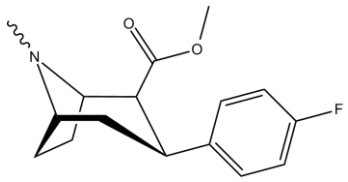

Figure 12: Fluorinated troparil analogue WIN 35,428

[^{18}F]-β-CFT reaches its highest striatal concentration approximately 225 minutes (approx. 2 $T_{½}$) after application [163].

1.6.2.4.2 RTI-31

The troparil analogue has a chloride linked to its phenyl ring and is approximately 64-fold more potent than cocaine, 6-times more than WIN 35,428 and 26-fold more effective as RTI 51 (self-administration by rhesus monkeys). The metabolic stability of RTI-31 *in-vivo* is considerably improved compared to cocaine (30 min vs. 2 min, respectively [165]). A displacement experiment of H-WIN 35,428 from striatal dopamine transporter sites by other troparil analogues was carried out. RTI-31 and WIN 35,428 exhibited the slowest exchange rates whereas RTI-55 and RTI-51 showed intermediate rates [143].

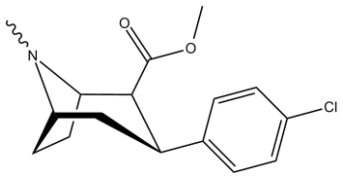

Figure 13: Chlorinated troparil analogue RTI-31

From the radiochemical point of view, the substance has lost a functional group when the fluorine atom was replaced by chlorine. The only practicable way to label the compound is via radioactive ^{11}C (without structural changes).

1.6.2.4.3 RTI-51

The compound, also known as bromopane, has a *para*-bound bromine at its aromatic ring. The expected properties are situated between its analogues RTI-31 and RTI-55. The substance is classified as a nonselective inhibitor [166]. An uptake and binding inhibition experiment was performed to measure the IC_{50} values for DAT, NET, and SERT (rat tissue). The results for the uptake of RTI-51 were 0.9 /0.8/1.2 nM and 1.7/37/10.6 nM for the binding inhibition, respectively [167].

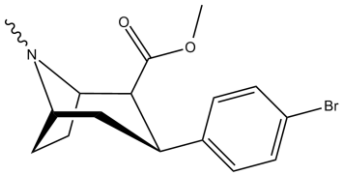

Figure 14: Brominated troparil analogue RTI-51

The action at the DAT is considered to be the decisive factor for the effects of these drugs, so a closer look on this aspect was taken. In an additional experiment, binding inhibition values in rat, rhesus monkey and human caudate-putamen tissue were measured. The obtained IC_{50} values for RTI-51 were 1.7/0.33/0.55 nM for DAT,NET and SERT, respectively. The values are extremely low compared to the values of cocaine (89/75/81 nM), obtained with the same experimental set-up [167].

1.6.2.4.4 RTI-55

RTI-55 is a phenyltropane-based compound mostly used in research. In the literature the substance is also known as beta-CIT (β-CIT). The structure of troparil was modified by adding a *para*-iodine to the aromatic ring. Iodine is - in contrast to the other halogens - off bulbous nature. This, combined with a low electronegativity, leads to a remarkable increase of the electron density around the aromatic structure, known as a positive feature for binding in the lipophilic pocket [154]. Experiments have shown that RTI-55 is at least 8-fold more potent than cocaine and also has a longer period of action [168].

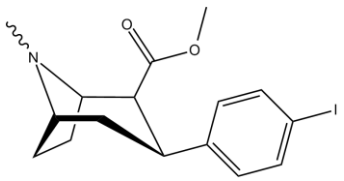

Figure 15: β-CIT: iodinated troparil analogue

RTI-55 can be used as a biomarker for dopaminergic nerve cells to detect degeneration in an early stage [169]. The degeneration process is a strong hint for Parkinson's disease (PD). Research and diagnostic purposes in connection with PD are the main field of application for CIT radioligands [170-172].

Compared to RTI-31, the bigger halogen atom in RTI-55 increased the affinity for the SERT (IC_{50} = 3.78 nM [173]) by retaining the blocking activity for DAT (IC_{50} = 1.6 nM [173]) . According to literature, the radioligand can be used for imaging 5-HT and DAT binding sites simultaneously in the human brain *in-vivo* [174], but for higher resolved images, more selective radiotracers are needed [175].

[^{123}I]Nor-β-CIT, a desmethyl analog of β-CIT, is the compound with the highest *in-vitro* affinity to SERT among all tested CIT analogues so far. Nor-β-CIT (IC_{50} = 0.36 nM) is tenfold more affine than β-CIT (IC_{50} = 4.2 nM). However, the direct comparison of [^{123}I]β-CIT and [^{123}I]nor-β-CIT *in-vivo* has shown that [^{123}I]β-CIT exhibits faster kinetics and higher binding potential for 5-HTT than [^{123}I]nor-β-CIT. This indicates that [^{123}I]β-CIT is a more effective radiotracer for SERT *in-vivo* [174].

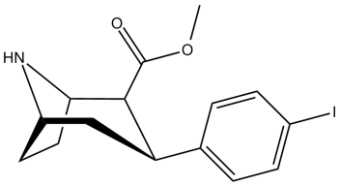

Figure 16: nor-β-CIT

The *para*-iodine allows labeling the compound without altering its structure by using radioactive iodine isotopes [176]. The half-life of ^{123}I is 13.2 hours and it decays by electron capture. When RTI-55 is labeled with ^{123}I, it is also known as iometopane. The long-lived isotope ^{125}I can also be used for labeling. A suitable technique to record the gamma rays is SPECT. It is also possible to label the compound with ^{11}C for PET experiments by introducing a radioactive methyl group [177].

1.6.2.4.5 FE@CIT

FE@CIT is derived from β-CIT. The highest uptake in an *in-vivo* experiment with rats was measured in the striatal regions followed by the thalamus and the cerebellum. The target-to-background ratio was determined with autoradiographic techniques and evaluated as good. Also, the images showed a good and differentiated uptake in the respective regions [178].

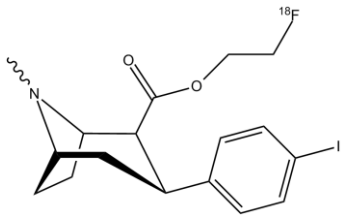

Figure 17: Structural formula of FE@CIT

A valuable feature of the compound is linked to its metabolic degradation. The point of attack for enzymes is the ester function. Its hydrolysis results in two fragments: a free β-CITacid, and the radiometabolite 2-[^{18}F]fluoroethanol ([^{18}F]FEtOH). [^{18}F]FEtOH is highly hydrophilic and is removed from the brain quickly. This process minimizes the background noise, and the recorded images are of a better quality. The remaining β-CIT fragments may occupy similar receptor types but they are invisible for the PET scanner.

1.6.2.4.6 PE2I and FE-PE2I

The troparil analogue PE2I exhibits high affinity to DAT (4 nM). *Ex-vivo* autoradiographic experiments have demonstrated high levels of accumulation in the striatum, the substantia nigra and ventral tegmental area. The peak concentration is reached 30 minutes after the injection. The uptake process into the striatum of rats and monkeys can be described as rapid and selective. *In-vivo* application of PE2I to humans showed high striatal accumulation, low radiation exposure, low non-specific binding and moderate scanning time. Further experiments confirmed the excellence of the radiotracer for detecting a reduction of available DATs in the brain [179].

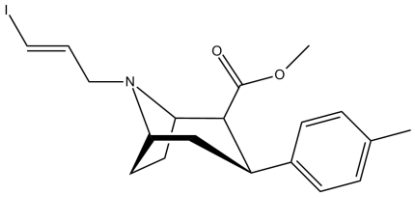

Figure 18: PE2I - a more advanced troparil analogue

[^{18}F]FE-PE2I is a further developed derivative of PE2I. In matters of labeling, it has the same qualities as FE@CIT. After application, the radioligand showed a distribution in accordance with known DAT locations in the brain. The binding behavior was reversible and kinetics were faster than the one from comparable substances [180]. However, several examples can be found in literature where a fluoroethyl labeled radioligand has a superior behavior to the methyl analog [181, 182].

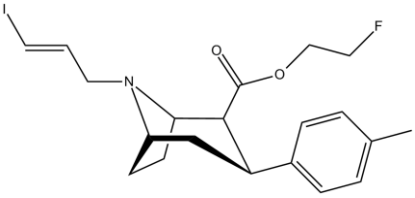

Figure 19: FE-PE2I (structural formula)

1.6.3 FE@IPCIT

FE@IPCIT (2-fluoroethyl 8-[(2E)-3-iodoprop-2-en-1-yl]-3-(4-iodophenyl)-8-azabicyclo[3.2.1]octane-2 carboxylate, figure 10) was designed by combining positive aspects of two radiopharmaceuticals: the established and well-proven radioligand RTI-55 (high metabolic stability), and the more recently developed compound FE-PE2I (high selectivity for DAT). The moiety containing the radioactive isotope is linked via an ester bonding to the precursor IPCITacid to yield [^{18}F]FE@IPCIT. The development from cocaine to FE@IPCIT is shown in figure 20.

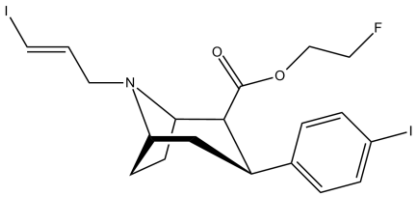

Figure 21: Candidate substance: FE@IPCIT

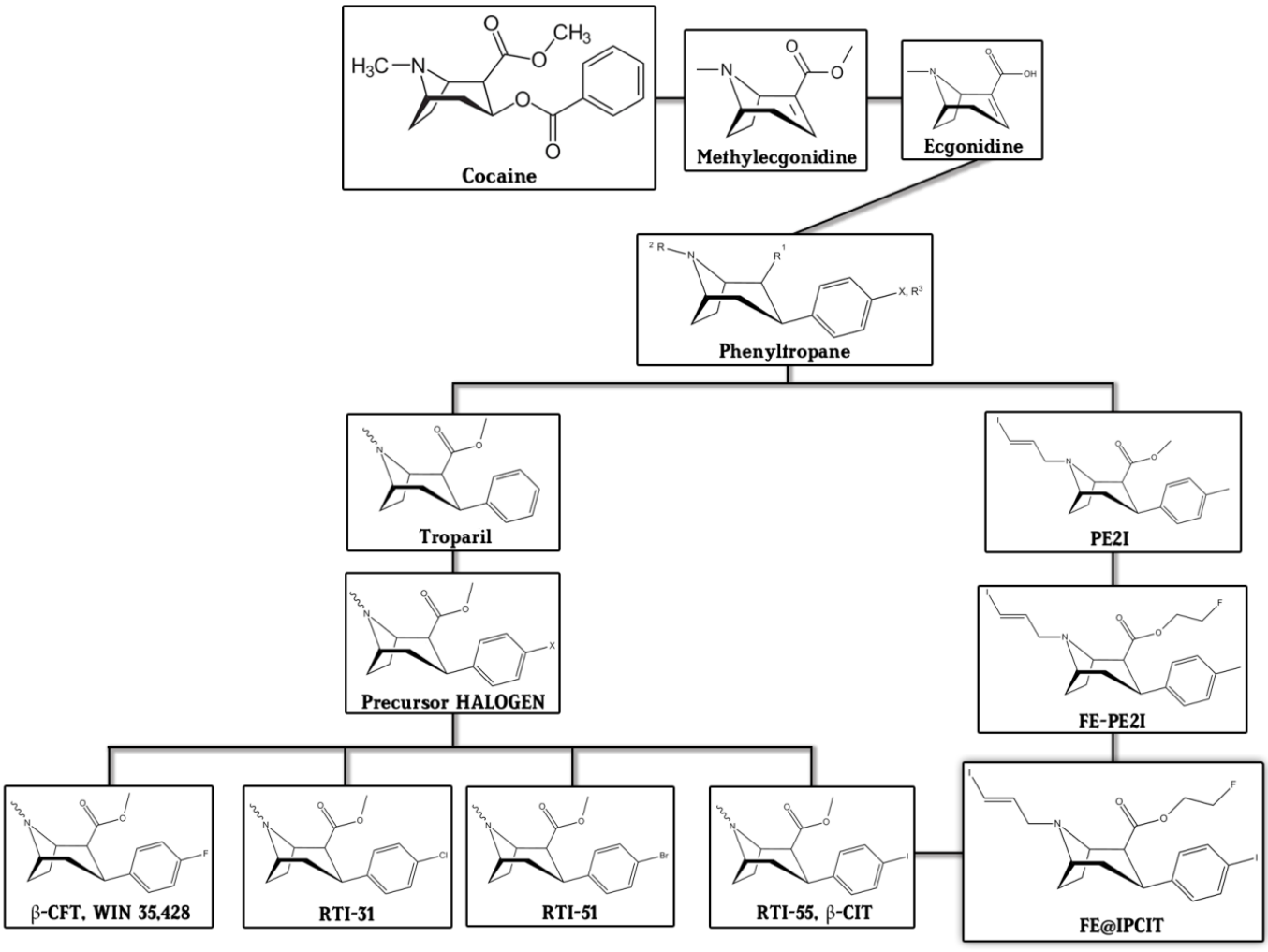

Figure 20: From cocaine to FE@IPCIT

1.6.3.1 *Synthesis of IPCITacid and FE@IPCIT*

The precursor is known as IPCITacid and its synthesis was done in cooperation with the Department of Drug and Natural Product Synthesis, Faculty of Science, University of Vienna [183].

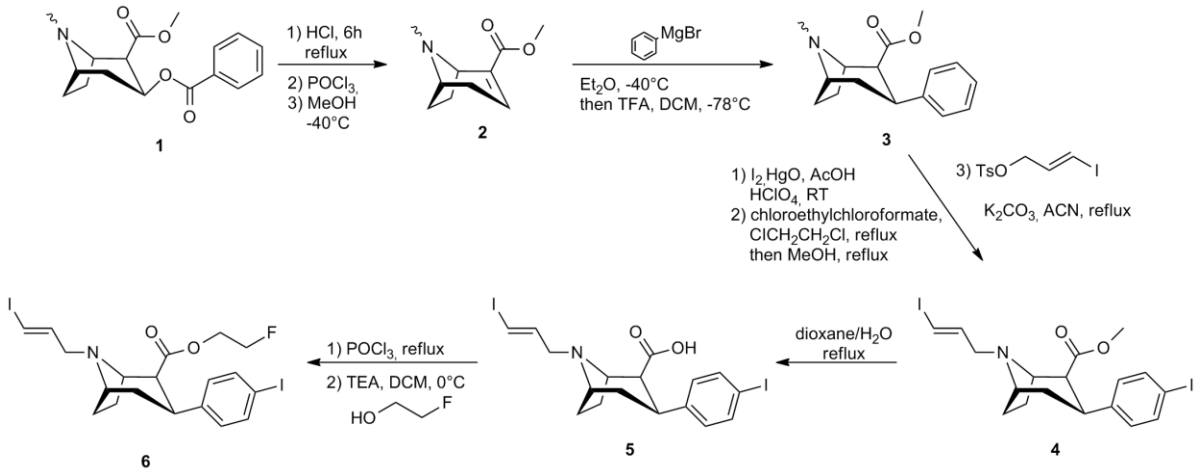

Figure 22: Schematic synthesis route for IPCITacid and FE@IPCIT

The synthesis starts with an acidic hydrolysis (6 M HCl) of cocaine (**1**). Two new functional groups emerge from this step: an alcohol moiety, which is eliminated with $POCl_3$, and an acidic group, which is esterified with MeOH. The yielded anhydromethylecgonidine (**2**) is purified by distillation (yield: 94.3 %). PhMrBr is attached via a Michael Addition to the α,β-unsaturated methyl ester and troparil (**3**) is obtained in 65.28 % yield. After the introduction of a *para*-iodo substituent at the phenyl ring, N-demethylation with chloroethyl chloroformate is performed. In the next step, N-alkylation with (E)-3-iodoally 4-methylbenzenesulfonate gives IPCIT (**4**) in 63.3 % yield (overall 12.7 %). IPCITacid (**5**) (yield: 38.7 %, overall-yield: 4.9 %) is obtained by a mild hydrolysis of the methyl ester (dioxane/water). Finally, the fluoroalkylation of IPCITacid gives the reference compound FE@IPCIT (**6**) in 85.0 % yield (overall 4.1 %).

1.6.3.2 *Preclinical tests*

1.6.3.2.1 Selectivity and Affinity

Affinity and selectivity are important characteristics for the evaluation of new compounds. FE@IPCIT was tested in preliminary standard DAT-membrane binding experiments. The competitive binding experiments were performed in a similar setting as described for NET by Allard et al. [184]. Figure 23 schematically explains the procedure. Three concentrations of non-radioactive FE@IPCIT (n = 3 for each concentration A,B, and C in figure 23) and one sample with radioactive reference compounds (WIN 35,425, total occupancy of receptors, 3 samples, 100 % in figure 23) to be used as control experiment were prepared. The control test tubes were filled with 350 µL assay buffer (100 mM NaCl, 50 mM TRIS-HCl pH 7.4), 100 µL membrane suspension (in assay buffer, 12.7 µg protein/unit, RBHDATM400UA, Perkin Elmer, Waltham, USA) and 50 µL ^{3}H-WIN 35,428 solution (3 nM in assay

buffer, 60-87 Ci/mmol, NET1033001MC, Perkin Elmer). The remaining glass tubes were divided in three groups and one concentration of non-radioactive FE@IPCIT (in assay buffer, 350 µL) was added to each triplicate (instead of pure assay buffer). The volumes of membrane solution and WIN-compound solution were the same as for the control sample. Incubation time was set to two hours at 4°C followed by quenching with ice-cold buffer. After centrifugation (40000 G, 15 min), the pellet was dissolved in a scintillator cocktail (2 mL Ultima GoldTM, biodegradable, Perkin Elmer) and β-counted for 20 minutes. Non-specific binding was tested with 10 µM GBR 12909 (Vanoxerine, Sigma Aldrich, Vienna Austria).

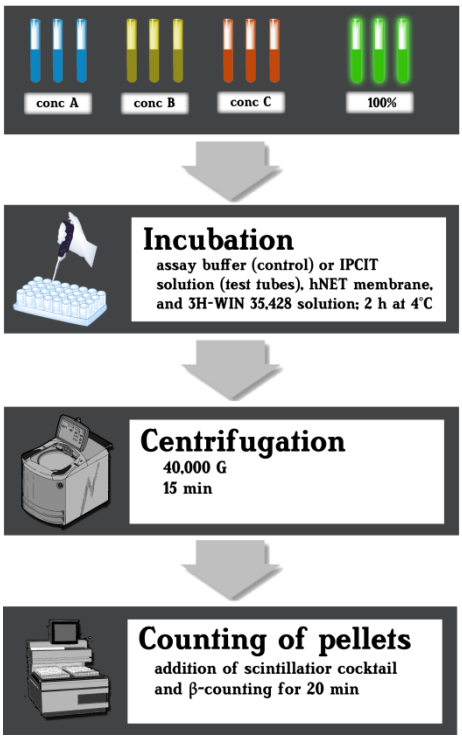

Figure 23: Schematic representation of affinity tests

Optimal conditions for SERT-affinity tests were determined as incubation at 25°C in a buffer consisting of 100 mM NaCl and 50 mM TRIS*HCl at pH = 7.4. The assay for NET-affinity tests was similar. Selectivity was determined as 115-fold towards DAT compared to NET and 1.8-fold for SERT. The K_i values are outlined in table 5 [183].

	DAT [nM]	NET [nM]	SERT [nM]
IPCITacid	36.99 ± 13	785 ± 179	71.4 ± 25.5
FE@IPCIT	1.33 ± 0.2	153 ± 53	2.4 ± 1

Table 5: Results of preclinical affinity tests of DAT ligands (K_i values)

1.6.3.2.2 BBB Penetration Experiments

A substance must have a certain lipophilicity to penetrate the BBB. Various concepts were developed to assess the BBB penetration of substances. Lipophilicity of FE@IPCIT was tested with HPLC according to Donovan and Pescatore [185]. The substance was dissolved in a mixture of toluene and triphenylene (logD and k' are known) and injected in a short polymeric ODP-50 column (Shodex®, Showa Denko Europe GmbH, Munich, Germany). Binary gradient elution (from 10 % MeOH and 90 % 25 mM phosphate buffer to 100 % MeOH within 9.4 min, flow rate 1.5 mL/min) was performed. LogD values are not very reliable for estimating BBB penetration of a substance. A calculation of tPSA (polar surface area) and IAM chromatography (immobilized artificial membrane chromatography) experiments were carried out in accordance to Yoon et al [186] and Tavares et al [187], respectively.

LogD was determined as 5.39 for FE@IPCIT and 0.87 for precursor IPCITacid. Calculated tPSA values for IPCIT and FE@IPCIT were 29.54 in both cases. IAM chromatography experiments revealed

permeability values (P_m values) of 8.94 for FE@IPCIT and 0.04 for the precursor IPCITacid. The obtained data was compared to the external standards PE2I (3.15) and RTI-55 (0.31), both of which are known to penetrate BBB [183].

2 Aim

[^{18}F]FE@IPCIT is a potential tracer for the dopamine transporter system. DATs are of great medical interest since they play a central role in many physiological and psychological processes. Serious illnesses, such as Parkinson's disease or major depression, are apparently associated with malfunction of the DAT system. It was discovered that monoamine transporter densities are decreased in these and similar diseases and can therefore be used as indicators [188-190].

[^{18}F]FE@IPCIT is supposed to combine the advantages of two prior DAT radioligands: RTI-55 and PE2I. Since decades, RTI-55 has proved itself to be a valuable radiopharmaceutical in clinical practice as well as in research. PE2I is a more recently developed compound. As mentioned in the introduction part, the substance showed huge potential in tests and experiments.

The aim of this thesis is to develop and optimize a module assisted synthesis route for [^{18}F]FE@IPCIT. However, this task can be divided in several subtasks: At the beginning, there is the development of efficient separation assays for analytical and semi-preparative HPLC. When this part is finished successfully, the manual synthesis of [^{18}F]BFE, a precursor, and [^{18}F]FE@IPCIT can start. The purpose of these experiments is to investigate various reaction parameters. Finally, after finding optimum reaction conditions, the reaction will be transferred on a synthesis module.

To work with radioactive isotopes is different compared to conventional chemistry. The main problem is the ionizing radiation: it does not allow extensive manual manipulation of the reaction. A further aspect is directly connected to the very nature of instable isotopes: the exponential loss of radionuclides during the synthesis. Especially short-lived radionuclides, preferentially used for PET, undergo massive radioactive decay during synthesis. Thus, time is a limiting factor in matters of the synthesis. And finally, the volumes of the samples are extremely small. Hence, highest concentration is required during every moment of synthesis work.

The products are potential radiopharmaceuticals. Therefore, samples, which do not correspond to the high quality requirements, have to be disposed, since the safety of patients has top priority.

3 Materials and Instrumentation

3.1 Materials

3.1.1 Solvents

Acetonitrile (ACN) was used in two grades of purity: high-purity ACN for synthesis (for DNA synthesis, ≥ 99.9 %) and for HPLC the ACN had HPLC grade as well as Methanol (MeOH, CHROMASOLV® for HPLC ≥ 99.9 %), ammonium formate (AMF), acetic acid (AcOH), ammonium acetate, pyridine abs., dichloromethane (DCM), petrol ether, ortho-dichlorobenzene (oDBC), and ethanol abs. (EtOH) were obtained from Sigma Aldrich (Vienna, Austria). The sterile water for reactions was purchased from Meditrade Medicare Medizinprodukte (Kufstein, Austria), while deionized water was provided by AKH Wien.

3.1.2 Catalytic Substances

Chemicals such as TBAH (tetrabutylammonium hydroxide · 30 H_2O, Sigma Aldrich), Cs_2CO_3, LiOH, Na_2succinate, KI, Et_3N (triethylamine), KOH, NaOH, NaH, NaI, and TRIS (tris(hydroxymethyl)aminomethane) were used for catalysis.

3.1.3 Chemicals

The reactants in the synthesis of 2-bromoethyl trifluoromethanesulfonate were 2-bromoethanol and trifluoromethane sulfonic anhydride. Kryptofix 222 (crypt-222, ABX Advanced Biochemical Compounds, Germany) and 18-crown-6 were used in the extraction process of fluoride-18 from $H_2{}^{18}O$.

3.1.4 Formulation of the Pharmaceutical

For the formulation of the radiopharmaceutical, 0.9 % saline solution (B. Braun, Melsungen, Germany), 3 % saline solution (Landesapotheke Salzburg, Austria), TWEEN 80 (polyoxyethylene sorbitan monooleate, Sigma Aldrich, Vienna, Austria), sodium dihydrogen phosphate monohydrate ($NaH_2PO_4 \cdot H_2O$), and disodium hydrogen phosphate dihydrate ($Na_2HPO_4 \cdot 2\ H_2O$) (Merck, Darmstadt, Germany) were used.

3.1.5 Miscellaneous

Anion-exchange cartridges (PS-CO_3) from Macherey-Nagel (Dueren, Germany) were used in the extraction process of radioactive fluoride. Solid phase extraction was performed with conditioned C18 plus SepPak® cartridges (10 mL EtOH, air, 20 mL H_2O, air) purchased from Waters (Waters®

Associated Milford, USA). Sterilization of the product was done with low-protein binding Millex® GS 0.22 µm (Millipore, Bedford, USA) filters.

Chemicals without further specifications were obtained from commercial sources such as Sigma-Aldrich (Vienna, Austria) or Merck (Darmstadt, Germany) and had at least analytical grade. The chemicals were used without further purification steps.

The target of the cyclotron was filled with $H_2{}^{18}O$ (HYOX18; enrichment > 98 %), which was purchased from Rotem Europe (Leipzig, Germany).

3.2 INSTRUMENTATION

A GE PETtrace cyclotron (General Electrics Medical System, Uppsala, Sweden) was used for the production of radionuclides.

Small-scale experiments with low activity (approx. 1 GBq) were executed manually in hoods with lead-shielding. After finding optimal parameters in manual experiments, the reaction was transferred to an automated synthesis module (Nuclear Interface, GE Healthcare, Sweden). The module was remotely operated by a commercially available laptop with appropriate software (raytest GmbH, Straubenhardt, Germany).

Quality control and characterization of products were done with analytical HPLC (Agilent Technologies 1200 Infinity Series and Merck-Hitachi LaChrom HPLC system, L-7100 pump, LaChrom L-7400 UV detector at 238 nm and 254 nm), using reverse phased column Chromolith® Performance RP-18e (length 100 mm, diameter 4.6 mm, Merck, Germany) for FE@IPCIT. Mobile phase was a mixture of ACN and aqueous solution (water/acetic acid = 97.5:2.5 v/v; 2.5 g/L ammonium acetate; pH = 3.5) in a ratio of 30:70. For the analysis of [^{18}F]BFE, a Phenomenex Prodigy™ 5 µm Phenyl-3 (PH-3) (100 Å, 250 x 4.6 mm, Phenomenex, Aschaffenburg, Germany) column was used with a mixture of ACN (30 %) and a water-based solution (2.5 g NH_4Ac, 25 mL CH_3COOH, 100 mL EtOH, and filled up with distilled water to 1000 mL; 70 %) as eluent (premix). A NaI radioactivity detection unit (Berthold Technologies, Bad Wildbach, Germany) or a raytest Socket 8103 (raytest GmbH, Straubenhardt, Germany) were used to classify the different radioactive species. Also the software for the HPLC systems was purchased from raytest (raytest GmbH, Straubenhardt, Germany).

Semi-preparative HPLC (Merck Hitachi, L6220 Intelligent pump, L-4000 UV detector) was used for product purification. The mobile phase had the same composition as in the analytical assay. For degassing of the eluent, a CMA/260 Degasser was used. A Chromolith® Performance RP-18e (Merck, Germany) column was used for reversed-phase chromatography. In this system, the radioactivity was

detected by a Radiomatic FLO-ONE/Beta Flow Scintillation Analyzer 150 TR (Packard Canberra Radiomatic, USA).

4 Method

4.1 Manually Operated Synthesis of [^{18}F]BFE and[^{18}F]FE@IPCIT

Experiment M.15 (4.1.1.2 Example Experiment for Manually Operated Synthesis: First Part – Extraction) is explained in greater detail to give a general understanding of the experimental procedure. Basically, all experiments were done according to this protocol. Exceptions are described in detail in section 5 (Experiments). Figure 24, figure 25, and figure 26 are schematic drawings and explain the principle of the experimental procedure. For the experiments, miniaturized equipment was used (volumes in between 0.1 and 5.0 mL).

4.1.1 Synthesis of [^{18}F]BFE

4.1.1.1 Set-up for Fluoride-18 Extraction

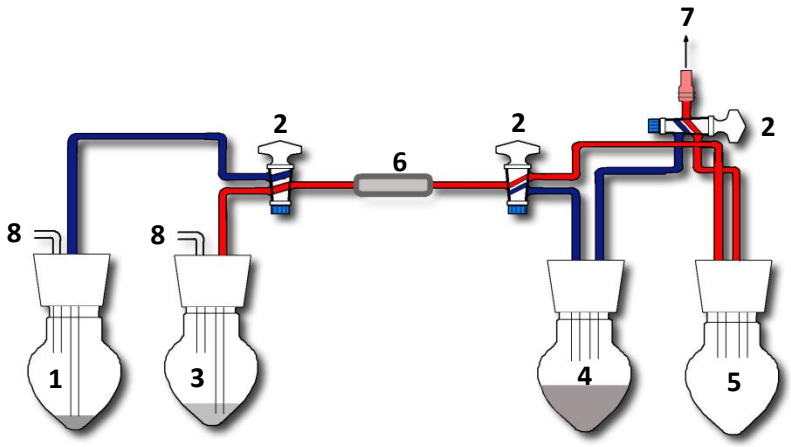

Figure 24: Schematic drawing: extraction of $^{18}F^-$ from $H_2{}^{18}O$ via an anion-exchange cartridge

(**1**) [^{18}F]F$^-$ in $H_2{}^{18}O$, (**2**) three-way cock, (**3**) elution solution, (**4**) waste ($H_2{}^{18}O$), (**5**) flask for eluted [^{18}F]F$^-$ and elution solution, (**6**) PS-HCO_3 cartridge, (**7**) vacuum pump, (**8**) air inlet

The scheme shows the set-up when fluoride-18 is already bound to the anion exchange cartridge (**6**). The next step is to draw elution solution (**3**) through the cartridge (marked in red). The course marked in blue depicts the extraction of [^{18}F]F$^-$ from $H_2{}^{18}O$.

4.1.1.2 Example Experiment for Manually Operated Synthesis: First Part – Extraction of $^{18}F^-$

Fluoride-18 (536 MBq, 10:25) was generated by a cyclotron and delivered in approx. 2.5 mL $H_2{}^{18}O$. The vial was transported to the lead-shielded working station. A syringe (20 mL) was used to draw the water with the radionuclide through an anion exchange cartridge (PS-HCO_3). The cartridge with the bound fluoride-18 was connected to an empty V-vial. To elute radioactive fluoride, 0.8 mL of an

elution mixture (22 mg Kryptofix® 222, 4.5 mg K_2CO_3, 0.7 mL ACN, and 0.3 mL H_2O) from a prepared stock was used. Subsequently, the activity on the ion exchange cartridge (14.27 MBq, 10:34) and in the vial (475 MBq, 10:33) was measured.

4.1.1.3 Set-up for [^{18}F]BFE Synthesis

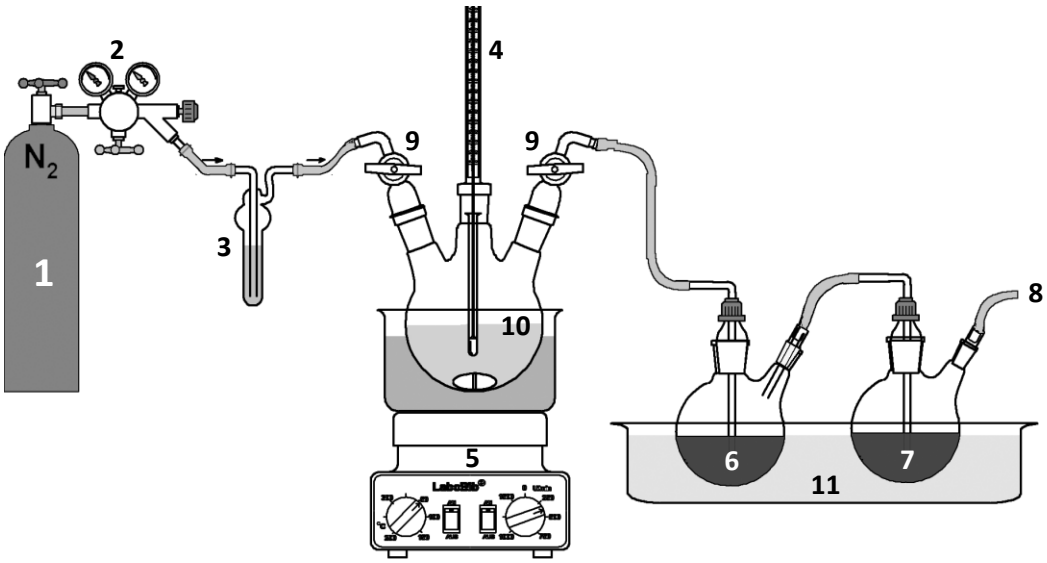

Figure 25: Schematic drawing of the experimental set-up for [^{18}F]BFE synthesis

1) gas bottle (nitrogen), (**2**) pressure reducer, (**3**) bubble counter, (**4**) thermometer, (**5**) magnetic stirrer with heating function and oil bath, (**6**) trap 1 containing an organic solvent, (**7**) trap 2 containing an organic solvent, (**8**) exhaust, (**9**) shut-off valve, (**10**) three-necked flask with magnetic stir bar, (**11**) ice bath

ad (**6**) & (**7**): first trap (**6**) normally contained all the radioactivity – second trap (**7**) was there as a safety measure

ad (**9**): valves are locked during the reaction; open during azeotropic drying and distillation

4.1.1.4 Example Experiment for Manually Operated Synthesis: Second Part - Azeotropic Drying of [^{18}F]F$^-$ and Synthesis of [^{18}F]BFE

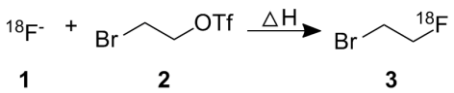

Figure 26: Reactants for [^{18}F]BFE synthesis: 2-Bromoethyl trifluoromethanesulfonate (BET) and ^{18}F$^-$

The vial was heated up to 100°C for approx. 15 minutes to remove water. Evaporation was supported by a gentle nitrogen current bubbling trough the solution. When the substance was dry, the vial was cooled down by dipping it into ice-cooled water. ACN (0.5 mL) was added and evaporated thrice (azeotropic drying, AZD). The measured activity was 352 MBq at 11:14.

A solution consisting of *o*-DCB (1 mL) and ethyl derivate (BET, 30 µL, **2**) was added to the dried fluoride-18 (**1**). The reaction vial was equipped with a magnetic stir bar and tightly sealed. Afterwards, it was heated up to 100°C for 15 minutes. An HPLC check (column: Phenomenex Prodigy™ 5 µm Phenyl-3 (PH-3), flow rate: 2 ml/min) of the crude reaction mixture showed that 90 % of the radioactivity in the sample originated from [^{18}F]BFE (**3**), the remaining 10 % were from [^{18}F]F$^-$ (no side products).

Distillation (10 min, 100°C) was performed to remove the volatile [^{18}F]BFE from the reaction mixture. [^{18}F]BFE was trapped in a vial filled with precooled DMSO (1 mL, 0°C) and a second vial was connected in series as a back-up trap. After distillation was done the purity of the distillate was determined by HPLC (RCI of [^{18}F]BFE = 95 %). Total activity in the first trap was 130.3 MBq at 11:45.

4.1.2 Synthesis of [^{18}F]FE@IPCIT

4.1.2.1 Set-up for [^{18}F]FE@IPCIT Synthesis

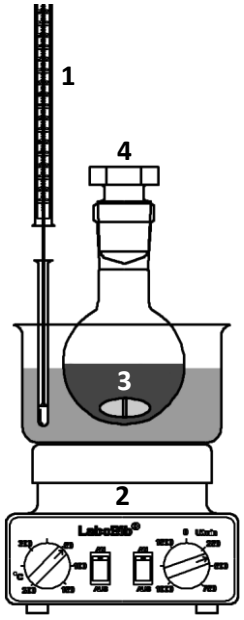

(**1**) thermometer

(**2**) magnetic stirrer with heating function and oil bath

(**3**) reaction flask (also reactor) with magnetic stirrer

(**4**) plug (sealed during the reaction) [191]

Figure 27: Schematic drawing of the set-up for [^{18}F]FE@IPCIT synthesis

4.1.2.2 Example Experiment for Manually Operated Synthesis: Third Part - Synthesis of [^{18}F]FE@IPCIT

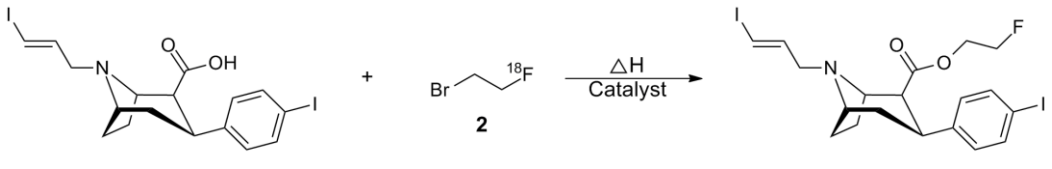

Figure 28: [^{18}F]FE@IPCIT forms in a single step by reacting the precursor IPCITacid with [^{18}F]BFE

For the synthesis of [^{18}F]FE@IPCIT, (**3**) 50 µL DMSO with trapped [^{18}F]BFE (**2**) was taken and mixed with a solution containing IPCITacid (50 µL, 2 mg/mL in DMSO, **1**) in a small V-vial. A magnetic stir bar and catalyst (TBAH, 1 µL, conc. 80 µmol/100 µL in H_2O) were added to the reaction mixture. The vial was tightly sealed and heated up to 100°C for 15 minutes while the mixture was stirred continuously. The reaction was stopped by quenching with water. HPLC analysis was performed and revealed 73 % [^{18}F]FE@IPCIT (RCI).

4.1.2.3 Digitalized Laboratory Protocol

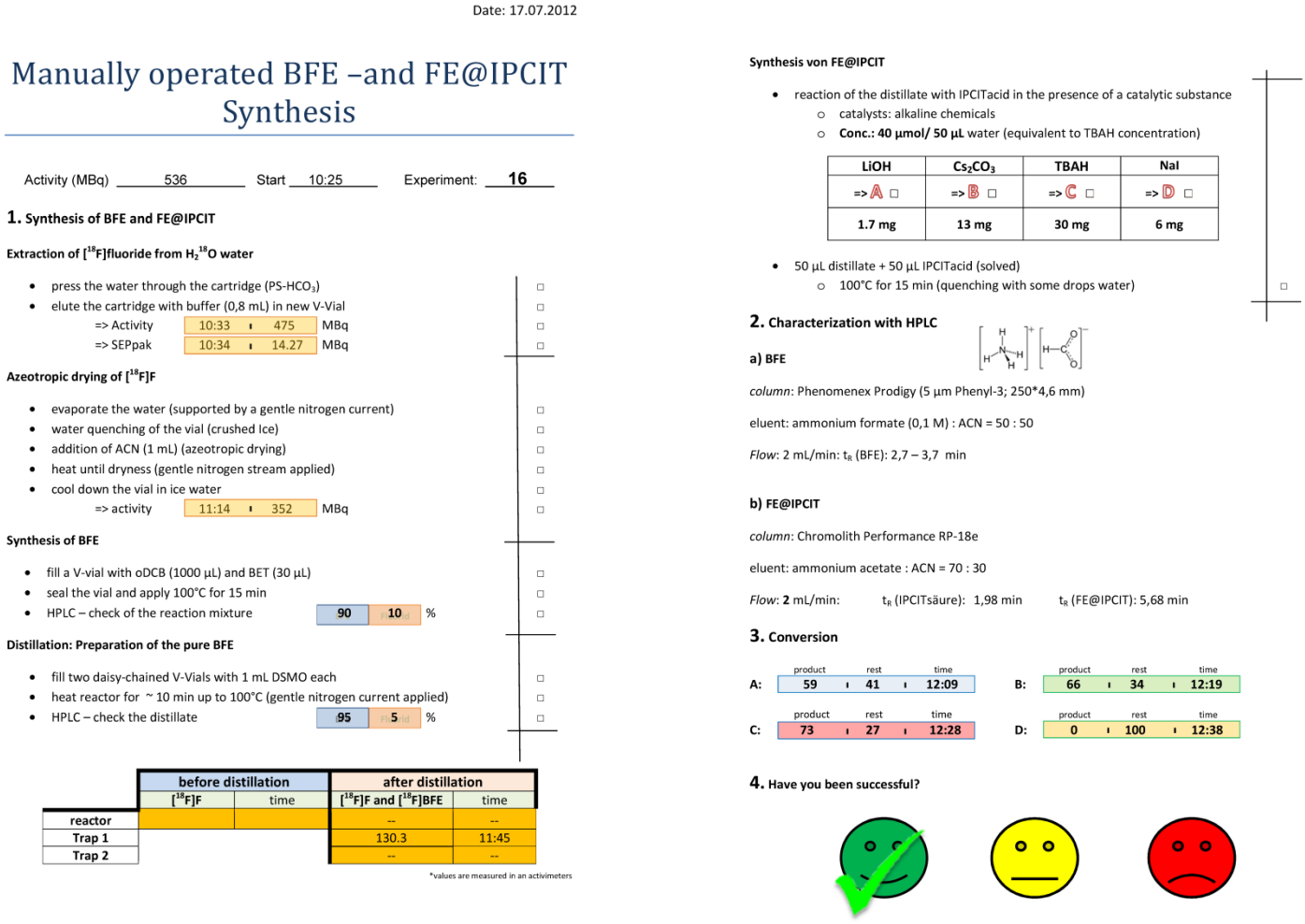

Date: 17.07.2012

Manually operated BFE –and FE@IPCIT Synthesis

Activity (MBq) 536 Start 10:25 Experiment: 16

1. Synthesis of BFE and FE@IPCIT

Extraction of [^{18}F]fluoride from $H_2{}^{18}O$ water

- press the water through the cartridge (PS-HCO_3)
- elute the cartridge with buffer (0,8 mL) in new V-Vial
  - => Activity 10:33 | 475 MBq
  - => SEPpak 10:34 | 14.27 MBq

Azeotropic drying of [^{18}F]F

- evaporate the water (supported by a gentle nitrogen current)
- water quenching of the vial (crushed Ice)
- addition of ACN (1 mL) (azeotropic drying)
- heat until dryness (gentle nitrogen stream applied)
- cool down the vial in ice water
  - => activity 11:14 | 352 MBq

Synthesis of BFE

- fill a V-vial with oDCB (1000 µL) and BET (30 µL)
- seal the vial and apply 100°C for 15 min
- HPLC – check of the reaction mixture 90 | 10 %

Distillation: Preparation of the pure BFE

- fill two daisy-chained V-Vials with 1 mL DSMO each
- heat reactor for ~ 10 min up to 100°C (gentle nitrogen current applied)
- HPLC – check the distillate 95 | 5 %

	before distillation		after distillation	
	[^{18}F]F	time	[^{18}F]F and [^{18}F]BFE	time
reactor			--	--
Trap 1			130.3	11:45
Trap 2			--	--

*values are measured in an activimeters

1

Synthesis von FE@IPCIT

- reaction of the distillate with IPCITacid in the presence of a catalytic substance
  - catalysts: alkaline chemicals
  - **Conc.: 40 µmol/ 50 µL** water (equivalent to TBAH concentration)

LiOH	Cs_2CO_3	TBAH	NaI
=> A	=> B	=> C	=> D
1.7 mg	13 mg	30 mg	6 mg

- 50 µL distillate + 50 µL IPCITacid (solved)
  - 100°C for 15 min (quenching with some drops water)

2. Characterization with HPLC

a) BFE

column: Phenomenex Prodigy (5 µm Phenyl-3; 250*4,6 mm)

eluent: ammonium formate (0,1 M) : ACN = 50 : 50

Flow: 2 mL/min: t_R (BFE): 2,7 – 3,7 min

b) FE@IPCIT

column: Chromolith Performance RP-18e

eluent: ammonium acetate : ACN = 70 : 30

Flow: **2** mL/min: t_R (IPCITsäure): 1,98 min t_R (FE@IPCIT): 5,68 min

3. Conversion

	product	rest	time
A:	59	41	12:09
B:	66	34	12:19
C:	73	27	12:28
D:	0	100	12:38

4. Have you been successful?

2

Figure 29: Laboratory protocol of a manual [^{18}F]FE@IPCIT synthesis

4.2 Module Assisted Synthesis of [^{18}F]BFE and [^{18}F]FE@IPCIT

4.2.1 Set-up for [^{18}F]BFE and [^{18}F]FE@IPCIT Synthesis

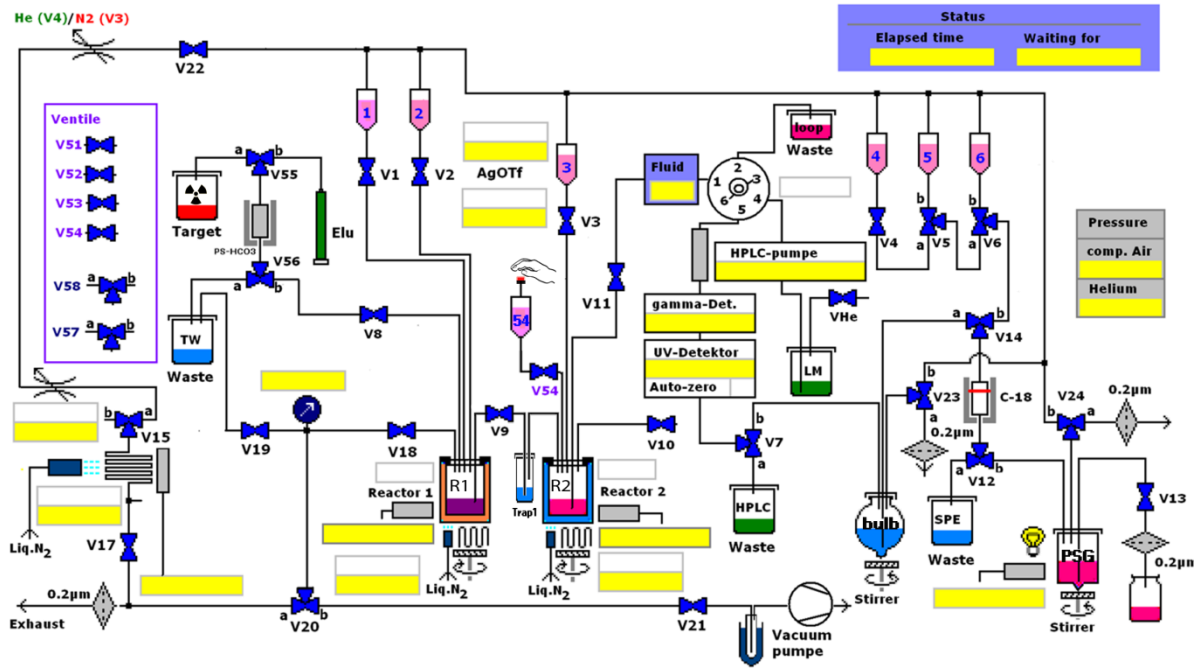

Figure 30: Schematic drawing of the synthesis module

	reservoir1	0.5 mL ACN
	reservoir2	30 µL BET in 500µL *o*-DCB
	reservoir3	400 µL IPCITacid solution (2 mg/mL) + TBAH (1 µL, 52 mg/50 µL)
	reservoir4	5 mL NaCl (0.9 %)
	reservoir5	1.5 mL EtOH
	reservoir6	10 mL water (sterile)
	reservoir54	1.5 mL water (sterile)
	reaction vessel 1 (reactor1)	drying of fluoride-18 and reaction with BET
	reaction vessel 2 (reactor2)	400 µL DMSO
bulb	bulb	80 mL water
	Target	$H_2{}^{18}O$ with [^{18}F]F^-
PSG	PSG	4 mL 0.9 NaCl + 1 mL 3 % NaCl + 1 mL phosphate buffer (125 mM, pH 7.4)
	V9	is closed except during the distillation of [^{18}F]BFE
	Trap1	400 µL ACN (gas-wash-bottle)
	HPLC	a semi-preparative HPLC is included into the synthesis module

4.2.2 Example Experiment for an Automated Module Synthesis

Experiment A.10 was selected to explain an automated synthesis with the Nuclear Interface synthesiser in detail. Other experiments were related to this procedure.

4.2.2.1 Protocol

Water with solvated $[^{18}F]F^-$ was passed through an anion exchange cartridge (PS-HCO_3) and $[^{18}F]F^-$ was fixed on cartridge, while the $[^{18}O]$water was disposed in the waste (TW). In the next step, elution solution (Kryptofix® 222, 0.8 mL) was used to eluate the $[^{18}F]F^-$ directly from the cartridge into reactor1. The remaining water was evaporated (15 min, 100°C), supported by a gentle He-current (2-4 kPa). Upon complete dryness, ACN (reservoir1) was released into the cooled reactor1 for further azeotropic drying (10 min, 100°C).

Afterwards, a mixture of *o*-DCB and BET (reservoir2) was transferred into reactor1 (at RT). All exhausts were closed before the reaction was started by raising the temperature (10 min, 100°C). When the reaction time was over, the distillation process was started (10 min, 100°C) and $[^{18}F]$BFE was evaporated. Supported by a helium stream, it was transported via V9 into the second reactor (reactor2, R2), which was filled with pure DMSO (RT). A small vial was connected between the two reactors in order to trap *o*-DCB and $[^{18}F]F^-$. When the distillation was finished, IPCITacid and a solution of catalyst and DMSO (reservoir3) were added. After sealing the reactor 2, the reaction was started by increasing the temperature (100°C for 15 min). As soon as the reaction time was over, the reaction was quenched with water (reservoir54, manually operated) and the reaction mixture was transferred to the HPLC module. Separation was carried out with a reversed phase column (Chromolith Performance RP-18e).

Caused by a software error, the product containing fraction was lost in the HPLC waste. In experiment a.88, the final steps of preparing a radiopharmaceutical and quality control were accomplished successfully. The procedure would have been the same for experiment A.10. Hence, the protocol of experiment A.8 is presented to describe the missing part(s):

During the separation process, only the product containing fraction was caught and transferred into a bulb filled with water (80 mL) to dilute the organic solvents. Subsequently, the mixture was transferred on an HPLC column for purification (C-18 SepPak®, conditioned). Water from reservoir10 was used to wash out all solvent residues. Afterwards, elution was done with ethanol (reservoir5) and completed with saline (reservoir4). Subsequently, the mixture was transferred into the final flask (PSG). By adding the required buffers, a ready-for-use pharmaceutical was prepared. Finally, the radiopharmaceutical was filtered through a sterile filter and quality control was performed. RCI for $[^{18}F]$FE@IPCIT was 12 % (decay corrected).

4.2.2.2 Digitalized Laboratory Protocol

Date: 13.08.20112

Module Assisted Synthesis of FE@IPCIT

1. Preparations

Activity (GBq) 12.3 **start time** 09:25 **Experiment**: **10**

F-18 cartridge (SEPpak)		□
elution buffer 0,8 mL	V-vial	□
ACN 0.5 mL	in V1	□
BET 30 µL in oDCB 0.5 mL	in V2	□
250 µL IPCITacid solved in DMSO (1 mg/mL)	in V3	□
switch on: N_2, DR, He		□
switch on: vacuum pump		□
switch on: heat/cool function		□
condition C18-SEPpak (10 mL EtOH, 20 mL H_20)		□
condition prep-column (SNAP-Säule)		□
80 mL water	bulb	□
10 mL water	V6	□
1.5 mL EtOH	V5	□
5 mL NaCl (0.9 %)	V4	□
4 mL 0.9 % NaCl + 1 mL 3 % NaCl	PSG	□
+ 1 mL phosphate buffer 125 mM		
sterile filter		□
liquid nitrogen		□
250 µL DMSO for BFE-distillation	reactor 2	□
TBAH for R2 (1 µL; 52 mg/ 50 µL)	**V3**	□
loop waste-vial		□
vial for the product		□
small trap (ACN)	between R1 and R2	□
bubble counter	after V10	□
water 1 mL	V54	□

1

2. BFE: Synthesis and Distillation

30 µL BET + 1000 µL oDCB with [^{18}F]fluoride for 10 Min at 100°C □

distillation 10 min at 100°C (supported by gentle He current) □

trapping of BFE in 400 µL DMSO in reactor 2 □

addition of 400 µL IPCITsäure-solution (1 mg/mL) □

3. FE@IPCIT: Synthesis and Purification

a) Synthesis

- 100°C for 15 min □
- quenching of the reaction (1 mL water) □

b) Purification of FE@IPCIT with prep. HPLC

column: Chromolith Performance RP-18e (SNAP)

eluent: ammonium acetate : ACN = 70 : 30

Flow: **5** mL/min: t_R (IPCITsäure): ~ 3 min t_R (FE@IPCIT): 9,80 min

3. Result

product		rest	
272	I	1428	MBq

4. Was the synthesis successful?

2

Figure 31: Protocol of a module assisted [^{18}F]FE@IPCIT synthesis

5 Experiments

5.1 Synthesis of 2-Bromoethyl Trifluoromethanesulfonate

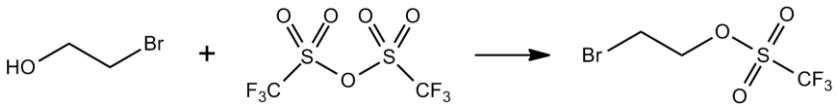

Figure 32: Schematic synthesis route for BET

Anhydrous pyridine (1.5 mL) and dry dichloromethane (20 mL) were poured into a 100 mL, 3-neck round-bottomed flask. All work was done under nitrogen atmosphere to avoid humidity. An ice-salt-water mixture was used to cool the flask down to -20°C. 2.98 mL (17.72 mmol) of trifluoromethane sulfonic anhydride were added (white precipitate formed). After five minutes, 1.76 mL (17.56 mmol) of 2-bromoethanol was added and the precipitate disappeared quickly. After 90 minutes, a new precipitate had formed. The reaction mixture was slowly warmed up to room temperature and constantly stirred. The mixture was filtered and the residue was washed three times (7 mL) with a mixture of DCM/hexane (1:1). To clean the filtrate, a silica column and 300 mL DCM/hexane (1:1) as mobile phase were used. Finally, a micro distillation was performed to obtain the colorless product (2.364 g, 9,2 mmol after drying in vacuo, 52 % conversion). The synthesis was done according to Wang et al. [192].

BET can be prepared in advance and stored at -20°C for the following [^{18}F]BFE syntheses.

5.2 Manually Operated Synthesis of [^{18}F]BFE and [^{18}F]FE@IPCIT

5.2.1 Legend

Equivalent or Equ.

In connection with the catalytic substances the terms “equivalent” and “equ” are used. In this context, one equivalent is defined as 1 µL of an aqueous solution of TBAH with a concentration of 80 µmol/100 µL.

Radiochemical Incorporation Yield

Radio**c**hemical **i**ncorporation **y**ield (RCIY) is a measure of how effective radioisotopes are incorporated by ligand molecules. RCIY is accessible with HPLC and expressed as a percentage of total radioactivity in the sample.

Time and activity

The starting time and the activity for every experiment are mentioned. Every time the activity was measured during an experiment, the interim was taken as well. Time is presented in parenthesis behind the corresponding activity value, e.g. MBq 100 (13:12).

Nomenclature of Experiments

Experiments are named according to the following pattern:

Experiment M.*xx* (M stands for manual synthesis and *xx* represents the number of the experiment)

Experiment A.*xx* (A stands for automated synthesis and *xx* represents the number of the experiment)

5.2.2 Protocols

5.2.2.1 Experiment M.1

purpose	Development of a set-up for the synthesis
miscellaneous	Dividing of radioactivity after azeotropic drying into three equal portions to perform the [^{18}F]BFE synthesis with three different reaction solvents;

activity$_{start}$ [GBq]	1.76	**starting time**	8:46

Extraction of [^{18}F]F$^-$ from $H_2{}^{18}O$ water

elution solution$_{cryptand}$	Kryptofix® 222	activity$_{vial}$ [MBq]	546
elution solution$_{volume}$ [mL]	0.8	activity$_{PS\text{-}HCO3}$ [MBq]	560

Azeotropic drying of [^{18}F]F$^-$

organic solvent$_{volume}$ [mL]	1	organic solvent$_{type}$	ACN
splitting of the radioactivity into 3 samples		activity$_{vial}$ [MBq]	500

Synthesis of [^{18}F]BFE

organic solvent$_{type}$ A	*o*-DCB	reaction time [min]	10
organic solvent$_{type}$ B	DMF	organic solvent$_{volume}$ [mL]	0.4
organic solvent$_{type}$ C	ACN	BET [µL]	30
temperature [°C]	100 (A), 100 (B), 80 (C)	activity vial A [MBq]	67
activity vial B [MBq]	136	activity vial C [MBq]	47

conclusion	No conversion of BET to [^{18}F]BFE; An equal sharing of the radioactivity into three portions could not have been accomplished: from approx. 500 MBq (after azeotropic drying), only 67, 136, and 47 MBq were found in the three vials; (probably the fluoride-18 sticks to the glass walls);

5.2.2.2 Experiment M.2

purpose	Solvent: evaluating different solvents for reaction BET to [^{18}F]BFE; Temperature: influence of temperature on the reaction;
miscellaneous	BET was dark red (should be colorless)

activity$_{start}$ [MBq]	918	**starting time**	9:12

Extraction of [^{18}F]F$^-$ from $H_2{}^{18}O$ water

elution solution$_{cryptand}$	Kryptofix® 222	activity$_{vial}$ [MBq]	651 (9:30)
elution solution$_{volume}$ [mL]	0.8		

Azeotropic drying of [^{18}F]F$^-$

temperature [°C]	110	organic solvent$_{volume}$ [mL]	1.2
organic solvent$_{type}$	ACN		

Synthesis of [^{18}F]BFE

organic solvent$_{type}$ (A)	*o*-DCB	reaction time [min]	10
organic solvent$_{type}$ (B)	DMF	organic solvent$_{volume}$ [mL]	0.5
organic solvent$_{type}$ (C)	ACN	temperature [°C]	110 (A), 100 (B), 85 (C)
BET [µL]	30		

Conversion: BET to [^{18}F]BFE (before distillation)

RCI$_{HPLC}$ [^{18}F]BFE (**A**) [%]	9	RCI$_{HPLC}$ [^{18}F]BFE (**B**) [%]	0
RCI$_{HPLC}$ [^{18}F]BFE (**C**) [%]	15		

conclusion	Splitting of the radioactivity was done <u>after</u> adding ACN (azeotropic drying step) and boiling it briefly to dissolve the [^{18}F]F$^-$. It still was not possible to divide the radioactivity equally. Experiment aborted because of a blocked tube during distillation of [^{18}F]BFE;

5.2.2.3 Experiment M.3

purpose	Conditions for trapping [^{18}F]BFE : solvents (DMF or DMSO) and various temperatures of the solvents (precooled or RT); Cotransport: Is there a cotransport of *o*-DCB during distillation?;
miscellaneous	It is known that *o*-DCB has negative effects on the reaction IPCITacid to [^{18}F]FE@IPCIT (therefore it cannot be used for trapping [^{18}F]BFE); oDBC is a suitable solvent for the reaction of BET to [^{18}F]BFE; *o*-DCB boils at 180°C; much higher than [^{18}F]BFE; this qualifies distillation as purification method for [^{18}F]BFE;

activity$_{start}$ [GBq]	1.10	**starting time**	9:15

Extraction of [^{18}F]F$^-$ from $H_2{}^{18}O$ water

elution solution$_{cryptand}$	Kryptofix® 222	elution solution$_{volume}$ [mL]	0.7

Azeotropic drying of [^{18}F]F$^-$

temperature [°C]	100	organic solvent$_{volume}$ [mL]	1
activity$_{vial}$ [MBq]	435 (10:23)	organic solvent$_{type}$	ACN

Synthesis of [^{18}F]BFE

organic solvent$_{type}$	*o*-DCB	reaction time [min]	10
temperature [°C]	100	BET in *o*-DCB [µL]	30
organic solvent$_{volume}$ [mL]	1.2	RCI$_{HPLC}$ [^{18}F]BFE [%]	80

Distillation: Purification of [^{18}F]BFE

splitting of the reaction mixture in 2 x 600 µL			
V-vial organic solvent$_{type}$ (A)	DMF	distillation temperature [°C]	100
V-vial organic solvent$_{type}$ (B)	DMSO	distillation time [min]	10
V-vial organic solvent$_{volume}$ [mL]	0.5	temperature of trap [°C]	RT
RCI$_{HPLC}$ [^{18}F]BFE (A) [%]	77	RCI$_{HPLC}$ [^{18}F]BFE (B) [%]	32
activity trap/reactor (A) [MBq]	37.5 / 24.6 (11:50)	activity trap/reactor (B) [MBq]	4 / 91.5 (11:50)

result	Nitrogen current: a more accurate regulation is required because too much *o*-DCB was carried over into the solvent of the trapping vial; A negative effect on the RCI of [^{18}F]FE@IPCIT was observed when high amounts of fluoride-18 were co-transported with [^{18}F]BFE into the trap; the most probable reason was a too strong nitrogen current;

5.2.2.4 Experiment M.4

purpose	Requirement of a catalyst: reaction between [^{18}F]BFE and IPCITacid without a catalytic substance; Concentration of precursor: solutions with different concentrations of IPCITacid are evaluated; What is the optimal reaction temperature for the reaction of IPCIT to [^{18}F]FE@IPCIT?;
miscellaneous	New set-up: a vial filled with DMSO between the primary trap (DMF) and the reactor shall absorb transported [^{18}F]F^- but not [^{18}F]BFE;

activity$_{start}$ [MBq]	742	**starting time**	10:00

Extraction of [^{18}F]F^- from $H_2{}^{18}O$ water

elution solution$_{cryptand}$	Kryptofix® 222	elution solution$_{volume}$ [mL]	0.7

Azeotropic drying of [^{18}F]F^-

temperature [°C]	100	organic solvent$_{volume}$ [mL]	1
organic solvent$_{type}$	ACN		

Synthesis of [^{18}F]BFE

organic solvent$_{type}$	*o*-DCB	reaction time [min]	10
temperature [°C]	100	BET in *o*-DCB [µL]	30
organic solvent$_{volume}$ [mL]	1	RCI$_{HPLC}$ [^{18}F]BFE [%]	87

Distillation: Purification of [^{18}F]BFE

gas-washing bottle$_{solvent}$	DMSO	gas-washing bottle$_{volume}$ [mL]	2
V-vial organic solvent$_{type}$ A	DMF	distillation temperature [°C]	100
V-vial organic solvent$_{volume}$ [mL]	0.5	distillation time [min]	10
RCI$_{HPLC}$ [^{18}F]BFE$_{washing\ bottle}$ [%]	92	temperature of trap [°C]	RT

Synthesis of [^{18}F]FE@IPCIT

catalyst	no	reaction time [min]	10
solvent$_{type}$	DMSO	solvent$_{volume}$ [µL]	50

temperature [°C]	60	130	150
IPCITacid [mg/mL]	1	1	1
product formation	no	no	no

conclusion	Concentration of [^{18}F]F^- was higher in the second vial (DMF) than in the first one (DMSO); Synthesis of [^{18}F]FE@IPCIT was performed with the DMSO solution; DMSO traps [^{18}F]BFE very effective (almost no [^{18}F]BFE reached the second vial filled with DMF);

5.2.2.5 Experiment M.5

purpose	TBAH as catalyst for the reaction of [^{18}F]BFE with IPCITacid; Is [^{18}F]BFE trapped quantitatively in the first DMSO filled vial?; Precursor concentration: 1 mg/mL or 2 mg/mL IPCITacid;
miscellaneous	Installation of 2 daisy-chained DMSO traps; Reaction temperature for [^{18}F]FE@IPCIT reaction:

activity$_{start}$ [MBq]	575	**starting time**	12:01

Extraction of [^{18}F]F$^-$ from $H_2{}^{18}O$ water

elution solution$_{cryptand}$	Kryptofix® 222	elution solution$_{volume}$ [mL]	0.7

Azeotropic drying of [^{18}F]F$^-$

temperature [°C]	100	organic solvent$_{volume}$ [mL]	1
activity$_{vial}$ [MBq]	327 (12:50)	organic solvent$_{type}$	ACN

Synthesis of [^{18}F]BFE

organic solvent$_{type}$ A	*o*-DCB	reaction time [min]	10
BET in *o*-DCB [µL]	30	organic solvent$_{volume}$ [mL]	1
temperature [°C]	100	RCI$_{HPLC}$ [^{18}F]BFE [%]	94

Distillation: Purification of [^{18}F]BFE

V-vial organic solvent$_{type}$	DMSO	distillation temperature [°C]	100
V-vial organic solvent$_{volume}$ [mL]	1	distillation time [min]	10
RCI$_{HPLC}$ [^{18}F]BFE [%]	98	activity$_{reactor}$ [MBq]	130 (13:20)
activity$_{DMSO1}$ [MBq]	114 (13:20)	activity$_{DMSO2}$ [MBq]	0.8 (13:20)

Synthesis of [^{18}F]FE@IPCIT

catalyst [equivalents]	1	solvent$_{volume}$ [µL]	50
catalyst$_{type}$	TBAH	solvent$_{type}$	DMSO

temperature [°C]	RT	100	130	150	RT	100	130	150
reaction time [min]	15	25	35	45	15	25	35	45
precursor [mg/mL]	1	1	1	1	2	2	2	2
product formation	yes	yes	yes	yes	yes	yes	yes	yes
RCI [^{18}F]FE@IPCIT [%]	3	55	56	56	5	43	48	49

conclusion	First trap contained almost the total activity in the form of [^{18}F]BFE; Formation of product: 100°C showed satisfying results (higher temperatures showed no improvement); Precursor concentration: 1 mg/mL shows good yields; were not increased by higher concentrations;

5.2.2.6 Experiment M.6

purpose	Precursor concentration: evaluation of concentrations of 1 mg/mL and below; Optimizing of temperature: 100°C and 130°C;
miscellaneous	Two vials in series filled with DMSO are now standard elements in the setting; Installation of a bubble counter for visualizing the nitrogen current;

activity$_{start}$ [GBq]	1.00	**starting time**	9:50

Extraction of [^{18}F]F$^-$ from $H_2{}^{18}O$ water

elution solution$_{cryptand}$	Kryptofix® 222	elution solution$_{volume}$ [mL]	0.7

Azeotropic drying of [^{18}F]F$^-$

temperature [°C]	100	organic solvent$_{volume}$ [mL]	1
organic solvent$_{type}$	ACN		

Synthesis of [^{18}F]BFE

organic solvent$_{type}$ A	*o*-DCB	organic solvent$_{volume}$ [mL]	1
BET in *o*-DCB [µL]	30	RCI$_{HPLC}$ [^{18}F]BFE [%]	83
temperature [°C]	100	reactor activity [MBq]	448
reaction time [min]	10		

Distillation: Purification of [^{18}F]BFE

V-vial organic solvent$_{type}$	DMSO	distillation temperature [°C]	100
V-vial organic solvent$_{volume}$ [mL]	1	distillation time [min]	10
RCI$_{HPLC}$ [^{18}F]BFE [%]	90	trap 2 [MBq]	20.8
trap 1 [MBq]	217 (11:20)		

Synthesis von [^{18}F]FE@IPCIT

catalyst [equivalents]	1	reaction time [min]	15
catalyst$_{type}$	TBAH	solvent$_{volume}$ [µL]	50
solvent$_{type}$	DMSO		

precursor [mg/mL]	0.25	0.5	1	2	0.25	0.5	1	2
temperature [°C]	100	100	100	100	130	130	130	130
product formation	no	no	no	no	no	no	no	no

conclusion	Approx. 50 % of the activity from the reactor can be trapped as [^{18}F]BFE; Bubble counter is an effective tool for the regulation of the nitrogen flow; No product was formed (reason unknown);

5.2.2.7 Experiment M.7

purpose	Catalyst solution: 2,5 equivalents of TBAH (2,5 volume);
miscellaneous	The reactor mixture ([^{18}F]BFE reaction) was distilled two times because the yield ([^{18}F]BFE) was comparably low (11 % of the reactor activity; mean value: approx. 50 %); Catalyst: addition of the double volume of solution (concentration not changed);

activity$_{start}$ [GBq]	1.70	**starting time**	14:20

Extraction of [^{18}F]F$^-$ from $H_2{}^{18}O$ water

elution solution$_{cryptand}$	Kryptofix® 222	elution solution$_{volume}$ [mL]	0.7

Azeotropic drying of [^{18}F]F$^-$

organic solvent$_{volume}$ [mL]	1	temperature [°C]	100
organic solvent$_{type}$	ACN		

Synthesis of [^{18}F]BFE

organic solvent$_{type}$	*o*-DCB	reaction time [min]	10
BET in *o*-DCB [µL]	30	organic solvent$_{volume}$ [mL]	1
temperature [°C]	100	RCI$_{HPLC}$ [^{18}F]BFE [%]	78
activity reactor [MBq]	773 (15:09)		

Distillation: Purification of [^{18}F]BFE

V-vial organic solvent$_{type}$	DMSO	distillation temperature [°C]	100
V-vial organic solvent$_{volume}$ [mL]	1	distillation time [min]	10
RCI$_{HPLC}$ [^{18}F]BFE 1st distillation	86	RCI$_{HPLC}$ [^{18}F]BFE 2nd distillation	83

Synthesis of [^{18}F]FE@IPCIT

reaction time [min]	15	catalyst$_{type}$	TBAH
solvent$_{type}$	DMSO	solvent$_{volume}$ [µL]	50

	catalyst [equivalents]	precursor [mg/mL]	temperature [°C]	RCI [^{18}F]FE@IPCIT [%]
A	1	2	100	14
B	1	2	135	14
C	2.5 (incl. 2.5 equ. water)	2	135	no product

conclusion	Second distillation of the reaction mixture ([^{18}F]BFE reaction): increased yield of [^{18}F]BFE but less pure (distillate contained more *o*-DCB and [^{18}F]F$^-$); Catalyst: no product formation with double volume of catalyst solution;

5.2.2.8 Experiment M.8

purpose	Catalyst solution: two equivalents of TBAH (double concentration of TBAH); New organic solvent as trapping agent;
miscellaneous	solvent in primary trap: ACN filled vial

activity$_{start}$ [GBq]	1.30	**starting time**	9:42

Extraction of [^{18}F]F$^-$ from $H_2{}^{18}O$ water

elution solution$_{cryptand}$	Kryptofix® 222	activity$_{vial}$ [MBq]	1200 (09:46)
elution solution$_{volume}$ [mL]	0.7		

Azeotropic drying of [^{18}F]F$^-$

temperature [°C]	100	organic solvent$_{volume}$ [mL]	1
activity$_{vial}$ [MBq]	920 (10:24)	organic solvent$_{type}$	ACN

Synthesis of [^{18}F]BFE

organic solvent$_{type}$	*o*-DCB	reaction time [min]	10
BET in *o*-DCB [µL]	30	organic solvent$_{volume}$ [mL]	1
temperature [°C]	100	RCI$_{HPLC}$ [^{18}F]BFE [%]	85
activity reactor [MBq]	825 (10:39)		

Distillation: Purification of [^{18}F]BFE

V-vial organic solvent$_{type}$	ACN	distillation temperature [°C]	100
V-vial organic solvent$_{volume}$ [mL]	1	distillation time [min]	10
RCI$_{HPLC}$ [^{18}F]BFE (ACN trap)	66	activity ACN trap [MBq]	500
re-distillation$_{ACN}$ into DMSO RCI$_{HPLC}$ [^{18}F]BFE [%]		82	

Synthesis of [^{18}F]FE@IPCIT

catalyst$_{type}$	TBAH	solvent$_{volume}$ [µL]	50
solvent$_{type}$	DMSO	catalyst solutionvolume [µL]	1

	catalyst [equ]	precursor [mg/mL]	temperature [°C]	reaction time [min]	RCI [^{18}F]FE@IPCIT [%]
A	1	2	100	20	28
A’	1	2	100	60	52
B	2	2	100	20	7
B’	2	2	100	60	9

conclusion	ACN traps [^{18}F]BFE effectively; Strong nitrogen current was applied and carried over *o*-DCB and ^{18}F$^-$ into the trap; A second distillation of [^{18}F]BFE from the ACN solution into DMSO produced a mixture of ACN, DMSO and [^{18}F]BFE; Catalyst: higher concentrated catalyst solution did not show improved conversion rates;

5.2.2.9 Experiment M.9

purpose	Catalyst solution: 2 equivalents of TBAH (double concentration of TBAH)

activity$_{start}$ [MBq]	923	**starting time**	10:10

Extraction of $^{18}F^-$ from $H_2{}^{18}O$ water

elution solution$_{cryptand}$	Kryptofix® 222	activity$_{vial}$ [MBq]	660 (11:04)
elution solution$_{volume}$ [mL]	0.8		

Azeotropic drying of $^{18}F^-$

temperature [°C]	100	organic solvent$_{volume}$ [mL]	1
activity$_{vial}$ [MBq]	437 (12:02)	organic solvent$_{type}$	ACN

Synthesis of [^{18}F]BFE

organic solvent$_{type}$	*o*-DCB	reaction time [min]	10
BET in *o*-DCB [µL]	30	organic solvent$_{volume}$ [mL]	1
temperature [°C]	100	RCI$_{HPLC}$ [^{18}F]BFE [%]	91

conclusion	Distillation of [^{18}F]BFE failed – in both traps there was no activity after distillation and there was also no activity in the reactor left – probably the distillation system was inadequately sealed;

5.2.2.10 Experiment M.10

purpose	Catalyst: added volumes were still 1 µL but the concentration was increased; Reaction time: evaluation of three different time frames for [^{18}F]FE@IPCIT reaction;
miscellaneous	Catalyst solution: 5-fold concentration of TBAH in one equivalent of water; Time frames: 15, 40 and 60 minutes;

activity$_{start}$ [GBq]	1.00	**starting time**	13:40

Extraction of $^{18}F^-$ from $H_2{}^{18}O$ water

elution solution$_{cryptand}$	Kryptofix® 222	activity$_{vial}$ [MBq]	896 (14:00)
elution solution$_{volume}$ [mL]	0.8		

Azeotropic drying of $^{18}F^-$

temperature [°C]	100	organic solvent$_{volume}$ [mL]	1
activity$_{vial}$ [MBq]	599 (14:59)	organic solvent$_{type}$	ACN

Synthesis of [^{18}F]BFE

organic solvent$_{type}$ A	*o*-DCB	reaction time [min]	10
BET in *o*-DCB [µL]	24	organic solvent$_{volume}$ [mL]	1
temperature [°C]	100	RCI$_{HPLC}$ [^{18}F]BFE [%]	91
activity reactor [MBq]	560 (15:10)		

Distillation: Purification of [^{18}F]BFE

V-vial organic solvent$_{type}$	DMSO	distillation temperature [°C]	100
V-vial organic solvent$_{volume}$ [mL]	1	distillation time [min]	10
RCI$_{HPLC}$ [^{18}F]BFE (1st trap) [%]	97	activity 1st trap [MBq]	271 (15:31)
activity 2nd trap [MBq]	9.2 (15:30)	activity$_{reactor}$ after dest [MBq]	120 (15:40)

Synthesis of [^{18}F]FE@IPCIT

temperature [°C]	100	catalyst$_{type}$	TBAH
solvent$_{type}$	DMSO	solvent$_{volume}$ [µL]	50

	catalyst [equ]	precursor [mg/mL]	reaction time [min]	RCI [^{18}F]FE@IPCIT [%]
A	1	1	15	62
A$_1$	1	1	15	65
B	5	2	15	0
B$_1$	5	2	15	0
A’	1	1	40	63
A$_1$’	1	1	40	68
B’	5	2	40	0
B$_1$’	5	2	40	0
A’’	1	1	60	0
A$_1$’’	1	1	60	0
B’’	5	2	60	0
B$_1$’’	5	2	60	0

conclusion	Catalyst: so far, higher concentrations than one equ. were not useful; Reaction time: 15 minutes seem to be an optimal time frame;

5.2.2.11 Experiment M.11

purpose	Precise examination of the catalyst concentration: two identical samples were prepared except for one difference: one vs. two equivalents of catalyst (in 1 µL)
miscellaneous	Two equ. of the catalyst were dissolved in the same volume of solvent as one equ.

$activity_{start}$ [MBq]	497	**starting time**	12:50

Extraction of $^{18}F^-$ from $H_2{}^{18}O$ water

$elution\ solution_{cryptand}$	Kryptofix® 222	$activity_{vial}$ [MBq]	497 (12:50)
$elution\ solution_{volume}$ [mL]	0.8		

Azeotropic drying of $^{18}F^-$

temperature [°C]	100	$organic\ solvent_{volume}$ [mL]	1
$activity_{vial}$ [MBq]	362 (13:35)	$organic\ solvent_{type}$	ACN

Synthesis of [^{18}F]BFE

$organic\ solvent_{type}$	*o*-DCB	reaction time [min]	40
BET in *o*-DCB [µL]	30	$organic\ solvent_{volume}$ [mL]	1
temperature [°C]	100	RCI_{HPLC} [^{18}F]BFE [%]	89

Distillation: Purification of [^{18}F]BFE

V-vial $organic\ solvent_{type}$	DMSO	distillation temperature [°C]	100
V-vial $organic\ solvent_{volume}$ [mL]	1	distillation time [min]	10
RCI_{HPLC} [^{18}F]BFE [%]	98		

Synthesis of [^{18}F]FE@IPCIT

reaction time [min]	15	$catalyst_{type}$	TBAH
temperature [°C]	100	precursor [mg/mL]	1
$solvent_{type}$	DMSO	$solvent_{volume}$ [µL]	50

	A	B	C	D
catalyst [equ]	1	1	2	2
RCI [^{18}F]FE@IPCIT [%]	38	55	0	0

conclusion	Both samples with high TBAH concentration failed

5.2.2.12 Experiment M.12

purpose	Catalysts: testing of other chemicals as catalytic substances; Distillation time: is a longer time frame beneficial?;
miscellaneous	Potential catalysts had the same concentration as TBAH (80 µmol/100 µL solvent) and alkaline chemicals; Distillation time: 90 minutes;

$activity_{start}$ [GBq]	1.08	**starting time**	10:57

Extraction of $^{18}F^-$ from $H_2{}^{18}O$ water

$elution\ solution_{cryptand}$	Kryptofix® 222	$activity_{vial}$ [MBq]	840 (11:12)
$elution\ solution_{volume}$ [mL]	0.7	$activity_{PS\text{-}HCO3}$ [MBq]	167 (11:13)

Azeotropic drying of $^{18}F^-$

temperature [°C]	100	$organic\ solvent_{volume}$ [mL]	1
$activity_{vial\_before\_ACN}$ [MBq]	640 (11:30)	$organic\ solvent_{type}$	ACN
$activity_{vial\_end}$ [MBq]	590 (11:44)		

Synthesis of [^{18}F]BFE

$organic\ solvent_{type}$	*o*-DCB	reaction time [min]	15
$activity_{after\_addition\_o\text{-}DCB}$ [MBq]	419 (11:57)	temperature [°C]	100
BET in *o*-DCB [µL]	30	$organic\ solvent_{volume}$ [mL]	1
RCI_{HPLC} [^{18}F]BFE [%]	78		

Distillation: Purification of [^{18}F]BFE

V-vial $organic\ solvent_{type}$	DMSO	distillation temperature [°C]	100
V-vial $organic\ solvent_{volume}$ [mL]	1	distillation time [min]	90
RCI_{HPLC} [^{18}F]BFE [%]	65	activity 1st trap [MBq]	98 (13:46)
activity 2nd trap [MBq]	16 (13:46)	$activity_{reactor}$ after dest [MBq]	58 (14:10)

conclusion	The experiment was stopped because of the high *o*-DBC concentration in the primary trap (long distillation time allowed oDBC to migrate from the reactor into the trap)

5.2.2.13 Experiment M.13

purpose	Catalysts: testing of new various chemicals as catalytic substances;
miscellaneous	Potential catalysts had the same concentration as TBAH (80 µmol/100 µL solvent) and alkaline chemicals;

activity$_{start}$ [GBq]	1.17	**starting time**	10:09

Extraction of $^{18}F^-$ from $H_2{}^{18}O$ water

elution solution$_{cryptand}$	Kryptofix® 222	activity$_{vial}$ [MBq]	765 (10:13)
elution solution$_{volume}$ [mL]	0.8	activity$_{PS\text{-}HCO3}$ [MBq]	217 (10:14)

Azeotropic drying of $^{18}F^-$

temperature [°C]	100	organic solvent$_{volume}$ [mL]	1
activity$_{vial}$ [MBq]	621 (10:40)	organic solvent$_{type}$	ACN

Synthesis of [^{18}F]BFE

organic solvent$_{type}$	*o*-DCB	reaction time [min]	15
BET in *o*-DCB [µL]	30	organic solvent$_{volume}$ [mL]	1
temperature [°C]	100	RCI$_{HPLC}$ [^{18}F]BFE [%]	79

Distillation: Purification of [^{18}F]BFE

V-vial organic solvent$_{type}$	DMSO	distillation temperature [°C]	100
V-vial organic solvent$_{volume}$ [mL]	1	distillation time [min]	10
RCI$_{HPLC}$ [^{18}F]BFE [%]	99.1	activity 1st trap [MBq]	188 (11:21)
activity 2nd trap [MBq]	11 (11:22)	activity$_{reactor}$ after dest [MBq]	136 (11:23)

Synthesis of [^{18}F]FE@IPCIT

reaction time [min]	10 and 15	catalyst$_{type}$	basic chemicals
temperature [°C]	100	precursor [mg/mL]	1
solvent$_{type}$	DMSO	solvent$_{volume}$ [µL]	50

	LiOH (A)	Cs_2CO_3 (B)	NaOH (C)	NEt_3* (D)	TBAH (E)
catalyst [equ]	1	1	1	1	1
RCI [^{18}F]FE@IPCIT (10 min) [%]	79	85	0	1	0
RCI [^{18}F]FE@IPCIT (15 min) [%]	83	80	0	2	0

*directly added 1 µL into the reaction mixture

conclusion	Catalytic substances: LiOH and Cs_2CO_3 showed a high level of catalytic activity;

5.2.2.14 Experiment M.14

purpose	Catalytic substances: retesting of the chemicals, which showed catalytic activity in experiment M.13

activity$_{start}$ [MBq]	780	**starting time**	09:40

Extraction of $^{18}F^-$ from $H_2{}^{18}O$ water

elution solution$_{cryptand}$	Kryptofix® 222	activity$_{vial}$ [MBq]	750 (09:40)
elution solution$_{volume}$ [mL]	0.8	activity$_{PS\text{-}HCO3}$ [MBq]	14 (09:41)

Azeotropic drying of $^{18}F^-$

organic solvent$_{volume}$ [mL]	1	temperature [°C]	100
organic solvent$_{type}$	ACN		

Synthesis of [^{18}F]BFE

organic solvent$_{type}$	*o*-DCB	reaction time [min]	15
BET in *o*-DCB [µL]	30	organic solvent$_{volume}$ [mL]	1
temperature [°C]	100	RCI$_{HPLC}$ [^{18}F]BFE [%]	84
activity$_{reactor}$ [MBq]	525 (10:27)		

Distillation: Purification of [^{18}F]BFE

V-vial organic solvent$_{type}$	DMSO	distillation temperature [°C]	100
V-vial organic solvent$_{volume}$ [mL]	1	distillation time [min]	15
RCI$_{HPLC}$ [^{18}F]BFE [%]	93	activity 1st trap [MBq]	222 (10:43)
activity 2nd trap [MBq]	9.7 (10:43)	activity$_{reactor}$ after dest [MBq]	204 (10:47)

Synthesis of [^{18}F]FE@IPCIT

reaction time [min]	15	catalyst$_{type}$	basic chemicals
temperature [°C]	100	precursor [mg/mL]	1
catalyst [equivalents]	1	solvent$_{volume}$ [µL]	50
solvent$_{type}$	DMSO		

	LiOH (A)	Cs_2CO_3 (B)	NEt_3* (C)	TBAH (D)
RCI [^{18}F]FE@IPCIT [%]	39	44	0	64

*directly added 1 µL into the reaction mixture

conclusion	Catalytic activity: confirmed for LiOH, Cs_2CO3 (and TBAH)

5.2.2.15 Experiment M.15

purpose	Test of different reaction mechanism: addition of iodide [193, 194]; Catalysts: testing of various new chemicals as catalytic substances;
miscellaneous	NaI and KI: sole use as catalysts; Catalytic mixture of NaI or KI with TBAH;

$activity_{start}$ [MBq]	536	**starting time**	10:25

Extraction of $^{18}F^-$ from $H_2{}^{18}O$ water

$elution\ solution_{cryptand}$	Kryptofix® 222	$activity_{vial}$ [MBq]	475 (10:33)
$elution\ solution_{volume}$ [mL]	0.8	$activity_{PS\text{-}HCO3}$ [MBq]	14 (10:34)

Azeotropic drying of $^{18}F^-$

temperature [°C]	100	$organic\ solvent_{volume}$ [mL]	1
$activity_{vial}$ [MBq]	352 (11:14)	$organic\ solvent_{type}$	ACN

Synthesis of [^{18}F]BFE

$organic\ solvent_{type}$	*o*-DCB	reaction time [min]	15
BET in *o*-DCB [µL]	30	$organic\ solvent_{volume}$ [mL]	1
temperature [°C]	100	RCI_{HPLC} [^{18}F]BFE [%]	90

Distillation: Purification of [^{18}F]BFE

V-vial $organic\ solvent_{type}$	DMSO	distillation temperature [°C]	100
V-vial $organic\ solvent_{volume}$ [mL]	1	distillation time [min]	15
RCI_{HPLC} [^{18}F]BFE [%]	95	activity 1st trap [MBq]	130 (11:45)

Synthesis of [^{18}F]FE@IPCIT

reaction time [min]	15	$catalyst_{type}$	basic chemicals
temperature [°C]	100	precursor [mg/mL]	1
catalyst [equivalents]	1	$solvent_{volume}$ [µL]	50
$solvent_{type}$	DMSO		

	LiOH (A)	Cs_2CO_3 (B)	TBAH (C)	NaI (D)	KI (E)
RCI [^{18}F]FE@IPCIT [%]	59	66	73	0	0

conclusion	Mixture of NaI or KI with TBAH: white precipitate was formed immediately after adding of the second chemical => experiment was not carried out; Sole use of KI or NaI as catalysts did not show any conversion;

5.2.2.16 Experiment M.16

purpose	Test of different reaction mechanism: addition of iodide [193, 194]; Elution of $^{18}F^-$: another cryptand molecule to eluate fluoride-18 form the cartridge;
miscellaneous	Catalytic mixture: NaI with NaH and KI with NaH; Elution of $^{18}F^-$: use of 18-crown-6 ether solution (15 mg 18-crown-6, 4.5 mg K_2CO_3, 0.7 mL ACN, and 0.3 mL H_2O) instead of Kryptofix® 222 solution;

activity$_{start}$ [MBq]	272	**starting time**	15:23

Extraction of $^{18}F^-$ from $H_2{}^{18}O$ water

elution solution$_{type}$	18-crown-6 ether	activity$_{vial}$ [MBq]	240 (15:26)
elution solution$_{volume}$ [mL]	0.8	activity$_{PS\text{-}HCO3}$ [MBq]	22 (15:25)

Azeotropic drying of $^{18}F^-$

temperature [°C]	100	organic solvent$_{volume}$ [mL]	1
activity$_{vial}$ [MBq]	194 (15:52)	organic solvent$_{type}$	ACN

Synthesis of [^{18}F]BFE

organic solvent$_{type}$	*o*-DCB	reaction time [min]	15
BET in *o*-DCB [µL]	30	organic solvent$_{volume}$ [mL]	1
temperature [°C]	100	RCI$_{HPLC}$ [^{18}F]BFE [%]	64

Distillation: Purification of [^{18}F]BFE

V-vial organic solvent$_{type}$	DMSO	distillation temperature [°C]	100
V-vial organic solvent$_{volume}$ [mL]	1	distillation time [min]	15
activity 1st trap [MBq]	15 (16:35)		

conclusion	RCI of [^{18}F]BFE dropped from avg. 90 % to 64 %; Distillation of [^{18}F]BFE did not yield enough activity (very low activity already before distillation) for further synthesis;

5.2.2.17 Experiment M.17

purpose	Test of different reaction mechanism: addition of iodide [193, 194]; Elution of $^{18}F^-$: another cryptand molecule to eluate fluoride-18 from the cartridge;
miscellaneous	Catalytic mixture: NaI + NaH and KI + NaH; Elution of $^{18}F^-$: use of 18-crown-6 ether solution (15 mg 18-crown-6, 4.5 mg K_2CO_3, 0.7 mL ACN, and 0.3 mL H_2O) instead of Kryptofix® 222solution; TBAH was already dissolved in water for one day and stored in a fridge

activity$_{start}$ [MBq]	738	**starting time**	10:30

Extraction of $^{18}F^-$ from $H_2{}^{18}O$ water

elution solution$_{type}$	18-crown-6 ether	activity$_{vial}$ [MBq]	625 (10:35)
elution solution$_{volume}$ [mL]	0.8	activity$_{PS\text{-}HCO3}$ [MBq]	56 (10:35)

Azeotropic drying of $^{18}F^-$

temperature [°C]	100	organic solvent$_{volume}$ [mL]	1
activity$_{vial}$ [MBq]	498 (11:05)	organic solvent$_{type}$	ACN

Synthesis of [^{18}F]BFE

organic solvent$_{type}$	*o*-DCB	reaction time [min]	15
BET in *o*-DCB [µL]	30	organic solvent$_{volume}$ [mL]	1
temperature [°C]	100	RCI$_{HPLC}$ [^{18}F]BFE [%]	64

Distillation: Purification of [^{18}F]BFE

V-vial organic solvent$_{type}$	DMSO	distillation temperature [°C]	100
V-vial organic solvent$_{volume}$ [mL]	1	distillation time [min]	15
RCI$_{HPLC}$ [^{18}F]BFE [%]	82	activity 1st trap [MBq]	80 (11:43)
activity 2nd trap [MBq]	12 (11:44)	activity$_{reactor}$ after dest [MBq]	205 (11:43)

Synthesis of [^{18}F]FE@IPCIT

reaction time [min]	15	catalyst$_{type}$	basic chemicals
temperature [°C]	100	precursor [mg/mL]	1
catalyst [equivalents]	1	solvent$_{volume}$ [µL]	50
solvent$_{type}$	DMSO		

	NaH (A)	TBAH (B)	NaI + NaH (C)	KI + NaH (D)
RCI [^{18}F]FE@IPCIT [%]	0	0	0	0

conclusion	RCI of [^{18}F]BFE was again worse than average (90 %) with only 64 %; Reaction of IPCITacid to [^{18}F]FE@IPCIT completely failed in all cases; TBAH should be prepared freshly for every experiment;

5.2.2.18 Experiment M.18

purpose	Catalysts: testing of various new chemicals as catalytic substances;
miscellaneous	TBAH was freshly prepared

activity$_{start}$ [MBq]	325	**starting time**	11:51

Extraction of $^{18}F^-$ from $H_2{}^{18}O$ water

elution solution$_{cryptand}$	Kryptofix® 222	activity$_{vial}$ [MBq]	297 (11:54)
elution solution$_{volume}$ [mL]	0.8	activity$_{PS\text{-}HCO3}$ [MBq]	9 (11:54)

Azeotropic drying of $^{18}F^-$

temperature [°C]	100	organic solvent$_{volume}$ [mL]	1
activity$_{vial}$ [MBq]	192 (13:00)	organic solvent$_{type}$	ACN
drying time [min]	40		

Synthesis of [^{18}F]BFE

organic solvent$_{type}$	*o*-DCB	reaction time [min]	15
BET in *o*-DCB [µL]	30	organic solvent$_{volume}$ [mL]	1
temperature [°C]	100	RCI$_{HPLC}$ [^{18}F]BFE [%]	83

Distillation: Purification of [^{18}F]BFE

V-vial organic solvent$_{type}$	DMSO	distillation temperature [°C]	100
V-vial organic solvent$_{volume}$ [mL]	1	distillation time [min]	15
RCI$_{HPLC}$ [^{18}F]BFE	99.5	activity 1st trap [MBq]	70 (13:33)
activity 2nd trap [MBq]	3 (13:36)	activity$_{reactor}$ after dest [MBq]	62 (13:35)

Synthesis of [^{18}F]FE@IPCIT

reaction time [min]	15	catalyst$_{type}$	basic chemicals
temperature [°C]	100	precursor [mg/mL]	1
catalyst [equivalents]	1	solvent$_{volume}$ [µL]	50
solvent$_{type}$	DMSO		

	NaH in H_2O (A)	TBAH (B)	NaI + NaH (C)	KI + NaH (D)	NaH in DMF (E)
RCI [^{18}F]FE@IPCIT [%]	0	78	0	0	0

conclusion	Catalytic activity: TBAH showed good conversion (indicating that reactants were in best order but the tested substances were not catalytically active)

5.2.2.19 Experiment M.19

purpose	Simulation of a module synthesis: developer name **M**odule **S**imulation **E**xperiment (MSE); Evaluation of several new alkaline substances as catalysts;
miscellaneous	MSE: [^{18}F]BFE was not trapped in solvent and then added to another solution with IPCITacid and a catalyst as before; this time the evaporated [^{18}F]BFE was conducted directly in a vial with a precursor (1 mg/mL) and a catalyst (TBAH) (as planned for the automated synthesis); Distillation of [^{18}F]BFE: simultaneously in two traps ("standard" and "MSE"); standard was the same experimental procedure as in Experiment M.1-18; New catalysts: used in a significantly higher concentration than TBAH (same volume);

activity$_{start}$ [GBq]	2.70	**starting time**	10:35

Extraction of $^{18}F^-$ from $H_2{}^{18}O$ water

elution solution$_{cryptand}$	Kryptofix® 222	activity$_{vial}$ [MBq]	2400 (10:37)
elution solution$_{volume}$ [mL]	0.8	activity$_{PS\text{-}HCO3}$ [MBq]	379 (10:38)

Azeotropic drying of $^{18}F^-$

temperature [°C]	100	organic solvent$_{volume}$ [mL]	1
activity$_{vial}$ [MBq]	1770 (11:10)	organic solvent$_{type}$	ACN

Synthesis of [^{18}F]BFE

organic solvent$_{type}$	*o*-DCB	reaction time [min]	15
BET in *o*-DCB [µL]	30	organic solvent$_{volume}$ [mL]	1
temperature [°C]	100	RCI$_{HPLC}$ [^{18}F]BFE	83

Distillation: Purification of [^{18}F]BFE

V-vial organic solvent$_{type}$	DMSO	distillation temperature [°C]	100
V-vial organic solvent$_{volume}$ [mL] for MSE	0.4	distillation time [min]	11
V-vial organic solvent$_{volume}$ [mL] for trap$_{standard}$	1	RCI$_{HPLC}$ [^{18}F]BFE trap$_{standard}$ [%]	87
activity$_{MSE}$ [MBq]	444 (11:49)	activity trap$_{standard}$ [MBq]	257 (11:48)

Synthesis of [^{18}F]FE@IPCIT

reaction time [min]	15	catalyst$_{type}$	basic chemicals
temperature [°C]	100	precursor [mg/mL]	1
solvent$_{type}$	DMSO	solvent$_{volume}$ [µL]	50

	TRIS (A)	Na_2 succinic acid (B)	KI + Cs_2CO_3 (C)	TBAH (MSE)
catalyst amount [µMol/ 50 µL]	240	185	92	40 (1 equ)
RCI [^{18}F]FE@IPCIT [%]	0	31	21	12

conclusion	MSE revealed a RCI of 12 % [^{18}F]FE@IPCIT

5.3 Module Assisted Synthesis of [^{18}F]BFE and [^{18}F]FE@IPCIT

5.3.1 Experiment A.1

purpose	Basic research: transfer of the reaction from manually operated syntheses to an automatized system; First goal: synthesis of [^{18}F]BFE;
miscellaneous	Trapping of [^{18}F]BFE: an external vial filled with DMSO was used for trapping of [^{18}F]BFE in the distillation process (instead of reactor 2 of the module); Temperature of the trap: precooled (0°C);

activity$_{start}$ [GBq]	1.58	**start time**	09:28

Synthesis of [^{18}F]BFE

trap: solvent$_{type}$	ACN
trap: solvent$_{volume}$	1000 µL

Activity Table

activity reactor1$_{after_dist}$	400 MBq

conclusion	Distillation: No [^{18}F]BFE was trapped --> whole activity remained in the reactor

5.3.2 Experiment A.2

purpose	Basic research: transfer of the reaction from manually operated syntheses to an automatized system;
miscellaneous	Trapping of [^{18}F]BFE: an external vial with DMF was used for trapping in the distillation process (instead of reactor 2 of the module); DMF was used as solvent for all reactions and for trapping [^{18}F]BFE;

activity$_{start}$ [GBq]	3.06	**start time**	08:37

Synthesis [^{18}F]BFE

trap: solvent$_{type}$	DMF
trap: solvent$_{volume}$ [µL]	500
V2	30 µL BET in 0.5 mL DMF

Activity Table

activity reactor1$_{elution_PS\text{-}HCO3}$ [MBq]	2110
activity reactor1$_{before_dist}$ [MBq]	1900
activity reactor1$_{after_dist}$ [MBq]	630 (09:57)
activity in trap$_{DMF}$ [MBq]	500 (09:58)

conclusion	Distillation: activity in the trap was caused by fluoride-18 (not [^{18}F]BFE)

5.3.3 Experiment A.3

purpose	Basic research: transfer of the reaction from manually operated syntheses to an automatized system
miscellaneous	Synthesis was divided into two parts: production of [^{18}F]BFE in the module and manual synthesis of [^{18}F]FE@IPCIT; trapping of [^{18}F]BFE in an external trap (instead of reactor 2);

activity$_{start}$ [GBq]	1.03	**start time**	09:25

Synthesis [^{18}F]BFE

trap: solvent$_{type}$	ACN
trap: solvent$_{volume}$ [µL]	1000
gas-wash bottle$_{solvent}$	DMF
gas-wash bottle$_{volume}$ [µL]	500
gas-wash bottle$_{activity}$ [MBq]	0.7

Activity Table

activity reactor1$_{elution_PS\text{-}HCO3}$ [MBq]	300
activity in trap$_{ACN}$ [MBq]	17
RCI$_{HPLC}$ [^{18}F]BFE in trap$_{ACN}$ [%]	64
RCI$_{HPLC}$ [^{18}F]BFE gas- wash bottle [%]	82

Synthesis [^{18}F]FE@IPCIT

	IPCITacid in ACN [µL]	ACN [µL]	IPCITacid [mg/mL]	temp. [°C]	time [min]	RCI [^{18}F]FE@IPCIT [%]
A_1	25	25	1	RT	10	0
B	12,5	37,5	0.5	RT	10	0
A_2	25	25	1	80	20	0
A_3	25	25	1	80	30	0

conclusion	Solvents for the trap (supposed to be ACN) and gas-wash (supposed to be DMF) bottle were interchanged; *o*-DCB and fluoride-18 were in the trap – in higher concentration than in the gas-washing bottle;

5.3.4 Experiment A.4

purpose	Basic research: transfer of the reaction from manually operated syntheses to an automatized system;
miscellaneous	Synthesis was divided in two sequential steps: production of [^{18}F]BFE in the module and manual synthesis of [^{18}F]FE@IPCIT in V-vials; Trapping of [^{18}F]BFE was realized in an external trap (instead of reactor 2);

activity$_{start}$ [MBq]	982	**start time**	10:02

Synthesis [^{18}F]BFE

trap: solvent$_{type}$	DMSO
trap: solvent$_{volume}$ [µL]	800
distillation time [min]	15
V2 [µL]	30 BET/1000 *o*-DCB
RCI$_{HPLC}$ [^{18}F]BFE in trap$_{DMSO}$ [%]	54
RCI$_{HPLC}$ [^{18}F]BFE in reactor1$_{post_dist}$ [%]	50

Activity Table

activity reactor1$_{elution_PS\text{-}HCO3}$ [MBq]	460
activity reactor1$_{before_dist}$ [MBq]	250 (11:00)
activity reactor1$_{after_dist}$ [MBq]	150 (11:20)

conclusion	Too much *o*-DCB was transported into the trap and for this reason, the synthesis was stopped

5.3.5 Experiment A.5

purpose	Distillation: R2 was used to trap [^{18}F]BFE (directly from R1)
miscellaneous	IPCITacid was dissolved in the DMSO (1 mg/mL) of R2, so the distillation was realized directly into a mixture for precursor and solvent; Catalyst: no catalytic substance was used;

activity$_{start}$ [GBq]	2.20	**start time**	14:29

Synthesis [^{18}F]BFE

reactor2: solvent$_{type}$	DMSO + IPCITacid
reactor2: solvent$_{volume}$ [µL]	400
distillation time [min]	10
V2 [µL]	30 BET/500 *o*-DCB
reaction time$_{[18F]BFE_synth}$ [min]	15
RCI$_{HPLC}$ [^{18}F]BFE reactor2 content [%]	40
RCI$_{HPLC}$ [^{18}F]FE@IPCIT reactor2 content [%]	0

Activity Table

activity reactor1$_{elution_PS\text{-}HCO3}$ [GBq]	2.1 (14:30)
activity reactor1$_{post_AZD}$ [GBq]	2.1 (14:32)
activity reactor1$_{before_dist}$ [GBq]	2.1 (14:50)
activity reactor1$_{after_dist}$ [MBq]	530 (15:10)
activity reactor2$_{after_dist}$ [MBq]	350 (15:10)
activity reactor2$_{after_quenching}$ [MBq]	240 (15:17)
activity reactor1$_{finally_remaining}$ [MBq]	50
activity loop waste [MBq]	2

conclusion	Distillation of [^{18}F]BFE from R1 to R2 was successful; Synthesis of [^{18}F]FE@IPCIT was not successful;

5.3.6 Experiment A.6

purpose	Catalyst: introduction of TBAH as catalytic substance
miscellaneous	Catalyst: mixture of DMSO and TBAH of R2 ([^{18}F]BFE in this mixture);

activity$_{start}$ [GBq]	13.60	**start time**	10:08

Synthesis [^{18}F]BFE

reactor2: solvent$_{type}$	DMSO + IPCITacid + TBAH
reactor2: solvent$_{volume}$ [µL]	400
RCI$_{HPLC}$ [^{18}F]BFE loop waste$_{crude}$ [%]	87
RCI$_{HPLC}$ [^{18}F]FE@IPCIT loop waste$_{crude}$ [%]	0

Activity Table

activity reactor1$_{elution_PS\text{-}HCO3}$ [GBq]	11.7 (10:30)
activity reactor1$_{post_AZD}$ [GBq]	11.4 (10:55)
activity reactor1$_{before_dist}$ [GBq]	8 (11:07)
activity reactor1$_{after_dist}$ [GBq]	3.5 (11:21)
activity reactor2$_{after_dist}$ [MBq]	900 (11:21)
activity reactor2$_{after_quenching}$ [GBq]	3.4 (11:35)
activity loop waste [MBq]	105

conclusion	No [^{18}F]FE@IPCIT was synthesized

5.3.7 Experiment A.7

purpose	Regulation of the helium flow: finding the optimal pressure for distillation
miscellaneous	Empty vial between R1 and R2 (supposed to trap less volatile compounds than [^{18}F]BFE); Bubble counter: experimental installation for visualizing the flow rate;

activity$_{start}$ [GBq]	21.40	**start time**	10:40

Synthesis [^{18}F]BFE + [^{18}F]FE@IPCIT

reactor2: solvent$_{type}$	DMSO + IPCITacid
reactor2: solvent$_{volume}$ [µL]	400
RCI$_{HPLC}$ [^{18}F]BFE in R2$_{post_dest}$ [%]	91
RCI$_{HPLC}$ loop waste$_{[18F]FE@IPCIT}$ [%]	6

Activity Table

activity reactor1$_{elution_PS\text{-}HCO3}$ [GBq]	13 (11:10)
activity reactor1$_{post_AZD}$ [GBq]	12.2 (11:36)
activity reactor1$_{before_dist}$ [GBq]	10 (11:45)
activity reactor1$_{after_dist}$ [GBq]	4.3 (12:00)
activity reactor2$_{after_dist}$ [GBq]	2.0 (12:00)
activity reactor2$_{after_quenching}$ [GBq]	1.7 (12:19)
activity loop waste [MBq]	435 (12:26)
activity reactor1$_{finally_remaining}$ [MBq]	500 (12:20)
activity bubble counter[MBq]	128 (12:30)
activity trap b/t. R1 & R2 (MBq)	728 (12:26)

conclusion	Helium current: a pressure of 2 - 4 kPa during distillation resulted in a suitable flow rate; trap proved itself to be useful (could theoretically be replaced with small silica column);

5.3.8 Experiment A.8

purpose	Catalytic substance: replacement of TBAH by Cs_2CO_3 (1 µL, 52 mg/50 µL)
miscellaneous	Content of R2 during distillation: DMSO, IPCITacid Cs_2CO_3 (more stable chemical)

activity$_{start}$ [GBq]	15.50	start time	10:20

Synthesis [^{18}F]BFE + [^{18}F]FE@IPCIT

reactor2: solvent$_{type}$	DMSO
reactor2: solvent$_{volume}$ [µL]	400
RCI$_{HPLC}$ [^{18}F]FE@IPCIT in loop waste [%]	2

Activity Table

activity reactor1$_{elution_PS\text{-}HCO3}$ [GBq]	11.7 (10:40)
activity reactor1$_{post_AZD}$ [GBq]	14 (11:04)
activity reactor1$_{before_dist}$ [GBq]	10.2
activity reactor1$_{after_dist}$ [GBq]	3.96 (11:32)
activity reactor2$_{after_dist}$ [GBq]	1.62 (11:32)
activity loop waste [GBq]	2.4 (11:40)
activity reactor1$_{finally_remaining}$ [MBq]	540 (11:50)

conclusion	Catalytic activity: [^{18}F]FE@IPCIT was formed but conversion was insufficient (2 %); Helium flow: an optimal flow rate for distillation results form a pressure of 3 - 6 kPa;

5.3.9 Experiment A.9

purpose	New method: adding precursor and catalyst after trapping [^{18}F]BFE Catalytic substance: changed back to TBAH;
miscellaneous	Trapping [^{18}F]BFE: pure DMSO in reactor2 for trapping [^{18}F]BFE; Reaction: IPCITacid and catalyst were added right before the reaction was started; Precursor concentration: final concentration of IPCITacid in R2 was 1 mg/mL;

activity$_{start}$ [GBq]	20.06	**start time**	09:40

Synthesis [^{18}F]BFE + [^{18}F]FE@IPCIT

reactor2 solvent$_{type}$	DMSO
reactor2 solvent$_{volume}$ [µL]	250
V3 content$_{type}$	DMSO + IPCITacid + cat
V3 content$_{volume}$ [µL]	250
Catalyst$_{type}$	TBAH
RCI$_{HPLC}$ [^{18}F]FE@IPCIT in loop waste [%]	15

Activity Table

activity reactor1$_{elution_PS\text{-}HCO3}$ [GBq]	18
activity reactor1$_{post_AZD}$ [GBq]	14 (10:40)

conclusion	Exhaust valve of R2 was blocked: distillation worked but only a little amount of [^{18}F]BFE was transferred; New procedure: promising results were obtained with the modified procedure (RCI of [^{18}F]FE@IPCIT: 15 %);

5.3.10 Experiment A.10

purpose	Production of a radiopharmaceutical
miscellaneous	Gas-washing bottle: installation of an ACN filled vial between R1 and R2; Trapping [^{18}F]BFE: pure DMSO in reactor2 for trapping [^{18}F]BFE; Detailed protocol of this experiment is given in the section "4.2.2 Example Experiment for an Automated Module Synthesis";

activity$_{start}$ [GBq]	12.30	**start time**	09:40

Synthesis [^{18}F]BFE + [^{18}F]FE@IPCIT

reactor2 solvent$_{type}$	DMSO
reactor2 solvent$_{volume}$ [µL]	250
V3 content$_{type}$	DMSO + IPCITacid + cat
V3 content$_{volume}$ [µL]	250
Catalyst$_{type}$	TBAH
Catalyst$_{concentration}$ [mg/100µL]	104
Catalyst$_{volume}$ [µL]	1
total activity$_{waste}$ [GBq]	1.7
activity of [^{18}F]FE@IPCIT [MBq]	272
RCI$_{HPLC}$ [^{18}F]FE@IPCIT in HPLC waste [%]	16

conclusion	Production of a pharmaceutical: failed because of technical difficulties with HPLC (program error); the positive result from the last experiment (5.3.9 Experiment A.9) was confirmed in this experiment by a RCI of 16 % for [^{18}F]FE@IPCIT;

5.4 HPLC

HPLC was a fundamental tool in the development of a synthesis route for [^{18}F]FE@IPCIT. Two different types were used: analytical HPLC for the identification of substances, and semi-preparative HPLC for the separation and purification of the product from the crude reaction mixture.

5.4.1 Analytical HPLC

5.4.1.1 Assay for Separation of Fluoride-18 and [^{18}F]BFE

Agilent Technologies 1200 Infinity Series HPLC (3.2 instrumentation) was used for identification and quantification (RCI).

column	Phenomenex Prodigy™ 5 µm Phenyl-3 (PH-3)
mobile phase$_{\text{organic component}}$	ACN (50 %)
mobile phase$_{\text{aqueous component}}$	0.1 M ammonium formate (50 %)
mode of mixing	premixing
flow rate [mL/min]	2
loop volume [µL]	20
detection	radio detector
sample solvent	*o*-DCB
sample	radioactive [^{18}F]BFE
retention time $_{18F^-}$ [min]	1.6 - 1.8 (k' = 1.29 - 1,57)
retention time$_{[18F]BFE}$ [min]	3.3 - 3.8 (k' = 3.7 - 4.29)

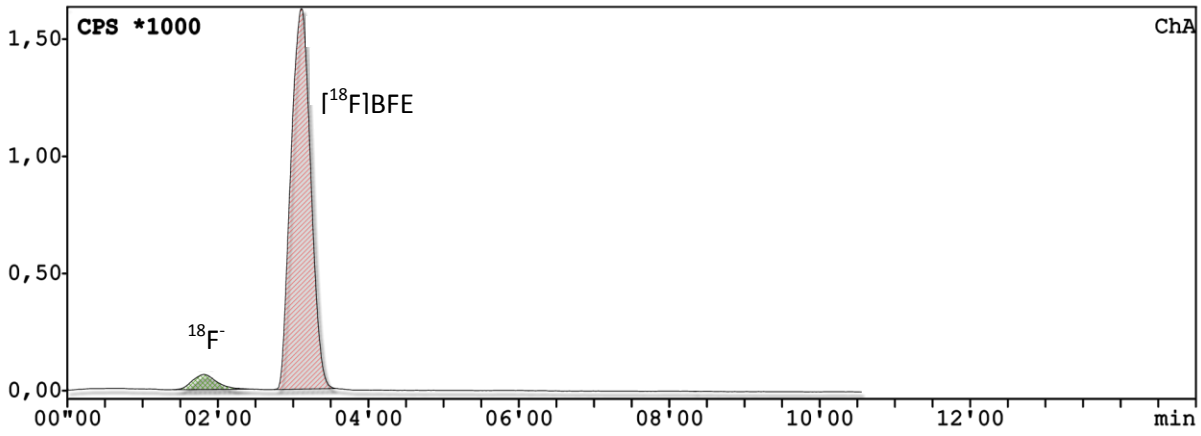

Figure 33: Chromatogram from fluoride-18 and [^{18}F]BFE (experiment M.16)

5.4.1.2 Assay for Separation of IPCITacid and [^{18}F]FE@IPCIT

column	Chromolith Performance RP-18e
mobile phase$_{\text{organic component}}$	ACN (30 %)
mobile phase$_{\text{aqueous component}}$	acidic water* (70 %)
mode of mixing	premix
flow rate [mL/min]	2

loop volume [µL]	20
detection	UV (or radio detection for [^{18}F]FE@IPCIT)
wave length [nm]	238 and 255
sample solvent	DMSO
sample	IPCITacid cold FE@IPCIT
retention time$_{IPCITacid}$ [min]	1.5 - 1.8 (k' = 1.14 - 1.57)
retention time$_{FE@IPCIT}$ [min]	3.7 - 4.0 (k' = 4.29 - 4.71)

*acidic water: 2.5 g NH_4Ac, 25 mL CH_3COOH, and filled up with water (dist.) to 1000 mL

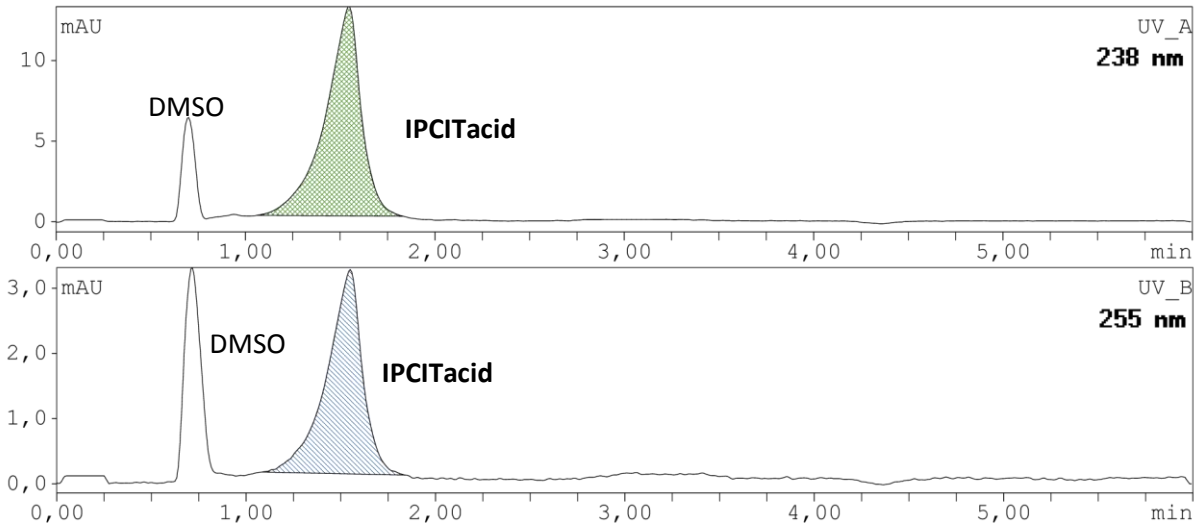

Figure 34: Chromatogram of IPCITacid (UV-detection); first peak is caused by the solvent of IPCITacid (DMSO)

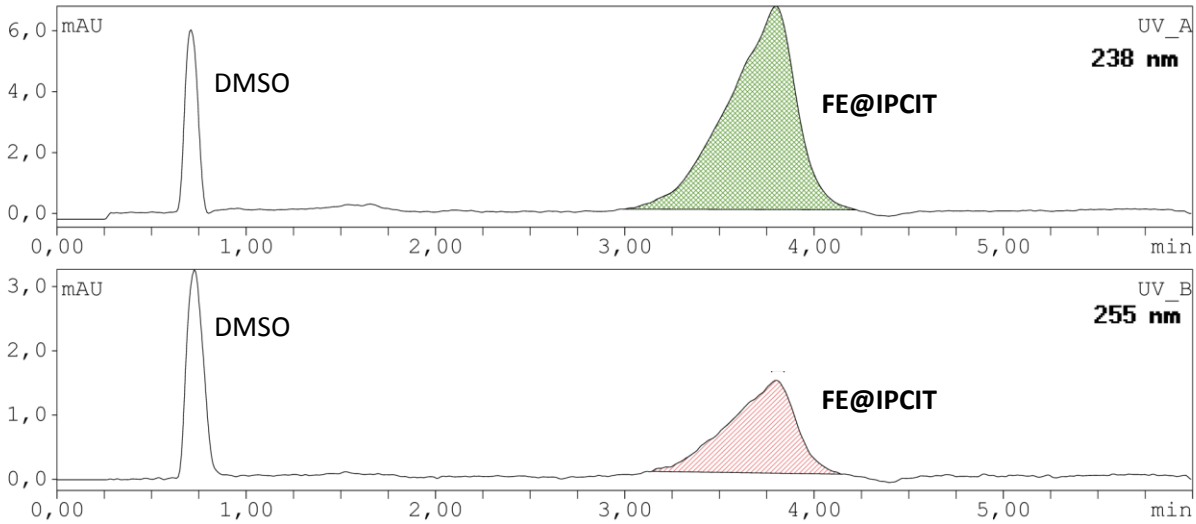

Figure 35: Chromatogram of FE@IPCIT (UV-detection); first peak is caused by the solvent of FE@IPCIT (DMSO)

5.4.2 Semi-preparative HPLC

5.4.2.1 Assay

column	Chromolith Performance RP-18e
mobile phase$_{\text{organic component}}$	ACN (30 %)
mobile phase$_{\text{aqueous component}}$	acidic water (70 %)
mode of mixing	premix
flow rate [mL/min]	5
loop volume [µL]	500
detection	UV
sample solvent	DMSO
sample	cold IPCITacid FE@IPCIT
wave length [nm]	238
retention time$_{\text{IPCITacid}}$ [min]	2.99 (k' = 2.52)
retention time$_{\text{FE@IPCIT}}$ [min]	9.75 (k' = 10.47)

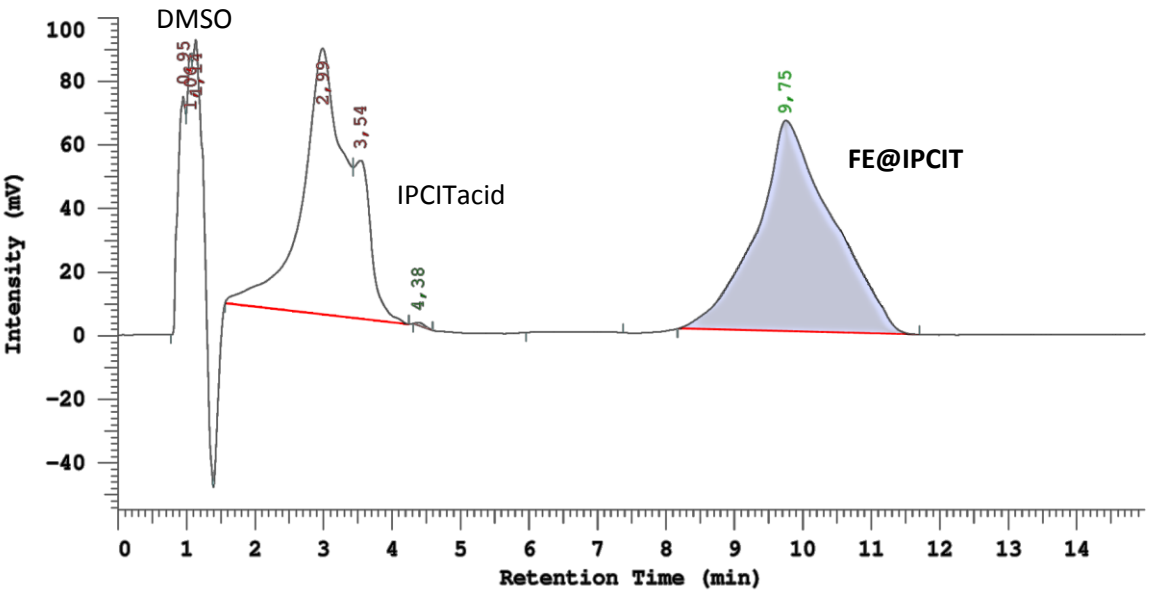

Figure 36: Chromatogram of FE@IPCIT by semi-preparative HPLC (colored area), IPCITacid elutes in the second peak

6 Results

In the tables, the experiments are abbreviated with “exp + number”.

6.1 Manually Operated Syntheses of [^{18}F]FE@IPCIT

6.1.1 Synthesis Results of [^{18}F]BFE and [^{18}F]FE@IPCIT

	activity$_{start}$ [MBq]	**RCI$_{[18F]BFE}$ [%]** (before dist.)	**RCI$_{[18F]BFE}$ [%]** (after dist.)	**activity$_{[18F]BFE}$ [MBq]**	**activity$_{[18F]BFE}$ [MBq]** (decay corrected)	**RCI$_{[18F]FE@IPCIT}$ [%]** (decay corrected)
exp 1	1764	-	-	-	-	-
exp 2	918	-	-	-	-	-
exp 3	1100	80	77	29	77	7
exp 4	742	87	92	-	-	-
exp 5	575	94	98	116	191	33
exp 6	1000	83	90	195	344	34
exp 7	1700	83	78	-	-	-
exp 8	1300	85	82	330	330	25
exp 9	923	91	-	-	-	-
exp 10	1000	91	97	263	524	52
exp 11	497	89	98	-	-	-
exp 12	1075	78	65	64	186	17
exp 13	1170	79	99	186	293	25
exp 14	780	84	93	206	307	39
exp 15	536	90	95	124	206	38
exp 16	272	64	-	-	-	-
exp 17	738	64	82	74	117	16
exp 18	325	83	99	70	133	41
exp 19	2700	83	87	610	967	36

[^{18}F]BFE syntheses were successful in 17 of 19 experiments. [^{18}F]BFE was produced in sufficient yields (16.8 ± 7.5 %, n = 12). The preparation of highly-pure [^{18}F]BFE was also accomplished (mean value [^{18}F]BFE: 78 ± 30 %; max. purity > 99 % [^{18}F]BFE after distillation, n = 17). The best results of extraction were obtained by 0.8 mL elution solution and Kryptofix® 222 as cryptand for [^{18}F]F^{-}. Azeotropic drying started with evaporating water at 100°C aided by a gentle nitrogen current (40 mL/min). When the substance was dry, a further 0.5 mL ACN was added and evaporated again. The act of adding ACN and evaporating was repeated two times. Synthesis of [^{18}F]BFE was performed in *o*-DCB (1 mL) as reaction solvent, 30 µL BET, and dried [^{18}F]F^{-}. The reaction time was 15 minutes, and the reaction temperature was 100°C. Purification was done by distilling [^{18}F]BFE for 15 minutes

at 100°C into a vial containing 1 mL precooled DMSO. The transport of [^{18}F]BFE was aided by a smooth nitrogen flow. The strength of the stream influenced the yield and purity significantly.

Optimum reaction parameters for [^{18}F]BFE synthesis

temperature	reaction time	precursor amount	solvent	solvent volume
100°C	15 min	30 µL	*o*-DCB	1 mL

[^{18}F]Fluoroalkylation was performed in manual syntheses with comparably low activities. The experiments were done to investigate reaction parameters such as precursor concentration, solvent, reaction temperature, catalytic substances (alkaline), and reaction time. The best results were obtained with a precursor concentration of 1 mg/mL. Higher concentrations had no negative effect, but RCI was also not improved. Concentrations below 1 mg/mL showed reduced RCIYs. Among all tested solvents, DMSO was the most advantageous for two reasons: The reaction of IPCITacid to [^{18}F]FE@IPCIT was successful, and DMSO was used as a trapping agent for [^{18}F]BFE during the distillation process. Temperatures were tested from RT (RCI of 2.9 %) up to 150°C. The best results were achieved at 100°C (RCI 55 % - 83 %). Regarding the reaction time, time frames in between 10 and 40 minutes were tested, thus best yields were obtained after 15 minutes reaction time. Extensive testing was done with catalytic substances as it is explained in section “6.1.2 Catalysts”.

Optimum reaction parameters for [^{18}F]FE@IPCIT synthesis

temperature	reaction time	precursor concentration	solvent	catalyst
100°C	15 min	1 mg/mL	DMSO	TBAH (1 equ)

6.1.2 Catalysts

Reaction mixtures were analyzed with HPLC. Results are given as percent RCI of [^{18}F]FE@IPCIT. Not listed experiments were not successful.

	TBAH	Cs_2CO_3	Na_2 succinic acid	KI + Cs_2CO_3	NEt_3	LiOH
exp 5	56					
exp 6	0					
exp 7	14					
exp 8	52					
exp 10	68					
exp 11	55					
exp 13	0	80			2	83
exp 14	64	44			0	39
exp 15	73	66				59
exp 18	78					
exp 19	12		31	21		

NaH, NaH (DMF), TRIS, KI, NI and NaOH were tested as well, but no catalytic effect was observed. Combinations of these chemicals, e.g. NaH with KI or NaI, did not show any conversion either. The best results were obtained with TBAH (1 µL, aqueous solution), Cs_2CO_3, and LiOH as catalytic substances. The highest grade of conversion was achieved with LiOH. An unexpected finding was that a higher concentration of TBAH influenced the conversion negatively.

6.2 Module Assisted Synthesis of [^{18}F]FE@IPCIT

experiment	**activity$_{start}$ [GBq]**	**duration [min]**	**activity$_{[18F]FE@IPCIT}$ [MBq]**	**activity$_{[18F]FE@IPCIT}$ [MBq]** (decay corrected)	**RCI $_{[18F]FE@IPCIT}$ [%]** (decay corrected)
7	21,40	106	26	51	0.24
8	15,50	80	50	83	0.53
10	12,30	261	272	1414	11.50

Although optimum conditions, as examined in manual syntheses, were used for module syntheses, only modest RCIYs were achieved (2.2 % overall in the best case). Furthermore, the reaction of IPCITacid to [^{18}F]FE@IPCIT revealed considerably low RCI yields (12 %). A smooth helium stream with an initial pressure of 2 - 4 kPa was used to accelerate azeotropic drying and distillation. A significant improvement was achieved by a modification of the distillation process. In the first attempts, evaporated [^{18}F]BFE was trapped in a mixture of DMSO, precursor and catalyst. The key step was to trap it in pure DMSO and add a solution of DMSO, precursor, and catalyst right before the reaction was started. By this action, the yield was remarkable improved (22-fold increased by comparison of exp. 8 to exp. 10).

7 Discussion

The main aim was to develop a synthesis route for the new potential DAT tracer [^{18}F]FE@IPCIT. At the beginning, manual experiments (n = 19) with comparably low activities (mean value: 1.006 ± 0.559 GBq) were performed to test and optimize various reaction parameters such as temperature, catalysts, time, precursor concentration, and solvents. After finding optimum conditions, the reaction was transferred to module assisted synthesis. Another goal was to establish a chromatographic identification and purification protocol for HPLC. FE@IPCIT is supposed to combine advantageous features from two other tracers, IPCIT and PE2I. The synthesis of the precursor IPCITacid was already done in a previous work [183].

In preliminary preclinical examinations, the affinity of FE@IPCIT to DAT, SERT, and NET was examined. The affinity to DAT was found to be high (1.33 ± 0.2 nM), but the affinity to SERT was not significantly lower (2.4 ± 1 nM). However, a selectivity of 1.8-fold towards SERT was regarded as high enough, due to the high abundance of dopamine transporter sites in the human brain (B_{max} ~ 200 pmol/g, human putamen) [195]. Lipophilicity was tested as an indicator for BBB penetration and selectivity. A compound needs a certain level of lipophilicity to penetrate the BBB. Too lipophilic substances show high unspecific binding. That means, they have a high affinity towards all kinds of lipophilic structures and plasma proteins. As a consequence, the bioavailability is low and the background noise increased. LogD values are a suitable measurement for lipophilicity. A method to access logD values is by using HPLC equipped with a polymeric ODP-50 column. LogD values are poor predictors for BBB penetration, but tPSA values can be calculated (29.54 for FE@IPCIT), which are more suitable to compare BBB penetration of different substances. According to Yoon et al., a tPSA value below 60 indicates BBB penetration [186]. Another experiment used in this context is IAM chromatography. This HPLC technique is used to evaluate new compounds by comparison with known substances. With 8.94, FE@IPCIT revealed a comparably high permeability value P_M (PE2I: 3.15 and RTI-55: 0.31) [183].

The synthesis work started with the manual preparation of [^{18}F]BFE. The cyclotron delivered fluoride-18 as solution of water ($H_2{}^{18}O$) and [^{18}F]F^-. The removal of water and iteratively azeotropic drying did not cause any significant problems. The best results were obtained with Kryptofix® 222 in the eluting solution (18-crown-6 ether in experiment M.16 and M.17, lower yields), 100-110°C for drying, and a gentle nitrogen current to accelerate evaporation. In the experiments M.1 and M.2, it was tried to split the activity. In the first attempt, splitting was done after azeotropic drying. *o*-DCB was added to the dried fluoride and the solution was divided in three portions, but most of the activity remained in the vial where the drying process was carried out.

The precursor, BET, was already prepared by another facility but it turned out that the quality was insufficient (experiments M.1 and M.2). The substance was dark red instead of colorless. Hence, by starting with the third experiment, freshly prepared BET was used (sufficient grade of purity was confirmed by NMR spectroscopy). Experiment M.3 was the first experiment with a successful [^{18}F]BFE synthesis. In experiment M.12, the reaction time was set to 15 minutes and showed good results. It has to be mentioned that a reaction time of ten minutes showed similar RCIY (experiment M.3 - M.11, 8 syntheses thereof finished successfully). A reaction temperature of 100°C examined in experiment M.3 and considered as promising. Henceforth, this temperature was used for all [^{18}F]BFE syntheses.

[^{18}F]BFE was purified by distillation. It was possible to use this technique, since [^{18}F]BFE was the most volatile compound in the reaction mixture. Several reasons support the use of distillation as purification technique: 1) the effective removal of *o*-DCB (reaction solvent), 2) almost quantitative purification from [^{18}F]F$^-$, 3) sufficient amounts of [^{18}F]BFE in the distillate (in 9 of 17 cases), 4) easy to adapt to module assisted syntheses, and 5) allowing an easy upscale (for higher activities). An important aspect was the complete tightness of the system. The removal of *o*-DCB was crucial because the reaction of [^{18}F]BFE with IPCITacid was sensitive to *o*-DCB, as findings of pretests showed.

Precooled DMSO proved to be the most appropriate trapping agent for evaporated [^{18}F]BFE referring to what was found out in experiments M.3, M.4, and M.5. The first of two gas-wash bottles, linked in series, contained almost the whole amount of [^{18}F]BFE, whereas in the second bottle only little activity was found (valid for all experiments with DMSO in the first trap). A further reason for the use of DMSO was that the [^{18}F]BFE-DMSO solution could be used without any further manipulation in the following [^{18}F]FE@IPCIT synthesis. It was discovered that ACN also traps [^{18}F]BFE in almost quantitative manner, but *o*-DCB and ^{18}F$^-$ were also retained in a high grade (experiment M.8). The experiment was not validated, but another experiment under similar conditions was performed: In Experiment A.3, ACN was also used as a trapping agent, leading to a similar result (RCIY [^{18}F]BFE 66 %).

The distillation was supported by a moderate nitrogen flow to facilitate the transfer of [^{18}F]BFE. The process of finding the optimal flow rate was challenging: In initial syntheses, gas-wash bottles were necessary due to difficulties with the regulation of the nitrogen current. A too strong current carried beside [^{18}F]BFE also *o*-DCB and fluoride-18 into the trap. In contrast, a too weak current resulted in low yields, since large quantities of [^{18}F]BFE remained in the reactor. After the installation of a bubble counter (experiment M.6), the gas flow was precisely adjustable and a gas-wash bottle was no longer required. Good results were achieved with a flow of ≤ 40 mL/min. In further experiments, the

procedure was optimized and it was finally accomplished to produce [^{18}F]BFE of high purity (> 99 %, experiments M.13 and M.18). In average, RCIYs were 20 - 30 % (not decay corrected). The decay corrected yields in percentage of total activity are shown in diagram 1.

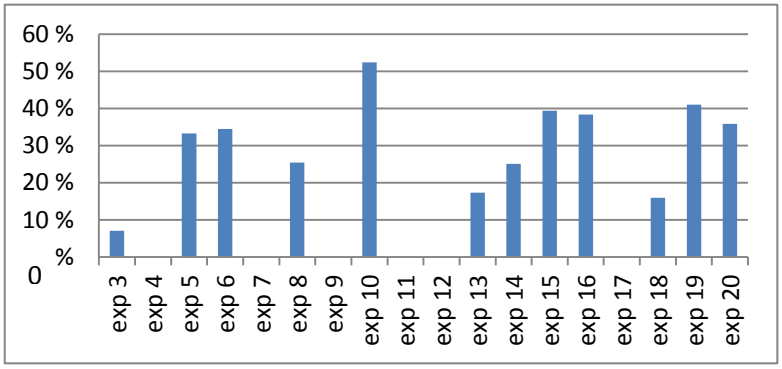

Diagram 1: Decay corrected RCI of [^{18}F]BFE in percent

Different organic solvents (DMSO, ACN, DMF, *o*-DCB) were screened in order to find a suitable one for the reaction of IPCITacid with [^{18}F]BFE. *o*-DCB showed good results in the synthesis of [^{18}F]BFE, but no reaction occurred between IPCITacid and [^{18}F]BFE in *o*-DCB, as preliminary experiments revealed. ACN was also tested, but a mixture of two solvents (ACN as reaction solvent and DMSO from trapping [^{18}F]BFE) did not yield any product (experiment M.8). Since DMSO was established as a trapping agent for [^{18}F]BFE in the distillation process, it was a logical consequence to try it as a reaction solvent as well. Overall, DMSO showed good results in the synthesis of [^{18}F]FE@IPCIT and was henceforth used for experiments (experiments M.4 - M.19).

Furthermore, different reaction temperatures were evaluated, from room temperature up to 150°C (experiments M.4 - M.7). Between one and three experiments were performed for every temperature.

temperature [C]	**RT**	**60**	**100**	**130**	**135**	**150**
RCI [^{18}F]FE@IPCIT [%]	4	-	55	40	14	55

These experiments revealed that temperatures of more than 100°C do not result in higher yields. Below 100°C, almost no product was formed (RCI: 4 %, experiment M.5). Hence, a reaction temperature of 100°C was used for all experiments from experiment M.8 on. The low RCI at 135°C (experiment M.7) was an unexpected result and is not consistent with comparable experiments. Most probably, the low RCI is attributable rather to an experimental error than to the temperature.

Moreover, various reaction times were tested. After a reaction time of 15 minutes, no more product was formed (experiments M.8 and M.10), thus a plateau was reached. In experiment M.13 it was shown that 10 minutes are sufficient for product formation. For further experiments, it seemed reasonable to use 15 minutes of reaction time to ensure a full conversion.

One more parameter to evaluate was the concentration of the precursor IPCITacid in the reaction mixture. In order to find the optimum condition, various concentrations from 0.25 up to 2 mg/mL

IPCITacid in DMSO were screened (experiment M.5, M.6, M.7, M.9, and M.11). It was shown that concentrations higher than 1 mg/mL did not result in higher yields whereas concentrations below 1 mg/mL did not allow optimal conversion. Finally, a concentration of 1 mg/mL was considered as most promising.

The reaction of IPCITacid with [^{18}F]BFE to [^{18}F]FE@IPCIT took only place in presence of a catalytic substance, which was proved in experiment A.4 and experiment A.5. Both experiments were performed without a catalyst and in both cases no [^{18}F]FE@IPCIT was formed – independently of reaction time and temperature.

Ten different alkaline chemicals were tested for their catalytic potential. Their conversion results are shown in diagram 2. Three substances, TBAH (experiment M.5 - M.19), Cs_2CO_3, and LiOH (both in experiments M.13, M.14 and M.15) showed good conversion rates. TBAH was an effective catalyst in terms of conversion to [^{18}F]FE@IPCIT (averaged RCI 43 ± 28.7 %, n = 11, best result 78 %). Since it is an organic substance, it may lack the (chemical) stability of inorganic compounds such as Cs_2CO_3 and LiOH. This was not relevant for manual synthesis, but it could be essential to have robust catalysts for automated synthesis. For application, TBAH was dissolved in water with a concentration of 80 µmol/100 µL (defined as one equivalent). The volume of the added catalyst solution was 1 µL. Both, volume and concentration, were optimal since every deviation from these parameters resulted in worse conversion rates (experiment M.7, M.8, M.10 and M.11). In experiment M.7, two identical samples were prepared – except for the volume of the added catalyst solution (2,5 µL vs. 1 µL). In the sample with an increased volume of the catalyst solution, no conversion was observed. The RCI of the control sample was 14 %. It was known that water has an aversive effect on the conversion rate. According to this, experiment M.8 was carried out with a higher concentrated TBAH solution (160 µmol/100 µL) to increase the amount of catalyst without adding a bigger volume of water (1 µL). Again, test samples (n = 2) and control samples were prepared (same conditions except for the concentration of the catalyst solution). The result confirmed the findings from experiment M.7: the samples with

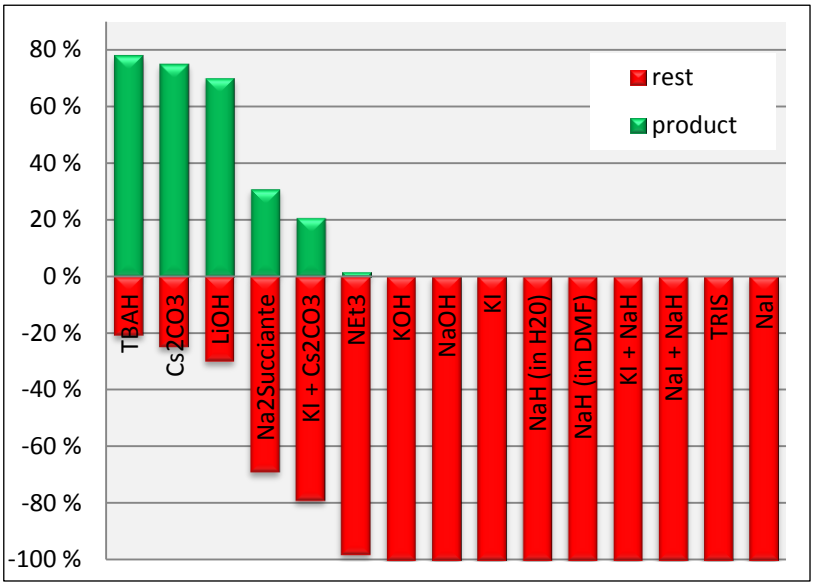

Diagram 2: Dependency of RCI on the catalytic substance in percent

increased TBAH content showed poor conversion rates (RCI: 7 % and 9 %), whereas the control samples resulted in an RCI of 28 and 52 %. In experiment M.9, the intention was to use stoichiometric amounts of TBAH (saturated solution, 400 µmol/100 µL). But, as it happened in experiments M.7 and M.8, the samples with high TBAH content showed again diminished product formation. Experiment M.11 had the same experimental design as experiment M.8. It confirmed that increased TBAH concentrations exhibit a negative effect on conversion rates (RCI: test samples 0 %, control samples 38 and 55 %, n = 2).

In most experiments, one sample was prepared with one equivalent TBAH as catalyst. This aspect was especially important when different potential catalytic substances were tested, because the conversion rate of TBAH was used for comparison and evaluation of catalytic activity.

Especially strong bases (NaH, NaOH) turned out to be inadequate catalysts (experiment M.13, M.18). Thereof only LiOH revealed a high catalytic activity (average RCI: 60 %, n = 3, 1 µL, 80 µmol/100 µL) and may be a suitable catalyst for module assisted syntheses. Even higher radiochemical incorporation was achieved with Cs_2CO_3 (average RCI: 63 %, n = 3, 1 µL, 80 µmol/100 µL).

The sodium salt of succinic acid was used in experiment M.19 and demonstrated catalytic properties (RCI 31 %). An unexpected finding was that the highly concentrated succinic acid solution (185 µmol/100 µL, 2.3 equ.) showed product formation since high concentrations of TBAH resulted in diminished conversions rates.

It was reported that the addition of KI or NaI improved conversion in similar experiments [193, 194]. However, no positive effects were observed in the presented experiments. The attempt to use a mixture of TBAH and KI or NaI as catalyst failed because the mixed substances precipitated immediately (experiment M.15). Also in experiment M.15, two samples were prepared using pure KI respectively NaI as catalyst. No product formation was observed for both samples. The negative effect of KI on the conversion rate was confirmed by experiment M.19: KI, water and Cs_2CO_3 were mixed and used as catalytic solution. The observed conversion rate (RCI: 21 %) was worse than for pure Cs_2CO_3.

After the optimization of reaction parameters in small-scale experiments, the next stage was to proceed with automated module syntheses. During manual syntheses, the activities were comparably low (mean value = 1.006 ± 7.51 GBq, max. 2.7 GBq, n = 19). On the contrary for module syntheses, where the average start activities were remarkable higher (9.95 ± 7.89 GBq, n = 10, min. 0.98 GBq, and max. 21.4 GBq).

Also for automated syntheses, the first step was the extraction of fluoride-18 from $H_2{}^{18}O$, delivered by the cyclotron. An ion exchange cartridge was used to bind the fluoride-18, while the $H_2{}^{18}O$ water was collected in a vial for recycling. The elution of the cartridge with a Kryptofix® 222 solution was followed by azeotropic drying in reactor1. Subsequently, BET (30 µL) dissolved in oDBC (500 µL) was added from reservoir2. The distillation was difficult because the regulation mechanism of the helium flow was imprecise. Finally, an initial pressure between 2 - 4 kPa (experiment A.7) resulted in a suitable flow. In experiments A.1 - 5, only the synthesis of [^{18}F]BFE was carried out in the module. During distillation, [^{18}F]BFE was transferred into an external vial for further use. The successful synthesis and trapping of [^{18}F]BFE in experiment A.5 allowed moving on to the next stage, which meant to trap [^{18}F]BFE in reactor2.

Another question came up concerning the precursor IPCITacid in connection with the distillation. Is it possible to trap [^{18}F]BFE in a solution of DMSO with dissolved IPCITacid and catalyst? The answer – "no" – was given in experiment A.7 and A.8, confirmed in experiment A.10 (experiment A.10 showed remarkably improved conversion). The best results for product formation were obtained in experiment A.10. In a first step, [^{18}F]BFE was trapped in pure DMSO. Then, as a second step, a mixture of IPCITacid and catalyst was added right before the reaction was started. This modification can be regarded as a key step in the automation process. A further improvement was achieved by installing a little vial (2.5 mL) in between the two reactors. It was meant to trap less volatile compounds than [^{18}F]BFE, which were co-transported by the nitrogen current.

The reaction time was set to 15 minutes, as was explored in manual synthesis. The reaction temperature of 100°C was also adopted from the manual syntheses.

The module provided only an insufficient number of reservoirs for the essential chemicals. In experiment A.10, the set-up was adapted to the requirements of the reaction: an additional reservoir (V54) filled with water was installed for quenching the reaction in R2. The semi-preparative HPLC purification step remained an uncertainty factor for several reasons, such as program errors, collection of wrong fractions, or timing problems.

An HPLC separation assay had to be developed before starting with the synthesis work. It was important, to have a tool, to check the reaction mixtures during the optimization process. For this task, analytical HPLC was the method of choice because of its low detection limits, reliable identification, and uncomplicated handling. For the separation of [^{18}F]F^- and [^{18}F]BFE, an existing separation assay from preliminary experiments was used, and it showed good results.

It has long been known that mixtures of organic solvents and aqueous solutions (buffers) are suitable mobile phases in HPLC separation. According to that, many different mixtures were tested - among

them ACN, DMF, MeOH, EtOH, petrol ether, and dimethyl ether - in combination with water-based solutions such as phosphate buffer (acidic and alkaline), acidic water and -mixture (both based on acetic acid), distilled water, various salts dissolved in water, and diluted hydrochloric acid (HCl). Some combinations with organic and aqueous solutions were not possible because a precipitate was formed. For this reason, all elution mixtures were prepared as a premix. For the case of gradient elution, some relevant proportions were pretested in volumetric flasks. It was checked if a precipitate was formed. An elution mixture of ACN (30 %) and acidic water (70 %) showed the best separation in combination with a Chromolith® Performance RP-18e column of FE@IPCIT. The flow rate was set to 2 mL/min, resulting in a short retardation time (3.8 min) for FE@IPCIT. The analytical set-up was transferred to the semi-preparative HPLC. The flow rate was set to 5 mL/min and FE@IPCIT was eluted as a discrete peak within ten minutes.

Altogether, it can be stated that the efficiency of the module syntheses was significantly lower than for manual syntheses. In three of ten experiments (experiments A.7, A.8, and A.10), [^{18}F]FE@IPCIT was synthesized successfully. Experiment A.7 and A.8 revealed only poor yields (0.5 % of initial activity), but in experiment A.10, 2.2 percent were obtained (not decay corrected). Although this seems rather low, the product activity was 272 MBq.

8 Conclusion

The thesis investigated the radiosynthesis of [^{18}F]FE@IPCIT, a new potential radiopharmaceutical for the DAT receptor, including the preparation of the precursor substance [^{18}F]BFE. The development of a synthesis route for [^{18}F]FE@IPCIT was divided in two stages: at the beginning, manual syntheses (n = 19) with comparable low activities (mean value: 1.006 ± 0.559 GBq) and, afterwards, module assisted preparations (n = 10) with high activities (mean value: 9.95 ± 7.89 GBq). Manual syntheses were performed to test and optimize reaction parameters, which were later applied on module syntheses.

Briefly, the synthesis of [^{18}F]BFE showed high RCI, but it was important to use optimum conditions. Of utmost importance was a constant, gentle gas flow during the distillation process. Furthermore, the choice of the trapping agent for evaporated [^{18}F]BFE was a crucial factor for the further synthesis. The reason was that the following reaction of IPCITacid and [^{18}F]BFE was sensitive to some organic solvents and [^{18}F]BFE was, obviously, only available in combination with the trapping solvent. All in all, DMSO proved to be the most suitable solvent for this task.

A major finding concerned the reaction of IPCITacid und [^{18}F]BFE: It only took place in presence of a catalyst. All substances, which were tested successfully, were alkaline chemicals. The best results were obtained with TBAH, LiOH, and Cs_2CO_3. Furthermore, it was reported that the addition of small amounts KI or NaI improved the conversion rate in similar reactions [193, 194]. However, these findings could not be confirmed in this work. Above all, the reaction parameters temperature and time were examined in greater detail. In numerous experiments was shown that a temperature of 100°C and a reaction time of 15 minutes were the most promising conditions – for both, manual- and module assisted syntheses.

The adaption of the reaction to the module was, as it turned out, more challenging as expected. In the final approach (4.2.2 Example Experiment for an Automated Module Synthesis), a remarkable improvement of the RCIY for [^{18}F]FE@IPCIT was achieved. The key step was to trap evaporated [^{18}F]BFE in pure DMSO (RT). Despite all optimizations, the efficiency of module assisted syntheses remained significantly lower than in manual synthesis. Nonetheless, the absolute product amount was increased, since the usage of the module allowed considerably higher starting activities.

In a nutshell, the amount of produced [^{18}F]FE@IPCIT (272 MBq) was enough for further scientific studies. Further preclinical investigations with [^{18}F]FE@IPCIT will be necessary to obtain a basis for final decision upon a clinical suitability of the tracer.

9 References

1. Snell, R.S., *Clinical neuroanatomy* 2010: Wolters Kluwer Health/Lippincott Williams & Wilkins.
2. Pope, J.A., *Medical Physics: Imaging* 1999: Heinemann.
3. Kelter, P.B., M.D. Mosher, and A. Scott, *Chemistry: The Practical Science* 2008: Houghton Mifflin.
4. Zumdahl, S.S. and D.J. DeCoste, *Introductory Chemistry* 2010: Brooks/Cole.
5. Jha, D.K., *Radioactivity And Radioactive Decay* 2004: Discovery Publishing House Pvt. Limited.
6. Alsfasser, R., E. Riedel, and H.J. Meyer, *Moderne Anorganische Chemie*. 6 ed 2007: De Gruyter.
7. Vesilind, P.A., S.M. Morgan, and L.G. Heine, *Introduction to Environmental Engineering* 2010: Cengage Learning.
8. Krebs, R.E., *The History And Use of Our Earth's Chemical Elements: A Reference Guide* 2006: GREENWOOD Publishing Group Incorporated.
9. Hall, E.J. and A.J. Giaccia, *Radiobiology For The Radiologist* 2006: Lippincott Williams&Wilki.
10. Powsner, R.A. and E.R. Powsner, *Essential Nuclear Medicine Physics* 2008: Wiley.
11. van Rijk, P.P., *Nuclear techniques in diagnostic medicine* 1986: Nijhoff.
12. Movahed, A., J.R. Buscombe, and G. Gnanasegaran, *Integrating Cardiology for Nuclear Medicine Physicians: A Guide to Nuclear Medicine Physicians* 2009: Springer Berlin Heidelberg.
13. Stigbrand, T., J. Carlsson, and G.P. Adams, *Targeted Radionuclide Tumor Therapy: Biological Aspects* 2008: Springer Science+Business Media B.V.
14. An, Z., *Therapeutic Monoclonal Antibodies: From Bench to Clinic* 2011: Wiley.
15. Thayalan, K., *Basic Radiological Physics* 2001, RP Bagh, Delphi: Jaypee Brothers Publishers.
16. Khan, F.M., *The Physics of Radiation Therapy* 2010: Walters Kluwer, Lippincott Williams & Wilkins.
17. Stoke, H.S., *General, Organic, and Biological Chemistry*. 6th ed 2012: Brooks Cole Pub Co.
18. Saha, G.B., *Basics of PET Imaging: Physics, Chemistry, and Regulations* 2010: Springer New York.
19. Dale L. Bailey, D.W.T., Peter E. Valk, Michael N. Maisey, *Positron Emission Tomography: Basic Sciences* 2005, London: Springer.
20. Institute, K.A.E.R. *Table of Nuclides*. 2010 05.02.2013]; Available from: http://atom.kaeri.re.kr/ton/nuc7.html.
21. Joe Rosen, L.Q.G., *Encyclopedia of Physical Science*. Vol. 1. 2010, New York.
22. Khalil, M.M., *Basic Sciences of Nuclear Medicine*. 1 ed 2011: Springer-Verlag Berlin Heidelberg. 83.
23. Miller, P.W., et al., *Synthesis of 11C, 18F, 15O, and 13N radiolabels for positron emission tomography.* Angew Chem Int Ed Engl, 2008. **47**(47): p. 8998-9033.
24. Stuart C. Yudofsky, R.E.H., *Essentials of Neuropsychiatry and Behavioral Neurosciences*. 2 ed 2010, Arlington: Amer Psychiatric Pub Inc.
25. Kilbourn, M.R., *Fluorine-18 Labeling of Radiopharmaceuticals* 1990, Washington D.C.: National Academy Press.
26. Park, B.K., N.R. Kitteringham, and P.M. O'Neill, *Metabolism of fluorine-containing drugs.* Annu Rev Pharmacol Toxicol, 2001. **41**: p. 443-70.
27. Stwertka, A., *A Guide to the Elements* 2002: Oxford University Press, USA.
28. Podgorsak, E.B., *Radiation Physics for Medical Physicists* 2010, Berlin Heidelberg: Springer Berlin Heidelberg.
29. Wall, E.v.d., *What's New in Cardiac Imaging?: Spect, Pet, and Mri* 1992, Dordrecht: Kluwer Academic Publishers.
30. G. Stöcklin , V.W.P., *Radiopharmaceuticals for Positron Emission Tomography - Methodological Aspects* 1993, Dordrecht: Kluwer Academic Publishers.

31. Schlyer, D., *PET Tracers and Radiochemistry.* Ann Acad Med Singapore, 2004. **33**: p. 146-154.
32. M. A. Harper, S.J., *Cerebral Blood Flow and Metabolism* 1990, Manchester: Manchester University Press.
33. Emran, A.M., *New Trends in Radiopharmaceutical Synthesis, Quality Assurance, and Regulatory Control: International Symposium Proceedings* 1991, New York: Plenum Press.
34. Wouter A. P. Breeman, A.M.V., *The 68Ge/68Ga generator has high potential, but when can we use 68Ga-labelled tracers in clinical routine?* Eur J Nucl Med Mol Imaging, 2007. **34(7)**: p. 978-981.
35. AGENCY, I.A.E., *CYCLOTRON PRODUCED RADIONUCLIDES: PHYSICAL CHARACTERISTICS AND PRODUCTION METHODS*, in *TECHNICAL REPORTS SERIES* 2009, INTERNATIONAL ATOMIC ENERGY AGENCY: Vienna.
36. Enghag, P., *Encyclopedia of the Elements: Technical Data - History - Processing - Applications* 2008, Weinheim: WILEY-VCH Verlag GmbH & Co. KGaA.
37. Bigott, H.M., et al., *Production, processing and uses of 94mTc.* Journal of Labelled Compounds and Radiopharmaceuticals, 2001. **44**(S1): p. S119-S121.
38. Martin A. Lodge, P., Henning Braess, PhD, Faaiza Mahmoud, MD, Jongdae Suh, MD, Nancy Englar, RN, Sandra Geyser-Stoops, BCNP, Jason Jenkins, CNMT, ¥Stephen L. Bacharach, PhD, Vasken Dilsizian, MD, *The Journal of Invasive Cardiology Developments in Nuclear Cardiology Transition from Single Photon Emission Computed Tomography to Positron Emission Tomography Computed Tomography* J Invasive Cardiol, 2005. **17(9)**: p. 591-496.
39. Chao, A., Tigner, M., *Handbook of Accelerator Physics and Engineering* 1999: World Scientific.
40. Biersack, H.J. and L.M. Freeman, *Clinical Nuclear Medicine* 2007: Springer London, Limited.
41. G. Tyler Miller, J. and S.E. Spoolman, *Sustaining the Earth: An Integrated Approach* 2008: Brooks/Cole.
42. Lewis, E.E., *Fundamentals of Nuclear Reactor Physics* 2008: Elsevier Science.
43. Bohrer, D., *Sources of Contamination in Medicinal Products and Medical Devices* 2012: Wiley.
44. Lee, Y.-S., *Radiopharmaceuticals for Molecular Imaging.* The Open Nuclear Medicine Journal, 2010. **2**: p. 178-185.
45. Prekeges, P.J., *Nuclear Medicine Instrumentation (Book)* 2012: Jones & Bartlett Learning.
46. Morin, R.L., T.C. Gerber, and C.H. McCollough, *Radiation Dose in Computed Tomography of the Heart.* Circulation, 2003. **107**(6): p. 917-922.
47. Brenner, D.J. and E.J. Hall, *Computed Tomography — An Increasing Source of Radiation Exposure.* New England Journal of Medicine, 2007. **357**(22): p. 2277-2284.
48. Ernst J. Rummeny, P.R., Walter Heindel, *Ganzkörper-MR-Tomographie*. 2 ed 2006, Stuttgart: Thieme Verlag.
49. Sid M. Shah, K.M.K., *Emergency Neurology: Principles and Practice* 1999, Cambridge, UK: Cambridge University Press. 14.
50. Kramme, R., *Medizintechnik: Verfahren, Systeme, Informationsverarbeitung*. 3 ed 2007, Heidelberg: Springer. 990.
51. Pichler, B.J., M.S. Judenhofer, and C. Pfannenberg, *Multimodal imaging approaches: PET/CT and PET/MRI.* Handb Exp Pharmacol, 2008. **185**(1): p. 109-32.
52. Judenhofer, M.S., et al., *Simultaneous PET-MRI: a new approach for functional and morphological imaging.* Nat Med, 2008. **14**(4): p. 459-65.
53. Kalra, M.K., S. Saini, and G.D. Rubin, *MDCT: From Protocols to Practice* 2008: Springer-Verlag Milan.
54. Vallabhajosula, S., *Molecular Imaging: Radiopharmaceuticals for PET and SPECT* 2009: Springer-Verlag.
55. Janson, J.C., *Protein Purification: Principles, High Resolution Methods, and Applications* 2012: Wiley.
56. Dong, M.W., *Modern HPLC for Practicing Scientists* 2006: Wiley.
57. Khopkar, S.M., *Basic Concepts Of Analytical Chemistry* 1998: New Age International (P) Ltd.
58. Gey, M.H., *Instrumentelle Analytik Und Bioanalytik: Biosubstanzen, Trennmethoden, Strukturanalytik, Applikationen* 2008: Springer.

59. Udo Huber, R.E.M., *Principles in preparative HPLC*, 2007, Agilent Technologies Inc.: Germany.
60. Wellings, D.A., *A Practical Handbook of Preparative HPLC* 2011: Elsevier Science.
61. Starr, C., C.A. Evers, and L. Starr, *Biology: Concepts and Applications* 2010: Brooks/Cole.
62. Südhof, T.C., *Neurotransmitter release.* Handb Exp Pharmacol, 2008. **184**: p. 1-21.
63. Karlson, P., et al., *Karlsons Biochemie und Pathologie* 2005: Thieme Georg Verlag.
64. Sicar, S., *Principles of Medical Physiology* 2008: Thieme Medical Pub.
65. Benbow, T.J., *Oxford English Dictionary Second Edition on CD-ROM (v. 4.0)*, 2009, Oxford University Press.
66. Ehlert, U., *Verhaltensmedizin* 2003: Springer-Verlag GmbH.
67. Pritchard, T.C. and K.D. Alloway, *Medical Neuroscience* 1998: John Wiley & Sons.
68. Dasgupta, A., *The Science of Drinking: How Alcohol Affects Your Body and Mind* 2011: Rowman & Littlefield Publishers.
69. Siegel, A. and H.N. Sapru, *Essential Neuroscience* 2010: Wolters Kluwer Health/Lippincott Williams & Wilkins.
70. Purves, D., *Neuroscience* 2012: Sinauer Associates.
71. Dunlop Bw, N.C.B., *THe role of dopamine in the pathophysiology of depression.* Archives of General Psychiatry, 2007. **64**(3): p. 327-337.
72. Wolfe, N., et al., *Neuropsychological profile linked to low dopamine: in Alzheimer's disease, major depression, and Parkinson's disease.* J Neurol Neurosurg Psychiatry, 1990. **53**(10): p. 915-7.
73. Chartier-Harlin, M.C., et al., *Alpha-synuclein locus duplication as a cause of familial Parkinson's disease.* Lancet, 2004. **364**(9440): p. 1167-9.
74. Ronald F. Pfeiffer, M.D., M.D. Zbigniew K. Wszolek, and P.D. Manuchair Ebadi, *Parkinson's Disease* 2012: Taylor & Francis Group.
75. Przuntek, H. and T. Müller, *Diagnosis and Treatment of Parkinson S Disease State of the Art: State of the Art* 1999: Springer Wien.
76. Rosenbaum, R.B., *Understanding Parkinson's Disease: A Personal And Professional View* 2006: Praeger.
77. Goldstein, D.S., *Adrenaline and the Inner World: An Introduction to Scientific Integrative Medicine* 2008: Johns Hopkins University Press.
78. Chiras, D.D., *Human Biology 5e* 2005: Jones & Bartlett Learning.
79. Landau, R., B. Achilladelis, and A. Scriabine, *Pharmaceutical Innovation: Revolutionizing Human Health* 1999: Chemical Heritage Press.
80. Excellence, N.I.f.H.a.C., *Depression - Treatment and management of depression in adults, including adults with a chronic physical health problem*, 2009.
81. Gendelman, H.E. and T. Ikezu, *Neuroimmune Pharmacology* 2008: Springer Science+Business Media, LLC.
82. Salzman, C., *Clinical Geriatric Psychopharmacology, 4e* 2005: Lippincott Williams & Wilkins.
83. Golan, D.E., *Principles of Pharmacology: The Pathophysiologic Basis of Drug Therapy* 2008: Wolters Kluwer.
84. Kompoliti, K. and L. Verhagen, *Encyclopedia of Movement Disorders* 2010: Elsevier Science.
85. Bear, M.F., B.W. Connors, and M.A. Paradiso, *Neuroscience* 2007: Lippincott Williams & Wilkins.
86. Hoyer, D., et al., *International Union of Pharmacology classification of receptors for 5-hydroxytryptamine (Serotonin).* Pharmacological Reviews, 1994. **46**(2): p. 157-203.
87. Hayes, D.J. and A.J. Greenshaw, *5-HT receptors and reward-related behaviour: a review.* Neurosci Biobehav Rev, 2011. **35**(6): p. 1419-49.
88. Brumback, R.A. and R.W. Leech, *Neuropathology and Basic Neuroscience* 1995: Springer-Verlag.
89. Schwab, S., et al., *NeuroIntensiv* 2011: Springer.
90. Medicine, I.B.L.P.D.D.J.M.P.C.N.U.P.S. and L.K.K.P.D.P.P.C.M.P.Y.U.S. Medicine, *The Neuron : Cell and Molecular Biology: Cell and Molecular Biology* 2001: Oxford University Press, USA.
91. Ernst, B. and A. Vögtli, *Moderne Pharmakokinetik* 2012: Wiley.

92. Acton, P., et al., *Quantification of dopamine transporters in the mouse brain using ultra-high resolution single-photon emission tomography.* European Journal of Nuclear Medicine and Molecular Imaging, 2002. **29**(5): p. 691-698.
93. Shimada, S., et al., *Cloning and expression of a cocaine-sensitive dopamine transporter complementary DNA.* Science, 1991. **254**(5031): p. 576-8.
94. Stehouwer, J.S. and M.M. Goodman, *Fluorine-18 Radiolabeled PET Tracers for Imaging Monoamine Transporters: Dopamine, Serotonin, and Norepinephrine.* PET Clin, 2009. **4**(1): p. 101-128.
95. Lever, J.R., et al., *Synthesis and in vivo studies of a selective ligand for the dopamine transporter: 3 beta-(4-[125I]iodophenyl) tropan-2 beta-carboxylic acid isopropyl ester ([125I]RTI-121).* Nucl Med Biol, 1996. **23**(3): p. 277-84.
96. Steele Jc, R.J.O.J., *Progressive supranuclear palsy: A heterogeneous degeneration involving the brain stem, basal ganglia and cerebellum with vertical gaze and pseudobulbar palsy, nuchal dystonia and dementia.* Archives of Neurology, 1964. **10**(4): p. 333-359.
97. Nutt, J.G., J.H. Carter, and G.J. Sexton, *The dopamine transporter: importance in Parkinson's disease.* Ann Neurol, 2004. **55**(6): p. 766-73.
98. Organization, W.H., *Neuroscience of Psychoactive Substance Use and Dependence* 2004: World Health Organization.
99. McFadden, R., *Introducing Pharmacology: For Nursing and Healthcare* 2009: Pearson.
100. Kilic, F., D.L. Murphy, and G. Rudnick, *A human serotonin transporter mutation causes constitutive activation of transport activity.* Mol Pharmacol, 2003. **64**(2): p. 440-6.
101. Cortes, R., et al., *Autoradiography of antidepressant binding sites in the human brain: localization using [3H]imipramine and [3H]paroxetine.* Neuroscience, 1988. **27**(2): p. 473-96.
102. Hrdina, P.D., et al., *Antidepressant binding sites in brain: autoradiographic comparison of [3H]paroxetine and [3H]imipramine localization and relationship to serotonin transporter.* J Pharmacol Exp Ther, 1990. **252**(1): p. 410-8.
103. Stockmeier, C.A., et al., *Quantitative subregional distribution of serotonin1A receptors and serotonin transporters in the human dorsal raphe.* Brain Res, 1996. **727**(1-2): p. 1-12.
104. Chinaglia, G., et al., *Serotoninergic terminal transporters are differentially affected in Parkinson's disease and progressive supranuclear palsy: an autoradiographic study with [3H]citalopram.* Neuroscience, 1993. **54**(3): p. 691-9.
105. Blier, P. and C. de Montigny, *Serotonin and drug-induced therapeutic responses in major depression, obsessive-compulsive and panic disorders.* Neuropsychopharmacology, 1999. **21**(2 Suppl): p. 91S-98S.
106. Purselle, D.C. and C.B. Nemeroff, *Serotonin transporter: a potential substrate in the biology of suicide.* Neuropsychopharmacology, 2003. **28**(4): p. 613-9.
107. Pacholczyk, T., R.D. Blakely, and S.G. Amara, *Expression cloning of a cocaine- and antidepressant-sensitive human noradrenaline transporter.* Nature, 1991. **350**(6316): p. 350-4.
108. Blakely, R.D., L.J. De Felice, and H.C. Hartzell, *Molecular physiology of norepinephrine and serotonin transporters.* Journal of Experimental Biology, 1994. **196**(1): p. 263-81.
109. Rommelfanger, K.S. and D. Weinshenker, *Norepinephrine: The redheaded stepchild of Parkinson's disease.* Biochem Pharmacol, 2007. **74**(2): p. 177-90.
110. Ahern, T.H., et al., *The effects of chronic norepinephrine transporter inactivation on seizure susceptibility in mice.* Neuropsychopharmacology, 2006. **31**(4): p. 730-8.
111. Ressler, K.J. and C.B. Nemeroff, *Role of norepinephrine in the pathophysiology and treatment of mood disorders.* Biol Psychiatry, 1999. **46**(9): p. 1219-33.
112. Biederman, J. and T. Spencer, *Attention-deficit/hyperactivity disorder (ADHD) as a noradrenergic disorder.* Biol Psychiatry, 1999. **46**(9): p. 1234-42.
113. Klimek, V., et al., *Reduced levels of norepinephrine transporters in the locus coeruleus in major depression.* J Neurosci, 1997. **17**(21): p. 8451-8.
114. Parrott, A., et al., *Understanding Drugs and Behaviour* 2005: Wiley.

115. Ruiz, P., E.C. Strain, and J. Langrod, *The Substance Abuse Handbook* 2007: Wolters Kluwer Health/Lippincott Williams & Wilkins.
116. Galanter, M. and H.D. Kleber, *The American Psychiatric Publishing Textbook of Substance Abuse Treatment, Fourth Edition* 2008: American Psychiatric Pub.
117. Maisto, S.A., M. Galizio, and G.J. Connors, *Drug Use and Abuse* 2010: Cengage Learning.
118. EANM, *The Radiopharmacy - The Radiopharmacy*, 2008: Vienna.
119. Gad, S.C., *Pharmaceutical Manufacturing Handbook: Production and Processes* 2008: Wiley.
120. Nicoletti, R., M. Oberladstätter, and F. König, *Messtechnik und Instrumentierung in der Nuklearmedizin: eine Einführung* 2007: Facultas.
121. Reba, R.C., D.J. Goodenough, and H.F. Davidson, *Diagnostic Imaging in Medicine* 1983: Nijhoff.
122. W. Wadsak, M.E., *Medizinische Radiochemie I*, 2011: Universität Wien.
123. Saha, G.B., *Physics and Radiobiology of Nuclear Medicine* 2006: Springer-Verlag New York.
124. Simon R. Cherry, J.A.S., Michael E. Phelps, *Physics in Nuclear Medicine: Expert Consult* 2012, Philadelphia: Saunders.
125. Little, K.Y., et al., *[125I]RTI-55 Binding to Cocaine-Sensitive Dopaminergic and Serotonergic Uptake Sites in the Human Brain.* Journal of Neurochemistry, 1993. **61**(6): p. 1996-2006.
126. S. Chen, R.J., J. Lei, H.-K. Kim, G. Flores, R. M. van Dam, P. Y. Keng, C.-J. Kim, *SYNTHESIS OF DIVERSE TRACERS ON EWOD MICRODEVICE FOR POSITRON EMISSION TOMOGRAPHY (PET)*, 2012, Solid-State Sensors, Actuators, and Microsystems Workshop: Hilton Head Island.
127. Hamacher, K., H.H. Coenen, and G. Stocklin, *Efficient stereospecific synthesis of no-carrier-added 2-[18F]-fluoro-2-deoxy-D-glucose using aminopolyether supported nucleophilic substitution.* J Nucl Med, 1986. **27**(2): p. 235-8.
128. E. K. J. Pauwels, M.J.R., J. H. M. B. Stoot, V. R. McCready, M. Bourguigno, B. Mazie`re, *FDG Accumulation and Tumor Biology.* Nuclear Medicine & Biology, 1998. **25**: p. 317–322.
129. John C. Kotz, P.M.T., Gabriela C. Weaver, *Chemistry and Chemical Reactivity*. Vol. 6. 2006, Belmont, USA: Thomson Brooks/Cole.
130. Cherry, S.R. and S.S. Gambhir, *Use of positron emission tomography in animal research.* Ilar J, 2001. **42**(3): p. 219-32.
131. Reichl, F.X. and J. Benecke, *TaschenAtlas der Toxikologie* 2002: Thieme.
132. Ungemach, F.R., R. Kroker, and W. Löscher, *Pharmakotherapie bei Haus- und Nutztieren* 2010: Enke.
133. Geschwinde, T., *Rauschdrogen* 2007: Springer London, Limited.
134. Schiffer, R.B., S.M. Rao, and B.S. Fogel, *Neuropsychiatry* 2003: Williams & Wilkins.
135. Bettelheim, F.A., et al., *Introduction to General, Organic, and Biochemistry* 2010: Brooks/Cole, Cengage Learning.
136. Richard K. Ries, M.D., et al., *Principles of Addiction Medicine* 2009: Wolters Kluwer.
137. Self, D.W. and J.K. Staley, *Behavioral Neuroscience of Drug Addiction* 2010: Springer.
138. U.S. Congress, O.o.T.A., *Biological components of substance abuse and addiction* 1993, Washington, D.C.: DIANE Publishing.
139. Stansfield, K.H. and U.o.S. Florida, *Enduring Changes in Reward Mechanisms After Developmental Exposure to Cocaine: The Role of the D2 Receptor* 2007: University of South Florida.
140. Hafen, B.Q., D. Soulier, and K.J. Frandsen, *Cocaine* 1982: Hazelden.
141. Treatment, C.f.S.A., *Treatment for Stimulant Use Disorders. Treatment Improvement Protocol* Vol. TIP Series No. 33. 1999, Rockville, MD: Center for Substance Abuse Treatment.
142. Wee, S., F.I. Carroll, and W.L. Woolverton, *A Reduced Rate of In Vivo Dopamine Transporter Binding is Associated with Lower Relative Reinforcing Efficacy of Stimulants.* Neuropsychopharmacology, 2005. **31**(2): p. 351-362.
143. Stathis, M., et al., *Rate of binding of various inhibitors at the dopamine transporter in vivo.* Psychopharmacology, 1995. **119**(4): p. 376-84.
144. Martinez, D., et al., *Imaging dopamine transmission in cocaine dependence: link between neurochemistry and response to treatment.* Am J Psychiatry, 2011. **168**(6): p. 634-41.

145. Freye, E., *Pharmacology and Abuse of Cocaine, Amphetamines, Ecstasy and Related Designer Drugs: A Comprehensive Review on Their Mode of Action, Treatment of Abuse and Intoxication* 2009: Springer.
146. Billman, G.E., *Mechanisms responsible for the cardiotoxic effects of cocaine.* Faseb J, 1990. **4**(8): p. 2469-75.
147. Phillips, K., et al., *Cocaine Cardiotoxicity: A Review of the Pathophysiology, Pathology, and Treatment Options.* American Journal of Cardiovascular Drugs, 2009. **9**(3): p. 177-196 10.2165/00129784-200909030-00005.
148. Gradman, A.H., *Cardiac effects of cocaine: a review.* Yale J Biol Med, 1988. **61**(2): p. 137-47.
149. Mehta, A. *Aspirin*. 2005 28.02.2012; 83:[Available from: http://pubs.acs.org/cen/coverstory/83/8325/8325aspirin.html.
150. Dunn, K.M., *Caveman Chemistry: 28 Projects, from the Creation of Fire to the Production of Plastics* 2003: Universal Pub.
151. Bülow, A., *Combinatorial Synthesis of Cocaine Analogues*, in *Department of Chemistry* 2004, University of Aarhus
152. Scheidweiler, K.B., et al., *Pharmacokinetics and Pharmacodynamics of Methylecgonidine, a Crack Cocaine Pyrolyzate.* Journal of Pharmacology and Experimental Therapeutics, 2003. **307**(3): p. 1179-1187.
153. Fandiño, A.S., S.W. Toennes, and G.F. Kauert, *Studies on Hydrolytic and Oxidative Metabolic Pathways of Anhydroecgonine Methyl Ester (Methylecgonidine) Using Microsomal Preparations from Rat Organs.* Chemical Research in Toxicology, 2002. **15**(12): p. 1543-1548.
154. Singh, S., *Chemistry, design, and structure-activity relationship of cocaine antagonists.* Chem Rev, 2000. **100**(3): p. 925-1024.
155. Wood, S.K., et al., *Prevention and reversal by cocaine esterase of cocaine-induced cardiovascular effects in rats.* Drug Alcohol Depend, 2010. **106**(2-3): p. 219-29.
156. Ritz, M.C., et al., *[3H]WIN 35,065-2: a ligand for cocaine receptors in striatum.* J Neurochem, 1990. **55**(5): p. 1556-62.
157. Carroll, F.I., et al., *Synthesis, Ligand Binding, and QSAR (CoMFA and Classical) Study of 3.beta.-(3'-Substituted phenyl)-, 3.beta.-(4'-Substituted phenyl)-, and 3.beta.-(3',4'-Disubstituted phenyl)tropane-2.beta.-carboxylic Acid Methyl Esters.* Journal of medicinal chemistry, 1994. **37**(18): p. 2865-2873.
158. Becker, D.E. and K.L. Reed, *Essentials of local anesthetic pharmacology.* Anesth Prog, 2006. **53**(3): p. 98-108.
159. Czoty, P.W., et al., *Lower reinforcing strength of the phenyltropane cocaine analogs RTI-336 and RTI-177 compared to cocaine in nonhuman primates.* Pharmacol Biochem Behav, 2010. **96**(3): p. 274-8.
160. Clouet, D.H., et al., *Mechanisms of Cocaine Abuse and Toxicity* 1988: U.S. Department of Health and Human Services, Public Health Service, Alcohol, Drug Abuse, and Mental Health Administration, National Institute on Drug Abuse.
161. Grunder, G., *Schizophrene Störungen: tiefere Einsichten durch bildgebende Verfahren* 2006: S Karger Ag.
162. Yang, B., et al., *Conformational, Aqueous Solvation, and pKa Contributions to the Binding and Activity of Cocaine, WIN 35 065-2, and the WIN Vinyl Analog.* Journal of the American Chemical Society, 1994. **116**(19): p. 8722-8732.
163. Broderick, P.A., D.N. Rahni, and E.H. Kolodny, *Bioimaging in Neurodegeneration* 2005: Humana Press.
164. Tsukada, H., et al., *Ketamine alters the availability of striatal dopamine transporter as measured by [(11)C]beta-CFT and [(11)C]beta-CIT-FE in the monkey brain.* Synapse, 2001. **42**(4): p. 273-80.
165. Wee, S., F.I. Carroll, and W.L. Woolverton, *A reduced rate of in vivo dopamine transporter binding is associated with lower relative reinforcing efficacy of stimulants.* Neuropsychopharmacology, 2006. **31**(2): p. 351-62.

166. Kimmel, H.L., F.I. Carroll, and M.J. Kuhar, *Locomotor stimulant effects of novel phenyltropanes in the mouse.* Drug Alcohol Depend, 2001. **65**(1): p. 25-36.
167. Kuhar, M.J., et al., *Studies of selected phenyltropanes at monoamine transporters.* Drug Alcohol Depend, 1999. **56**(1): p. 9-15.
168. Weed, M.R., et al., *Reinforcing and discriminative stimulus effects of beta-CIT in rhesus monkeys.* Pharmacol Biochem Behav, 1995. **51**(4): p. 953-6.
169. *Iometopane: (123)I beta-CIT, dopascan injection, GPI 200, RTI 55.* Drugs R D, 2003. **4**(5): p. 320-2.
170. Grosset, D., H. Fernandez, and M. Okun, *Parkinson's Disease: Clinican's Desk Reference* 2009: Manson Publishing Limited.
171. Thümler, R., *Parkinson-Krankheit: Ein Leitfaden Für Betroffene und Therapeuten* 1999: Springer-Verlag GmbH.
172. Cummings, J.L., et al., *The role of dopaminergic imaging in patients with symptoms of dopaminergic system neurodegeneration.* Brain, 2011. **134**(Pt 11): p. 3146-66.
173. Seibyl, J.P., et al., *Iodine-123-ß-CIT and Iodine-123-FPCIT SPECT Measurement of Dopamine Transporters in Healthy Subjects and Parkinson's Patients.* Journal of Nuclear Medicine, 1998. **39**(9): p. 1500-1508.
174. Reneman, L., et al., *Comparative in vivo study of iodine-123-labeled beta-CIT and nor-beta-CIT binding to serotonin transporters in rat brain.* Synapse, 1999. **34**(1): p. 77-80.
175. Hesse, S., et al., *Serotonin and dopamine transporter imaging in patients with obsessive-compulsive disorder.* Psychiatry Res, 2005. **140**(1): p. 63-72.
176. Carpinelli, A., et al., *Radiosynthesis of [123I]ßCIT, a selective ligand for the study of the dopaminergic and serotoninergic systems in human brain.* Applied Radiation and Isotopes, 2001. **54**(1): p. 93-95.
177. Nakano, T., et al., *Enhancement of in vivo binding of [123I]beta-CIT by MK-801 in rat brain.* Synapse, 1998. **30**(4): p. 402-8.
178. Mitterhauser, M., et al., *Synthesis and biodistribution of [18F]FE@CIT, a new potential tracer for the dopamine transporter.* Synapse, 2005. **55**(2): p. 73-9.
179. Emond, P., D. Guilloteau, and S. Chalon, *PE2I: a radiopharmaceutical for in vivo exploration of the dopamine transporter.* CNS Neurosci Ther, 2008. **14**(1): p. 47-64.
180. Schou, M., et al., *Synthesis, radiolabeling and preliminary in vivo evaluation of [18F]FE-PE2I, a new probe for the dopamine transporter.* Bioorg Med Chem Lett, 2009. **19**(16): p. 4843-5.
181. Chi, D.Y., et al., *Synthesis of no-carrier-added N-([18F]fluoroalkyl)spiperone derivatives.* Int J Rad Appl Instrum A, 1986. **37**(12): p. 1173-80.
182. Kiesewetter, D.O., et al., *Syntheses and D2 receptor affinities of derivatives of spiperone containing aliphatic halogens.* International Journal of Radiation Applications and Instrumentation. Part A. Applied Radiation and Isotopes, 1986. **37**(12): p. 1181-1188.
183. Mark, C., Bornatowicz, B., Fink, C., Wadsak W. , *Synthesis, radiosynthesis and first in-vitro evaluation of Novel PET-tracers for dopamine transporter: [11C]IPCIT and [18F]FE@IPCIT.* submitted.
184. Allard, P., J.O. Marcusson, and S.B. Ross, *[3H]WIN 35,428 binding in the human brain.* Brain Res, 1996. **706**(2): p. 347-50.
185. Donovan, S.F. and M.C. Pescatore, *Method for measuring the logarithm of the octanol-water partition coefficient by using short octadecyl-poly(vinyl alcohol) high-performance liquid chromatography columns.* J Chromatogr A, 2002. **952**(1-2): p. 47-61.
186. Yoon, C.H., et al., *Rapid screening of blood-brain barrier penetration of drugs using the immobilized artificial membrane phosphatidylcholine column chromatography.* J Biomol Screen, 2006. **11**(1): p. 13-20.
187. Tavares, A.A., et al., *Radiotracer properties determined by high performance liquid chromatography: a potential tool for brain radiotracer discovery.* Nucl Med Biol, 2012. **39**(1): p. 127-35.
188. Emre, M., *Cognitive Impairment and Dementia in Parkinson's Disease* 2010: Oxford University Press.

189. Rhoades, R.A. and D.R. Bell, *Medical Physiology: Principles for Clinical Medicine* 2009: Wolters Kluwer Health/Lippincott Williams & Wilkins.
190. Senda, M., Y. Kimura, and P. Herscovitch, *Brain Imaging Using Pet* 2002: Boston.
191. Lundkvist, C., et al., *Improved syntheses of the PET radioligands, [11C]FLB 457, [11C]MDL 100907 and [11C]β-CIT-FE, by the use of [11C]methyl triflate.* Journal of Labelled Compounds and Radiopharmaceuticals, 1998. **41**(6): p. 545-556.
192. Wang, Y., et al., *Reactivity and rearrangements of dialkyl- and diarylvinylsulfonium salts with indole-2- and pyrrole-2-carboxaldehydes.* Tetrahedron, 1999. **55**(35): p. 10659-10672.
193. A. Bauman, M.P., F. Rösch, *In Situ Generierung von [18F]IFE aus [18F]BFE* 2002, Mainz, Germany: Institut für Kernchemie, Johannes Gutenberg - Universität.
194. A. Bauman, M.P., F. Rösch, *Vergleichende Untersuchung zur 18F-Fluorethylierung mit den sekundären Markierungsvorläufern 2-[18F]Fluorethyltosylat und 2-Brom-1-[18F]fluorethan* 2002, Mainz, Germany: Institut für Kernchemie, Johannes Gutenberg - Universität.
195. Varrone, A., et al., *In vitro autoradiography and in vivo evaluation in cynomolgus monkey of [18F]FE-PE2I, a new dopamine transporter PET radioligand.* Synapse, 2009. **63**(10): p. 871-80.

10 Appendix

10.1 Abstract English

The thesis investigated the radiosynthesis of [^{18}F]FE@IPCIT, a new potential radiopharmaceutical for the dopamine transporter (DAT). The main aim was to develop and optimize a module assisted synthesis route, based on the results of a manual synthesis route.

Method: At the beginning, manual experiments (n = 19) with comparable low activities (mean value: 1.006 ± 0.559 GBq) were performed to test and optimize various reaction parameters (temperature, catalysts, time, precursor concentration, and solvents). Optimum conditions were applied on automated module syntheses, and the activities were increased (mean value: 9.95 ± 7.89 GBq, n = 10). Moreover, catalysts for the reaction of [^{18}F]BFE with IPCITacid, and the preparation of the precursor [^{18}F]BFE were explored in greater detail.

Result: Three highly catalytic substances for the radiosynthesis of [^{18}F]FE@IPCIT were identified: TBAH, LiOH, and Cs_2CO_3. For the preparation of [^{18}F]BFE, adequate yields (16.8 ± 7.5 %, n = 12) of great purity (mean value: 78 ± 30 %, n = 17) were achieved. Module assisted syntheses remained challenging: Despite optimizations, the efficiency was significantly lower than in manual synthesis. Nonetheless, it was finally accomplished to produce a sufficient amount of [^{18}F]FE@IPCIT (272 MBq) for further scientific examinations.

Conclusion: The module assisted synthesis of [^{18}F]FE@IPCIT has been developed to a level, which allows the production of adequate radiopharmaceutical for further studies.

10.2 Abstract German

In der vorliegenden Arbeit wurde die Synthese eines potentiellen Tracers, [^{18}F]FE@IPCIT, für den Dopamintransporter (DAT) evaluiert und entwickelt. Das Hauptziel war die Erarbeitung einer modulgestützten Syntheseroute, basierend auf den Ergebnissen einer manuellen Synthese.

Methode: Grundlegende Reaktionsparameter (Temperatur, Katalysatoren, Reaktionszeit, Präkursorkonzentration und Art des Lösungsmittels) wurden in manueller Synthese (n = 19) mit vergleichsweise niedrigen Aktivitäten (Mittelwert: 1.006 ± 0.559 GBq) getestet und optimiert. Die anschließenden Modulsynthesen benutzen bereits zu Beginn die optimalen Reaktionsbedingungen und wesentlich höhere Startaktivitäten (Mittelwert: 9.95 ± 7.89 GBq, n = 10). Der Hauptfokus wurde während der Entwicklungsphase auf das Auffinden und Testen von katalytischen Substanzen für die Reaktion von [^{18}F]BFE mit IPCITacid gelegt. Ein weiterer wichtiger Punkt betraf die Herstellung der Synthesevorstufe [^{18}F]BFE.

ERGEBNIS: Es konnten drei Substanzen mit hoher katalytischer Aktivität identifiziert werden: TBAH, LiOH und Cs_2CO_3. Die Synthese von [^{18}F]BFE lieferte hinreichende radiochemische Ausbeuten (16.8 ± 7.5 %, n = 12), von hoher Reinheit (Mittelwert: 78 ± 30 %, n = 17). Die Adaption der Reaktion auf das Synthesemodul gelang trotz anfänglicher Probleme und es konnte genügend [^{18}F]FE@IPCIT (272 MBq) produziert werden, um weitere wissenschaftliche Untersuchungen zu ermöglichen.

ZUSAMMENFASSUNG: Die Modulsynthese von [^{18}F]FE@IPCIT wurde auf einen Entwicklungsstand gebracht, der die Herstellung von ausreichend Tracer für weitere Studien sicherstellen kann.

10.3 CURRICULUM VITAE

Education

1992 – 1996	Primary school (VS Hörbranz)
1996 – 2004	Secondary school (BG Blumenstraße Bregenz)
2005 – 2007	Study of Medicine at the Medical University of Vienna (completed first level)
2007 – 2011	Study of Chemistry at the University of Vienna (completed with a Bachelor of Science degree)
2011 – 2013	Study of Chemistry at the University of Vienna (Master program) including an Erasmus-semester in Sweden at the University of Gothenburg

10.4 ACKNOWLEDGMENT

An dieser Stelle möchte ich mich bei allen Personen bedanken, die mich während meines Studiums und bei der Anfertigung dieser Arbeit unterstützt haben:

Professor Dr. Markus Mitterhauser und Professor Dr. Wolfgang Wadsak danke ich, dass sie es mir ermöglichten, in ihrer Arbeitsgruppe mitzuarbeiten, die benötigten Ressourcen zur Verfügung stellten und meine Masterarbeit dadurch erst ermöglichten.

An Professor Dr. Wolfgang Wadsak ein weiteres Dankeschön für die Bereitstellung des interessanten Themas und die stete Unterstützung während meiner Arbeit.

Mein besonderer Dank gilt meiner Betreuerin Christina Rami-Mark, MSc. Danke für deine kompetenten, guten Erklärungen auf fachliche Fragen, für deine Geduld und für die Unterstützung beim Schreiben meiner Masterarbeit, die weit größer war, als man es erwarten kann. Auch danke für den freundlichen Umgangston, sodass ich mich stets auf die Zusammenarbeit im Labor freuen konnte.

Ein Dankeschön auch an Mag. Lukas Nics für die Unterstützung bei den HPLC-Experimenten, den Versuch, mir das Funktionsprinzip einer Uhr zu erklären und die besondere Hilfsbereitschaft, die er im Zuge meiner Arbeit immer wieder gezeigt hat.

Abschließend möchte ich mich bei der ganzen Arbeitsgruppe für die freundliche Aufnahme, die Unterstützung bei den kleinen Widrigkeiten des Forscheralltages, den gemeinsamen Mittagessen und das rundum freundliche Arbeitsklima bedanken.

Meinen Eltern danke ich für ihre Unterstützung während des gesamten Studiums.